Proceedings of the CAS-CERN Accelerator School: Intensity Limitations in Particle Beams, Geneva, Switzerland, 2–11 November 2015, edited by W. Herr, CERN Yellow Reports: School Proceedings, Vol. 3/2017, CERN-2017-006-SP (CERN, Geneva, 2017)

Intrabeam Scattering: Anatomy of the Theory

M. Martini
CERN, Geneva, Switzerland

Abstract

This paper starts with an introduction to some elements of physical kinetics relevant to microscopic interactions in gas or plasma systems. The aim is to provide the necessary background for understanding charged particle beams. Emphasis is placed on the important role played by collisions in plasmas. We then give a detailed, albeit non-exhaustive, review of intrabeam scattering (IBS), which consists of the study of diffusion effects caused by multiple Coulomb scattering on charged particle beams, in both the transverse and the longitudinal beam dimensions. Finally, applications to the large hadron collider 7 TeV stored proton beam and the 'Extra Low Energy Antiproton' (ELENA) 100 keV decelerated antiproton beam are used to illustrate the behaviour of the IBS growth rates, for a high-energy storage ring well above the transition energy and an ultra-low-energy decelerator ring below the transition energy.

Keywords

Plasma kinetic; IBS paradigms; Piwinski framework; Bjorken-Mtingwa approach; IBS applications.

1 Introduction

Consider a system of N particles described by a 'density distribution' in a $6N$-dimensional phase space. In this space, the whole collection of N particles is represented by a single point. Under a stability condition, the particles occupy a finite volume in phase space. The density function behaves like an incompressible fluid when observed along the phase space trajectories, provided that all forces driving the system are *conservative* (i.e. derived from a potential): this is the crux of the matter. In practice, instead of using the full $6N$-dimensional space, it is more convenient to view the phase trajectories of all particles in the same six-dimensional phase space, which allows for better visualization of the particle density distribution. In the process of this reduction, however, difficulties could arise with interactions between the particles. In the presence of inter-particle collisions driven by *non-conservative* forces, the phase space volume containing the N particles does not remain incompressible; some particles may escape from it and others may enter it. *Liouville's formula*, modified by adding a 'collision term', becomes the *collision Boltzmann's equation*, which is still an active area of research. The reader may find it helpful to review the topic of particle collisions in plasmas and ionized gases, which are basically quasi-stationary, when we consider the case of a charged particle beam in a storage ring.

In what way is intrabeam scattering (IBS) in charged particle beams different from Coulomb scattering of plasma or gas particles in a 'closed box'? In storage rings, due to the curvature of the orbit, IBS can increase the beam density in phase space as a whole (i.e. transverse beam emittances and momentum spread can grow simultaneously) to above the ring transition energy, because of the coupling between the radial and longitudinal motions. While revisiting the methods used in IBS, our interest was drawn to the logical structure at the core of the subject, so we have decided to base our study on the theoretical framework of A. Piwinsky [1]. His original paper gives a clear presentation of the kinematics of the classical interaction process involved in multiple Coulomb scattering in charged particle beams, assuming weak-focusing accelerator or storage rings. His methodical approach makes all his papers fairly easy to grasp. Equipped with this framework, the essential features of IBS can be understood quite well. The alternative approach of J. Bjorken and S. Mtingwa [2] is based on the scattering matrix

https://doi.org/10.23730/CYRSP-2017-003.291

formalism from quantum electrodynamics, and the theory is applicable to strong-focusing machines. Both of these approaches are presented here, to provide a thorough grounding for the study of many aspects of IBS. However, Monte Carlo simulations of IBS based on a binary collision model [3–5] are not covered in this paper; nor are IBS models that implement the linear coupling between transverse betatron oscillations [6, 7].

2 Overview of the kinetics of gases and plasmas

The classical mechanics branch of dynamics is sometimes divided into kinematics and kinetics. Kinematics is the study of the properties of motion—i.e. the masses or forces which may be involved—without considering the causes, whereas kinetics aims to explain the change in motion as a result of the forces and torques applied. Kinetics refers also to the study of gases and plasmas, relating their macroscopic properties (such as pressure and temperature) to a microscopic model of which the constituents are many small particles. A plasma is a fully or partially ionized gas, i.e. an ensemble of particles made up of electrons, ions and neutrals moving under the influence of electromagnetic or gravity forces and particle interactions such as ionization or Coulomb scattering. Gases and plasmas are mostly non-relativistic. Unlike plasmas, a *plasma beam* is a directed stream of charged particles, generally relativistic, in which the motion depends on applied external fields; in a plasma beam the individual particles make small angles with the beam axis, and the particle energy spread is small relative to the total energy (typical of beams in accelerators and storage rings).

2.1 The Liouville (collisionless Boltzmann) equation

2.1.1 The many-particle phase space joint probability density

The dynamic state of a plasma is completely determined once given the instantaneous positions $\mathbf{r}_i(t)$ and momenta $\mathbf{p}_i(t)$ at time t for all particles in the $6N$-dimensional phase space $\{\mathbf{r} = \mathbf{r}_i(t),\ \mathbf{p} = \mathbf{p}_i(t) : i = 1, \ldots, N\}$, called Γ-space, where N is the number of plasma particles. The state of a plasma is a single point moving along a $6N$-dimensional trajectory $\{\mathbf{r}(t), \mathbf{p}(t)\}$ as time evolves; Γ-space is a many-particle phase space for the whole system of particles, often used in statistical mechanics and kinetic theory [8]. To simplify the notation, we assume that all particles in a plasma are of the same species (e.g. protons, electrons or ions). In a Cartesian frame we have $\{\mathbf{r}_i(t) = x_i\hat{\mathbf{x}} + y_i\hat{\mathbf{y}} + z_i\hat{\mathbf{z}},\ \mathbf{p}_i(t) = p_{x,i}\hat{\mathbf{x}} + p_{y,i}\hat{\mathbf{y}} + p_{z,i}\hat{\mathbf{z}}\}$ where $\hat{\mathbf{x}}$, $\hat{\mathbf{y}}$ and $\hat{\mathbf{z}}$ are unit vectors along the x-, y- and z-axes. The representative single point $M(t) = \prod_{i=1}^{N}\{\mathbf{r}_i(t), \mathbf{p}_i(t)\}$ of the N particles in Γ-space is called the *microstate*. Such a detailed model requires knowledge of $6N$ functions of time with initial conditions that are known only to a certain degree of precision and whose complete description cannot be achieved. When N is very large, say $N = 6 \times 10^{23}$ for one atom-gram of hydrogen, it makes sense to describe the plasma statistically instead.

To this end, we conceptualize a large number $\mathcal{N}$ of independent replicas of the same microstate of an N-particle system, each virtual replica being described by a different representative point $M(t)$ in Γ-space ($\mathcal{N}$ does not have to equal N). The abstract set of identical systems is called a statistical *ensemble*. Let $\mathrm{d}^{6N}\mathcal{N}(\mathbf{r}, \mathbf{p}, t)$ denote the number of representative points inside a infinitesimal phase space volume element $\mathrm{d}\Gamma = \mathrm{d}^{3N}\mathbf{r}\,\mathrm{d}^{3N}\mathbf{p} = \prod_{i=1}^{N}\mathrm{d}^3\mathbf{r}_i\,\mathrm{d}^3\mathbf{p}_i$ about a point $(\mathbf{r}, \mathbf{p})$ at time t, i.e. in the range $\{(\mathbf{r}, \mathbf{r} + \mathrm{d}\mathbf{r}), (\mathbf{p}, \mathbf{p} + \mathrm{d}\mathbf{p})\}$ about $(\mathbf{r}, \mathbf{p})$. Therefore, a normalized phase space probability density function $\rho(\mathbf{r}, \mathbf{p}, t)$ can be formally specified by

$$\rho(\mathbf{r}, \mathbf{p}, t) = \lim_{\mathcal{N}\to\infty} \frac{\mathrm{d}^{6N}\mathcal{N}(\mathbf{r}, \mathbf{p}, t)}{\mathcal{N}\,\mathrm{d}\Gamma}, \qquad \int \mathrm{d}\Gamma\,\rho(\mathbf{r}, \mathbf{p}, t) = 1\,, \tag{1}$$

where $\mathrm{d}\Gamma$ is a $6N$-dimensional hypercube of 'hypersides' $\mathrm{d}^{3N}\mathbf{r}$ and $\mathrm{d}^{3N}\mathbf{p}$.

Comment: As $\rho^{-1}(\mathbf{r}, \mathbf{p}, t)$ has the dimension of a reciprocal 'action', $[(\mathrm{J\,s})^{-1}]$, and because ρ^{-1} is proportional to $\mathrm{d}\Gamma = (\mathrm{d}\mathbf{r}\,\mathrm{d}\mathbf{p})^{3N}$ it is evocative to attach a Planck constant $h = 2\pi\hbar$ to each pair $\mathrm{d}\mathbf{r}\,\mathrm{d}\mathbf{p}$ so that $\mathrm{d}\Gamma = (\mathrm{d}\mathbf{r}\,\mathrm{d}\mathbf{p}/2\pi\hbar)^{3N}$, where $h^{3N} \approx \Delta\mathbf{r}\Delta\mathbf{p}$ is the smallest possible phase space cell size by

virtue of the Heisenberg uncertainty relation. However, this is ill-suited to the framework of classical physics!

This means that $\rho(\mathbf{r},\mathbf{p},t)\,\mathrm{d}\Gamma$ is the probability of finding a non-specific microstate in the volume $\mathrm{d}\Gamma = \mathrm{d}^{3N}\mathbf{r}\,\mathrm{d}^{3N}\mathbf{p}$ about $(\mathbf{r},\mathbf{p})$ at time t; that is, $\rho(\mathbf{r},\mathbf{p},t)\,\mathrm{d}^{3N}\mathbf{r}\,\mathrm{d}^{3N}\mathbf{p}$ is the probability that particle 1 is in the volume $\mathrm{d}^3\mathbf{r}_1\,\mathrm{d}^3\mathbf{p}_1$ about the point $(\mathbf{r}_1,\mathbf{p}_1)$, particle 2 is in the volume $\mathrm{d}^3\mathbf{r}_2\,\mathrm{d}^3\mathbf{p}_2$ about $(\mathbf{r}_2,\mathbf{p}_2)$, and so on, up to particle N located in the volume $\mathrm{d}^3\mathbf{r}_N\,\mathrm{d}^3\mathbf{p}_N$ about $(\mathbf{r}_N,\mathbf{p}_N)$ at time t. Then ρ is the N-particle joint probability density function for the plasma system. It is assumed that the density of microstates in Γ-space does not change too fast from one volume element to the next, so that $\rho(\mathbf{r},\mathbf{p},t)$ can be regarded as a continuous function. For a finite number $\mathcal{N}$, a so-called coarse-grained density is obtained which disregards the variations of ρ below some small resolution in Γ-space: $\rho(\mathbf{r},\mathbf{p},t) = \mathrm{d}^{6N}\mathcal{N}(\mathbf{r},\mathbf{p},t)/\mathcal{N}\,\mathrm{d}\Gamma$.

Properly normalized, $\rho(\mathbf{r},\mathbf{p},t)$ can be used to compute *macroscopic* values for various functions $\mathcal{O}(\mathbf{r},\mathbf{p})$:

$$\langle\mathcal{O}\rangle = \int \mathrm{d}\Gamma\,\rho(\mathbf{r},\mathbf{p},t)\mathcal{O}(\mathbf{r},\mathbf{p})\;. \tag{2}$$

A key property of an ensemble is that the microstate trajectories never intersect in Γ-space, because each trajectory is uniquely specified by $6N$ initial conditions $\{\mathbf{r}(0),\mathbf{p}(0)\}$. (In case trajectories might be crossed, a phase space configuration situated at the intersection would have multiple trajectories; but this is forbidden in classical physics!). Figure 1 shows two snapshots of the state of an ensemble of $\mathrm{d}^{6N}\mathcal{N}(\mathbf{r},\mathbf{p},t)$ microstate points in Γ-space at times t and $t+\mathrm{d}t$. It illustrates the evolution over the time interval $\mathrm{d}t$ of these microstates which occupy a tiny volume element $\mathrm{d}\Gamma(t) = \prod_{i=1}^{N}\mathrm{d}^3\mathbf{r}_i\,\mathrm{d}^3\mathbf{p}_i$ with border $C(t)$ around $(\mathbf{r},\mathbf{p})$ at time t. Meanwhile, the volume element $\mathrm{d}\Gamma(t)$ can become distorted in shape as a consequence of the particle motion and will occupy a new volume element $\mathrm{d}\Gamma(t+\mathrm{d}t)$ with border $C(t+\mathrm{d}t)$ at time $t+\mathrm{d}t$. Likewise, each microstate represented by a point $M(t) = \prod_{i=1}^{N}\{\mathbf{r}_i(t),\mathbf{p}_i(t)\}$ transforms gradually, to first order in time, into another point $M'(t+\mathrm{d}t)$:

$$M'(t+\mathrm{d}t) = \prod_{i=1}^{N}\left\{\mathbf{r}_i'(t+\mathrm{d}t) = \mathbf{r}_i(t) + \dot{\mathbf{r}}_i(t)\,\mathrm{d}t,\;\mathbf{p}_i'(t+\mathrm{d}t) = \mathbf{p}_i(t) + \dot{\mathbf{p}}_i(t)\,\mathrm{d}t\right\}. \tag{3}$$

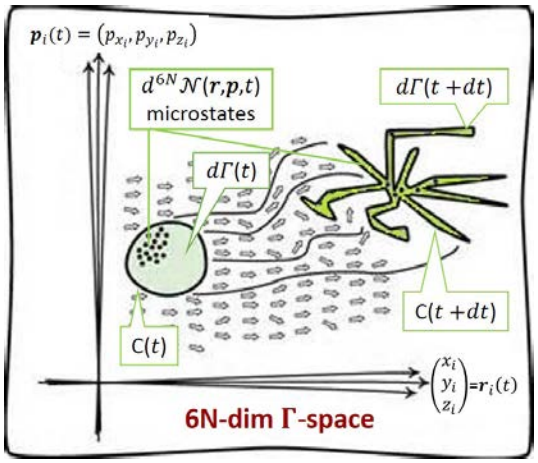

Fig. 1: Depiction of the motion during the time interval $\mathrm{d}t$ of a volume element $\mathrm{d}\Gamma(t) = \mathrm{d}^3\mathbf{r}(t)\,\mathrm{d}^3\mathbf{v}(t)$ about $(\mathbf{r}(t),\mathbf{v}(t))$ in Γ-space.

2.1.2 The single-particle phase space probability density

A simpler way to describe a plasma of N identical particles is to use the phase space for a single particle, called μ-space, in contrast to the Γ-space for the overall particle ensemble; this is the method typically

used in plasma physics, with Cartesian coordinates $\mathbf{r}$ and velocities $\mathbf{v}$ in place of the momenta $\mathbf{p}$, since plasma motion is often non-relativistic. When a particle moves, its representative point $\mu(t)$ traces out a trajectory in six-dimensional phase space such that at each instant the dynamic state of the N plasma particles is represented by N points in the phase space [9]. Likewise, a one-particle probability density function $\rho_1(\mathbf{r},\mathbf{v},t)$ can be defined such that $\mathrm{d}^6N(\mathbf{r},\mathbf{v},t)$ is the number of plasma particles contained in an infinitesimal phase volume element $\mathrm{d}\mu = \mathrm{d}^3\mathbf{r}\,\mathrm{d}^3\mathbf{v}$ (a hypercube of sides $\mathrm{d}^3\mathbf{r}$ and $\mathrm{d}^3\mathbf{v}$) about one unspecified representative 'point particle' $\mu(t) = (\mathbf{r},\mathbf{v}) = \{(x,y,z),(v_x,v_y,v_z)\}$ among N in μ-space:

$$\rho_1(\mathbf{r},\mathbf{v},t) = \lim_{N\to\infty}\frac{\mathrm{d}^6N(\mathbf{r},\mathbf{v},t)}{N\,\mathrm{d}\mu}, \qquad \int \mathrm{d}\mu\,\rho_1(\mathbf{r},\mathbf{v},t) = 1\,. \tag{4}$$

Comment: Here, with $\rho_1(\mathbf{r},\mathbf{v},t)$, every 'phase' volume element $(\mathrm{d}\mathbf{r}\,\mathrm{d}\mathbf{v})^3$ could be replaced by $\mathrm{d}\mu = (\mathrm{d}\mathbf{r}\,\mathrm{d}\mathbf{v}/2\pi\hbar)^3$.

Like Eq. (2), the distribution function $\rho_1(\mathbf{r},\mathbf{v},t)$ enables one to compute macroscopic values of functions $\mathcal{O}(\mathbf{r},\mathbf{v})$:

$$\langle\mathcal{O}\rangle = \int \mathrm{d}\mu\,\rho_1(\mathbf{r},\mathbf{v},t)\mathcal{O}(\mathbf{r},\mathbf{v})\,. \tag{5}$$

For instance, let us formulate the horizontal beam emittance in terms of the single-particle emittance given by the *Courant–Snyder invariant*

$$\begin{aligned}\varepsilon_x &= \gamma_x x_\beta^2 + 2\alpha_x x_\beta x'_\beta + \beta_x x'^2_\beta = \frac{x_\beta^2}{\beta_x} + \beta_x\left(x'_\beta - \frac{\beta'_x}{2\beta_x}x_\beta\right)^2,\\ x_\beta &= x - D_x\frac{\Delta p}{p_0}, \quad x'_\beta = x' - D'_x\frac{\Delta p}{p_0}\,,\end{aligned} \tag{6}$$

where $2\alpha_x = -\beta'_x,\ \gamma_x = (1+\alpha_x^2)/\beta_x,\ D_x$ is the momentum dispersion function and $x' = p_x/|\mathbf{p}|$. To write down the overall horizontal beam emittance, we switch back to the momentum variable (since a charge particle beam is mostly relativistic), $\mathbf{p} = m\gamma\mathbf{v}$ with $\gamma = (1-\mathbf{v}^2/c^2)^{-1/2}$. Hence, upon averaging Eq. (6) over N particles we obtain, using the notation $\langle\cdots\rangle = \sum_{i=1}^N(\cdots)/N$,

$$\begin{aligned}\varepsilon_x &= \int \mathrm{d}\mu\,\rho_1(x,p,t)\left(\frac{x_\beta^2}{\beta_x} + \beta_x\left[x'_\beta - \frac{\beta'_x}{2\beta_x}x_\beta\right]^2\right)\\ &= \left\langle\frac{x_\beta^2}{\beta_x}\right\rangle\left(1+\frac{\beta'^2_x}{4}\right) - \beta'_x\langle x'_\beta x_\beta\rangle + \beta_x\langle x'^2_\beta\rangle\,.\end{aligned} \tag{7}$$

The equation that governs the evolution of the phase space probability density function under specified initial conditions is generally known as the *Boltzmann equation*. Suppose that each particle of the plasma is subjected to an external force $\mathbf{F}(t)$. In the absence of particle interactions, a particle with coordinates around $\{\mathbf{r},\mathbf{v}\}$ at time t will be found after a time interval $\mathrm{d}t$ around the new coordinates $\{\mathbf{r}',\mathbf{v}'\}$ so that, to first order in t, we obtain

$$\mathbf{r}'(t+\mathrm{d}t) = \mathbf{r}(t) + \mathbf{v}(t)\,\mathrm{d}t\,, \qquad \mathbf{v}'(t+\mathrm{d}t) = \mathbf{v}(t) + \mathbf{a}(t)\,\mathrm{d}t\,, \tag{8}$$

where $\mathbf{v} = \dot{\mathbf{r}}$ and $\mathbf{a} = \dot{\mathbf{v}} = \mathbf{F}/m$ (with $\mathbf{a}$ being the acceleration of the particle and m its mass).

All the particles inside the phase space volume element $\mathrm{d}\mu(t) = \mathrm{d}^3\mathbf{r}\,\mathrm{d}^3\mathbf{v}$ with border $C(t)$ about $(\mathbf{r},\mathbf{v})$ at time t will occupy a new volume element $\mathrm{d}^3\mathbf{r}'\mathrm{d}^3\mathbf{v}'$ with border $C'(t+\mathrm{d}t)$ about $(\mathbf{r}',\mathbf{v}')$ after the time interval $\mathrm{d}t$. Figure 2 displays the state of $\mathrm{d}^6N(\mathbf{r},\mathbf{v},t)$ particles of plasma in μ-space at times t and $t+\mathrm{d}t$. Since we are considering the same particles at t and at $t+\mathrm{d}t$, the following equality holds, provided there are no inter-particle collisions or dissipative forces leading to non-conservation of phase space volume:

$$\begin{aligned}&\rho_1(\mathbf{r}',\mathbf{v}',t+\mathrm{d}t)\,\mathrm{d}^3\mathbf{r}'\,\mathrm{d}^3\mathbf{v}'\\ &\quad\equiv \rho_1(\mathbf{r},\mathbf{v},t)\,\mathrm{d}^3\mathbf{r}\,\mathrm{d}^3\mathbf{v}\,.\end{aligned} \tag{9}$$

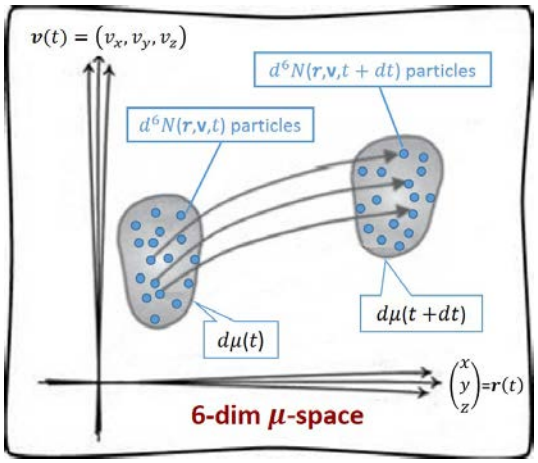

Fig. 2: Depiction of the motion during the time interval $\mathrm{d}t$ of a volume element $\mathrm{d}\mu(t) = \mathrm{d}^3\mathbf{r}(t)\,\mathrm{d}^3\mathbf{v}(t)$ about $(\mathbf{r}(t), \mathbf{v}(t))$ in μ-space.

The shape of the volume $\mathrm{d}\mu(t) = \mathrm{d}^3\mathbf{r}\,\mathrm{d}^3\mathbf{v}$ may change into $\mathrm{d}\mu(t+\mathrm{d}t) = \mathrm{d}^3\mathbf{r}'\,\mathrm{d}^3\mathbf{v}'$ during the particle motion over the time interval $\mathrm{d}t$. The new phase volume $\mathrm{d}\mu(t+\mathrm{d}t)$ and the initial one $\mathrm{d}\mu(t)$ are related by the determinant of the 6×6 Jacobian matrix J of the transformation (8):

$$\mathrm{d}^3\mathbf{r}'\mathrm{d}^3\mathbf{v}' = |\det \mathrm{J}|\,\mathrm{d}^3\mathbf{r}\,\mathrm{d}^3\mathbf{v}, \tag{10}$$

where

$$J = \frac{\partial(\mathbf{r}', \mathbf{v}')}{\partial(\mathbf{r}, \mathbf{v})} = \begin{pmatrix} \partial x'/\partial x & \partial y'/\partial x & \cdots & \partial v_z'/\partial x \\ \partial x'/\partial y & \partial y'/\partial y & \cdots & \partial v_z'/\partial y \\ \vdots & \vdots & \ddots & \vdots \\ \partial x'/\partial v_z & \partial y'/\partial v_z & \cdots & \partial v_z'/\partial v_z \end{pmatrix}. \tag{11}$$

We split the external force $\mathbf{F}$ into (i) a *velocity-independent* force $\tilde{\mathbf{F}}$ (e.g. an external force constraining the particles inside a box or an external electric field force $e\mathbf{E}$ accelerating charged particles) and (ii) a *velocity-dependent* force, customarily the Lorentz force due to an external magnetic field $\mathbf{B}$ confining the particles inside a torus. Thus, leaving $\tilde{\mathbf{F}}$ not fully specified at this stage, we get $\mathbf{F} = \tilde{\mathbf{F}} + e(\mathbf{v} \times \mathbf{B})$. Using Eq. (8) the partial derivatives in the Jacobian matrix can be written in the form

$$\begin{aligned} &\frac{\partial x'_{u=x,y,z}}{\partial x_{w=x,y,z}} = \delta_{u,w}, \qquad \frac{\partial v'_{u=x,y,z}}{\partial x_{w=x,y,z}} = \frac{\mathrm{d}t}{m}\frac{\partial \tilde{F}_u}{\partial x_w} = \frac{\mathrm{d}t}{m}\begin{pmatrix} \partial\tilde{F}_x/\partial x & \partial\tilde{F}_y/\partial x & \partial\tilde{F}_z/\partial x \\ \partial\tilde{F}_x/\partial y & \partial\tilde{F}_y/\partial y & \partial\tilde{F}_z/\partial y \\ \partial\tilde{F}_x/\partial z & \partial\tilde{F}_y/\partial z & \partial\tilde{F}_z/\partial z \end{pmatrix}, \\ &\frac{\partial x'_{u=x,y,z}}{\partial v_{w=x,y,z}} = \delta_{u,w}\,\mathrm{d}t, \quad \frac{\partial v'_{u=x,y,z}}{\partial v_{w=x,y,z}} = \delta_{u,w} + \frac{e\,\mathrm{d}t}{m}\frac{\partial(\mathbf{v}\times\mathbf{B})_{\hat{\mathbf{u}}=\hat{\mathbf{x}},\hat{\mathbf{y}},\hat{\mathbf{z}}}}{\partial v_w}, \end{aligned} \tag{12}$$

where $\delta_{u,w}$ is the Kronecker delta with the subscripts u and w alternately representing the coordinates x, y and z. For clarity, the Lorentz force term in the fourth part of (12) is explicitly written below as a submatrix of the Jacobian:

$$\begin{aligned} \frac{\partial(\mathbf{v}\times\mathbf{B})_{\hat{\mathbf{u}}=\hat{\mathbf{x}},\hat{\mathbf{y}},\hat{\mathbf{z}}}}{\partial v_{w=x,y,z}} &= \frac{\partial}{\partial v_w}\begin{vmatrix} \hat{\mathbf{x}} & \hat{\mathbf{y}} & \hat{\mathbf{z}} \\ v_x & v_y & v_z \\ B_x & B_y & B_z \end{vmatrix}_{\hat{\mathbf{u}}} \\ &= \frac{\partial}{\partial v_{w=x,y,z}}\Big[\big(v_yB_z - v_zB_y\big)\hat{\mathbf{x}} + \big(v_zB_x - v_xB_z\big)\hat{\mathbf{y}} \\ &\quad + \big(v_xB_y - v_yB_x\big)\hat{\mathbf{z}}\Big]_{\hat{\mathbf{u}}=\hat{\mathbf{x}},\hat{\mathbf{y}},\hat{\mathbf{z}}} \end{aligned}$$

$$= \begin{pmatrix} 0 & -B_z & B_y \\ B_z & 0 & -B_x \\ -B_y & B_x & 0 \end{pmatrix} .$$

The full Jacobian matrix with its determinant $|\det \mathrm{J}|$ (up to second order in $\mathrm{d}t$) are shown in Eqs. (13) and (14) below:

$$J = \begin{pmatrix} 1 & 0 & 0 & (\mathrm{d}t/m)\,\partial\tilde{F}_x/\partial x & (\mathrm{d}t/m)\,\partial\tilde{F}_y/\partial x & (\mathrm{d}t/m)\,\partial\tilde{F}_z/\partial x \\ 0 & 1 & 0 & (\mathrm{d}t/m)\,\partial\tilde{F}_x/\partial y & (\mathrm{d}t/m)\,\partial\tilde{F}_y/\partial y & (\mathrm{d}t/m)\,\partial\tilde{F}_z/\partial y \\ 0 & 0 & 1 & (\mathrm{d}t/m)\,\partial\tilde{F}_x/\partial z & (\mathrm{d}t/m)\,\partial\tilde{F}_y/\partial z & (\mathrm{d}t/m)\,\partial\tilde{F}_z/\partial z \\ \mathrm{d}t & 0 & 0 & 1 & -B_z\,e\,\mathrm{d}t/m & B_y\,e\,\mathrm{d}t/m \\ 0 & \mathrm{d}t & 0 & B_z\,e\,\mathrm{d}t/m & 1 & -B_x\,e\,\mathrm{d}t/m \\ 0 & 0 & \mathrm{d}t & -B_y\,e\,\mathrm{d}t/m & B_x\,e\,\mathrm{d}t/m & 1 \end{pmatrix} , \tag{13}$$

$$|\det \mathrm{J}| = 1 + \mathrm{dt}^2(\mathrm{e}^2/\mathrm{m}^2)(\mathrm{B}_\mathrm{x}^2 + \mathrm{B}_\mathrm{y}^2 + \mathrm{B}_\mathrm{z}^2) - \big(\partial\tilde{\mathrm{F}}_\mathrm{x}/\partial\mathrm{x} + (\partial\tilde{\mathrm{F}}_\mathrm{y}/\partial\mathrm{y})(\partial\tilde{\mathrm{F}}_\mathrm{z}/\partial\mathrm{z})\big)/\mathrm{m} + \mathcal{O}(\mathrm{dt}^3) . \tag{14}$$

It follows that $|\det \mathrm{J}| = 1$ to first order in $\mathrm{d}t$, and so (10) and (9) become

$$(\mathrm{d}^3\mathbf{r}'\,\mathrm{d}^3\mathbf{v}')(t+\mathrm{d}t) = (d^3\mathbf{r}\,\mathrm{d}^3\mathbf{v})(t), \qquad \big[\rho_1(\mathbf{r}',\mathbf{v}',t+\mathrm{d}t) - \rho_1(\mathbf{r},\mathbf{v},t)\big]\,\mathrm{d}^3\mathbf{r}\,\mathrm{d}^3\mathbf{v} = 0\,; \tag{15}$$

that is, volume elements in μ-space are invariants. This is *Liouville's theorem*, which states that the phase space probability density $\rho_1(\mathbf{r},\mathbf{v},t)$ behaves like an incompressible fluid. Using (8), Liouville's theorem (the second equation in (15)) can be rewritten as

$$\rho_1(\mathbf{r}+\mathbf{v}\,\mathrm{d}t,\ \mathbf{v}+\mathbf{a}\,\mathrm{d}t,\ t+\mathrm{d}t) = \rho_1(\mathbf{r},\mathbf{v},t). \tag{16}$$

With these results, the incompressibility condition of Liouville's theorem can be cast in differential form by expanding the left-hand side of (16) in a Taylor series for ρ_1 with respect to the variables $(\mathbf{r},\mathbf{v},t)$, yielding to first order in $\mathrm{d}t$,

$$\begin{aligned} &\rho_1(\mathbf{r}+\mathbf{v}\,\mathrm{d}t,\ \mathbf{v}+\mathbf{a}\,\mathrm{d}t,\ t+\mathrm{d}t) \\ &\quad= \rho_1(\mathbf{r},\mathbf{v},t) + \left[\frac{\partial\rho_1(\mathbf{r},\mathbf{v},t)}{\partial t} + \frac{\mathrm{d}\mathbf{r}}{\mathrm{d}t}\cdot\frac{\partial\rho_1(\mathbf{r},\mathbf{v},t)}{\partial\mathbf{r}} + \frac{\mathrm{d}\mathbf{r}}{\mathrm{d}t}\cdot\frac{\partial\rho_1(\mathbf{r},\mathbf{v},t)}{\partial\mathbf{v}}\right]\mathrm{d}t \\ &\quad= \rho_1(\mathbf{r},\mathbf{v},t) + \left[\frac{\partial\rho_1(\mathbf{r},\mathbf{v},t)}{\partial t} + \mathbf{v}\cdot\frac{\partial\rho_1(\mathbf{r},\mathbf{v},t)}{\partial\mathbf{r}} + \mathbf{a}\cdot\frac{\partial\rho_1(\mathbf{r},\mathbf{v},t)}{\partial\mathbf{v}}\right]\mathrm{d}t \\ &\quad= \rho_1(\mathbf{r},\mathbf{v},t) + \left[\frac{\partial\rho_1(\mathbf{r},\mathbf{v},t)}{\partial t} + \mathbf{v}\cdot\nabla_r\rho_1(\mathbf{r},\mathbf{v},t) + \mathbf{a}\cdot\nabla_v\rho_1(\mathbf{r},\mathbf{v},t)\right]\mathrm{d}t\,, \end{aligned} \tag{17}$$

where notation similar to $\frac{\partial}{\partial\mathbf{u}} = \nabla_u$ (for $\mathbf{u} = \mathbf{r},\mathbf{v}$) has been used for the del operators $\nabla_r = \hat{\mathbf{x}}\frac{\partial}{\partial x} + \hat{\mathbf{y}}\frac{\partial}{\partial y} + \hat{\mathbf{z}}\frac{\partial}{\partial z}$ and $\nabla_v = \hat{\mathbf{x}}\frac{\partial}{\partial v_x} + \hat{\mathbf{y}}\frac{\partial}{\partial v_y} + \hat{\mathbf{z}}\frac{\partial}{\partial v_z}$. Substituting the right-hand side of (16) into the left-hand side of (17) gives the so-called *Liouville's formula*

$$\frac{\partial\rho_1(\mathbf{r},\mathbf{v},t)}{\partial t} + \mathbf{v}\cdot\nabla_r\rho_1(\mathbf{r},\mathbf{v},t) + \mathbf{a}\cdot\nabla_v\rho_1(\mathbf{r},\mathbf{v},t) = 0\,. \tag{18}$$

Liouville's formula can also be written in terms of the total derivative $\mathrm{d}\rho_1/\mathrm{d}t$ for the evolution of a volume element as it moves in μ-space (different from $\partial\rho_1/\partial t$, which refers to the change in a volume element at a specific μ-space location):

$$\frac{\mathrm{d}\rho_1(\mathbf{r},\mathbf{v},t)}{\mathrm{d}t} \equiv \frac{\partial\rho_1(\mathbf{r},\mathbf{v},t)}{\partial t} + \mathbf{v}\cdot\nabla_r\rho_1(\mathbf{r},\mathbf{v},t) + \mathbf{a}\cdot\nabla_v\rho_1(\mathbf{r},\mathbf{v},t) = 0\,. \tag{19}$$

This means that $\rho_1(\mathbf{r},\mathbf{v},t)$ is constant along a system phase space trajectory; Eq. (19) is also called the *collisionless Boltzmann equation*.

2.2 The Boltzmann collision integral

The collisionless Boltzmann equation is an equation of motion for a one-particle probability density function $\rho_1(\mathbf{r}, \mathbf{v}, t)$, which is especially suitable for describing dilute gas. In the absence of interactions, the particles are mutually independent and ρ_1 obeys the one-particle Liouville's equation. So far we have introduced the normalized probability density $\rho(\mathbf{r}, \mathbf{v}, t)$ in Γ-space, Eq. (1), and the reduced one-particle probability density $\rho_1(\mathbf{r}, \mathbf{v}, t)$ in μ-space, Eq. (4). Another useful interpretation of the one-particle probability density is obtained when one multiplies ρ_1 by the number of particles N inside a phase space domain in μ-space; this is the one-particle *density distribution* in phase space, denoted by f_1 (see [9]):

$$f_1(\mathbf{r}, \mathbf{v}, t) = \frac{\mathrm{d}^6 N(\mathbf{r}, \mathbf{v}, t)}{\mathrm{d}^3\mathbf{r}\,\mathrm{d}^3\mathbf{v}}, \qquad \int \mathrm{d}^3\mathbf{r}\,\mathrm{d}^3\mathbf{v}\, f_1(\mathbf{r}, \mathbf{v}, t) = N\,. \tag{20}$$

Here $\mathrm{d}^6 N(\mathbf{r}, \mathbf{v}, t)$ is the number of particles contained within the phase volume $\mathrm{d}\mu(t) = \mathrm{d}^3\mathbf{r}\,\mathrm{d}^3\mathbf{v}$ around $(\mathbf{r}, \mathbf{v})$ at time t. Liouville's equation says that if during the time interval $\mathrm{d}t$, we move along with a representative particle in the phase volume element $\mathrm{d}^3\mathbf{r}\,\mathrm{d}^3\mathbf{v}$ (enclosing N particles) and observe the net number $\delta^6 N$ of particles that enter this volume element, we will find that $\delta^6 N \equiv 0$ (note the difference in meaning of 'd' and 'δ'). Thus, we get

$$\delta^6 N = \left[\frac{\partial f_1(\mathbf{r}, \mathbf{v}, t)}{\partial t} + \mathbf{v}\cdot\nabla_r f_1(\mathbf{r}, \mathbf{v}, t) + \mathbf{a}\cdot\nabla_v f_1(\mathbf{r}, \mathbf{v}, t)\right]\mathrm{d}^3\mathbf{r}\,\mathrm{d}^3\mathbf{v}\,\mathrm{d}t \equiv 0 \tag{21}$$

or, in analogy to (19),

$$\frac{\mathrm{d}f_1(\mathbf{r}, \mathbf{v}, t)}{\mathrm{d}t} \equiv \frac{\partial f_1(\mathbf{r}, \mathbf{v}, t)}{\partial t} + \mathbf{v}\cdot\nabla_r f_1(\mathbf{r}, \mathbf{v}, t) + \mathbf{a}\cdot\nabla_v f_1(\mathbf{r}, \mathbf{v}, t) = 0$$

(where, as before, $\mathbf{a} = \mathbf{F}/m$ is the particle acceleration, with m being the mass of the particle and $\mathbf{F}$ an externally supported force).

The collisionless Boltzmann equation has to be adapted to handle the effects arising from interactions between particles. The Boltzmann collision term discussed below considers only binary elastic collisions. For short-range interactions, two-particle collisions are defined in terms of the pair correlation function $f_2(\mathbf{r}, \mathbf{v}, \mathbf{r}_1, \mathbf{v}_1, t)$. The two colliding particles become dependent, and their density functions $f_1(\mathbf{r}, \mathbf{v}, t)$ and $f_1(\mathbf{r}_1, \mathbf{v}_1, t)$ before collision must be replaced by the two-particle density distribution f_2, which is no longer constant along the phase space trajectories; Eq. (19) needs to be modified by

$$\frac{\mathrm{d}f_2(\mathbf{r}, \mathbf{v}, \mathbf{r}_1, \mathbf{v}_1, t)}{\mathrm{d}t} = \left[\frac{\delta f_2(\mathbf{r}, \mathbf{v}, \mathbf{r}_1, \mathbf{v}_1, t)}{\delta t}\right]_{\text{coll}}. \tag{22}$$

The right-hand side of (22), $[\delta f_2(\mathbf{r}, \mathbf{v}, \mathbf{r}_1, \mathbf{v}_1, t)/\delta t]_{\text{coll}}$, is called the 'collision integral', and designates symbolically the rate of change of the distribution due to the two-particle collisions, which is still to be worked out. A heuristic validation of the Boltzmann equation including collisions in gases and plasmas will be carried out. In the end, this heuristic approach will give the same result as more fundamental derivations. The binary collisions occur in charged and neutral plasmas and involve atoms or molecules in a dilute gas. Multiple coulomb interactions in a plasma, although they may be as important as binary collisions, are ignored here. For binary collisions in the time interval $\mathrm{d}t$, the interaction result is characterized by the net rate at which collisions either decrease or increase the number of particles in a μ-space volume element $\mathrm{d}^3\mathbf{r}\,\mathrm{d}^3\mathbf{v}$ (cf. [9, 10]).

Figure 3 shows the numbers of particles $\mathrm{d}^6 N_1$ and $\mathrm{d}^6 N_2$ that, at two instants t and $t+\mathrm{d}t$, are within a phase space volume element $\mathrm{d}\mu = \mathrm{d}^3\mathbf{r}\,\mathrm{d}^3\mathbf{v}$, possibly distorted by the particle motion. It illustrates particles entering and leaving the phase volume by virtue of collisions during the interval $\mathrm{d}t$. Some of the particles that were at first in $\mathrm{d}^3\mathbf{r}\,\mathrm{d}^3\mathbf{v}$ may be removed from it, and particles originally outside this volume element may end up inside it.

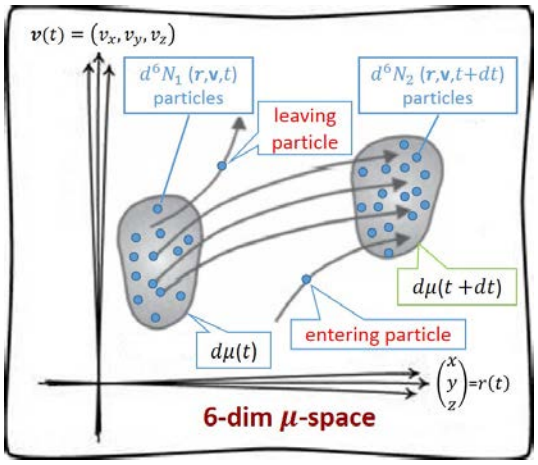

Fig. 3: Evolution of the number of particles in a volume element $\mathrm{d}^3\mathbf{r}(t)\,\mathrm{d}^3\mathbf{v}(t)$ over a time interval $\mathrm{d}t$ in μ-space

The net loss or gain of particles resulting from collisions in the time interval $\mathrm{d}t$ is, by (19) and (22),

$$\delta^6 N = \left[\frac{\delta f_2(\mathbf{r},\mathbf{v},\mathbf{r}_1,\mathbf{v}_1,t)}{\delta t}\right]_{\text{coll}} \mathrm{d}^3\mathbf{r}\,\mathrm{d}^3\mathbf{v}\,\mathrm{d}t, \qquad \delta^6 N = \delta^6 N^+ - \delta^6 N^- \,. \tag{23}$$

Here, $\delta^6 N^-$ is the loss part, due to collisions for which a particle within $\mathrm{d}^3\mathbf{r}$ of $\mathbf{r}$ has a velocity *before* collision that is within $\mathrm{d}^3\mathbf{v}$ of $\mathbf{v}$; similarly, $\delta^6 N^+$ is the gain part, caused by collisions for which a particle within $\mathrm{d}^3\mathbf{r}$ of $\mathbf{r}$ has a velocity *after* collision that is within $\mathrm{d}^3\mathbf{v}$ of $\mathbf{v}$.

For $\delta^6 N^-$, the velocities of the particles may be split into two groups: one contains velocities in the slice $\mathrm{d}^3\mathbf{v}$ about $\mathbf{v}$, and the other includes all other velocities, referred to as $\mathbf{v}_1$. The number of particles removed from the phase volume element $\mathrm{d}^3\mathbf{r}\,\mathrm{d}^3\mathbf{v}$ in time $\mathrm{d}t$ is the total number of collisions that the particles $\mathbf{v}$ have with all the other particles $\mathbf{v}_1$ during the time interval $\mathrm{d}t$. To compute $\delta^6 N^-$, each collision between a pair of particles must satisfy the following: one particle of the first group (called the $\mathbf{v}$-particle) in the phase volume $\mathrm{d}^3\mathbf{r}\,\mathrm{d}^3\mathbf{v}$ about $(\mathbf{r},\mathbf{v})$ is scattered out of the velocity slice $\mathrm{d}^3\mathbf{v}$ in the time $\mathrm{d}t$ as a result of a collision with a particle of the second group (a $\mathbf{v}_1$-particle), which has a velocity in $\mathrm{d}^3\mathbf{v}_1$ about $\mathbf{v}_1$ and a location in $\mathrm{d}^3\mathbf{r}_1$ about $\mathbf{r}_1$ (a priori not necessarily the same as $\mathrm{d}^3\mathbf{v}$). Then

$$\delta^6 N^- = \left(\int_{(\mathbf{r}_1,\mathbf{v}_1)} f_2(\mathbf{r},\mathbf{v},\mathbf{r}_1,\mathbf{v}_1,t)\,\mathrm{d}^3\mathbf{r}_1\,\mathrm{d}^3\mathbf{v}_1\right)\mathrm{d}^3\mathbf{r}\,\mathrm{d}^3\mathbf{v}\,. \tag{24}$$

Recall that $\mathrm{d}^3\mathbf{r}_1$ must be such that during δt, the $\mathbf{v}_1$-particles in $\mathrm{d}^3\mathbf{r}_1$ experience a collision with the $\mathbf{v}$-particles inside $\mathrm{d}^3\mathbf{r}$. We set up $\mathrm{d}^3\mathbf{r}_1$ by considering a scattering event in the frame of the single $\mathbf{v}$-particle, as shown in Fig. 4. The particles inside $\mathrm{d}^3\mathbf{r}_1\,\mathrm{d}^3\mathbf{v}_1$ about $(\mathbf{r}_1,\mathbf{v}_1)$ may be viewed as a $\mathbf{v}_1$-particle flux incident on this $\mathbf{v}$-particle. Figure 4 illustrates the scattering where the $\mathbf{v}_1$-particle flux approaches the $\mathbf{v}$-particle from the right at a velocity of $|\mathbf{v}_1-\mathbf{v}|$ with an *impact parameter* between b and $b+\mathrm{d}b$, in a collision plane lying between the angles ϕ and $\phi+\mathrm{d}\phi$. Accordingly, all $\mathbf{v}_1$-particles in the volume of the cylinder of length $|\mathbf{v}_1-\mathbf{v}|\,\mathrm{d}t$ and base area $b\,\mathrm{d}b\,\mathrm{d}\phi$ experience a collision with the $\mathbf{v}$-particles in time $\mathrm{d}t$. So

$$\mathrm{d}^3\mathbf{r}_1 = b\,\mathrm{d}b\,\mathrm{d}\phi\,|\mathbf{v}_1-\mathbf{v}|\,\mathrm{d}t\,. \tag{25}$$

Substituting (25) into (24) transforms the equation into

$$\delta^6 N^- = \left(\int_{(\mathbf{v}_1,b,\phi)} f_2(\mathbf{r},\mathbf{v},\mathbf{r}_1,\mathbf{v}_1,t)\,\mathrm{d}^3\mathbf{v}_1\,|\mathbf{v}_1-\mathbf{v}|\,b\,\mathrm{d}b\,\mathrm{d}\phi\right)\mathrm{d}^3\mathbf{r}\,\mathrm{d}^3\mathbf{v}\,\mathrm{d}t\,. \tag{26}$$

For $\delta^6 N^+$, consider all particle-pair collisions that send one particle into the velocity slice $\mathrm{d}^3\mathbf{v}$ about $\mathbf{v}$ in the time interval $\mathrm{d}t$, which is the *inverse* of the original collision $(\mathbf{v},\mathbf{v}_1) \rightleftarrows (\mathbf{v}',\mathbf{v}_1')$. The

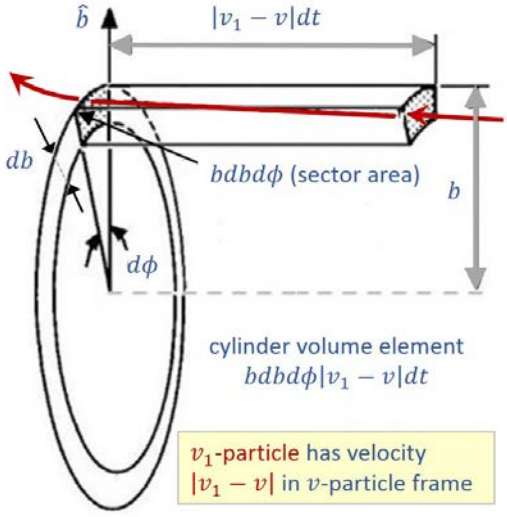

Fig. 4: Sketch of scattering for $\delta^6 N^-$ in the $\mathbf{v}$-particle frame, where a $\mathbf{v}_1$-particle moves from the right towards the $\mathbf{v}$ particle sitting in the vertical collision plane.

primed variables represent the inverse collision of the unprimed ones in (26). In analogy to (24), $\delta^6 N^+$ can be written as

$$\delta^6 N^+ = \left(\int_{(\mathbf{r}_1', \mathbf{v}_1')} f_2(\mathbf{r}', \mathbf{v}', \mathbf{r}_1', \mathbf{v}_1', t)\, \mathrm{d}^3\mathbf{r}_1'\, \mathrm{d}^3\mathbf{v}_1' \right) \mathrm{d}^3\mathbf{r}'\, \mathrm{d}^3\mathbf{v}' \,. \tag{27}$$

Equivalently, from the conservation of momentum and energy for elastic collisions between identical particles, i.e.

$$\mathbf{v} + \mathbf{v}_1 = \mathbf{v}' + \mathbf{v}_1', \quad \mathbf{v}^2 + \mathbf{v}_1^2 = \mathbf{v}'^2 + {\mathbf{v}_1'}^2 \quad \Longrightarrow \quad |\mathbf{v} - \mathbf{v}_1| = |\mathbf{v}' - \mathbf{v}_1'| \,,$$

we obtain

$$\delta^6 N^+ = \left(\int_{(\mathbf{v}_1', b, \phi)} f_2(\mathbf{r}', \mathbf{v}', \mathbf{r}_1', \mathbf{v}_1', t)\, \mathrm{d}^3\mathbf{v}_1'\, |\mathbf{v}_1' - \mathbf{v}'|\, b\, \mathrm{d}b\, \mathrm{d}\phi \right) \mathrm{d}^3\mathbf{r}'\, \mathrm{d}^3\mathbf{v}'\, \mathrm{d}t \,. \tag{28}$$

In order to combine Eqs. (26)–(28) and express $\delta^6 N$ as a single integral with variables of integration $\mathbf{v}_1$, b and ϕ, the integrands of $\delta^6 N^+$ and $\delta^6 N^-$ have to be compatible. To verify this, one can use the phase volume-invariant techniques based on change of variables involving unit Jacobian determinants (see [10] and the above proof of Liouville's theorem, for example). In particular, the phase volume $\mathrm{d}^3\mathbf{r}\, \mathrm{d}^3\mathbf{v}\, \mathrm{d}^3\mathbf{r}_1\, \mathrm{d}^3\mathbf{v}_1$ is a *collisional invariant*:

$$\mathrm{d}^3\mathbf{r}\, \mathrm{d}^3\mathbf{v}\, \mathrm{d}^3\mathbf{r}_1\, \mathrm{d}^3\mathbf{v}_1 = \mathrm{d}^3\mathbf{r}'\, \mathrm{d}^3\mathbf{v}'\, \mathrm{d}^3\mathbf{r}_1'\, \mathrm{d}^3\mathbf{v}_1' \,.$$

It follows that

$$\delta^6 N = \left(\int_{(\mathbf{v}_1, b, \phi)} \left[f_2(\mathbf{r}', \mathbf{v}', \mathbf{r}_1', \mathbf{v}_1', t) - f_2(\mathbf{r}, \mathbf{v}, \mathbf{r}_1, \mathbf{v}_1, t) \right] \mathrm{d}^3\mathbf{v}_1\, |\mathbf{v}_1 - \mathbf{v}|\, b\, \mathrm{d}b\, \mathrm{d}\phi \right) \mathrm{d}^3\mathbf{r}\, \mathrm{d}^3\mathbf{v}\, \mathrm{d}t \,, \tag{29}$$

where there is no extra integration over $\mathbf{v}_1'$ thanks to the above collisional invariant. Substituting (29) into (21) and cancelling the products $\mathrm{d}^3\mathbf{r}\, \mathrm{d}^3\mathbf{v}\, \mathrm{d}t$, the total time-derivative $\mathrm{d}f_1/\mathrm{d}t$ turns into

$$\begin{aligned} \frac{\mathrm{d}f_1(\mathbf{r}, \mathbf{v}, t)}{\mathrm{d}t} &\equiv \frac{\partial f_1(\mathbf{r}, \mathbf{v}, t)}{\partial t} + \mathbf{v} \cdot \nabla_r f_1(\mathbf{r}, \mathbf{v}, t) + \mathbf{a} \cdot \nabla_v f_1(\mathbf{r}, \mathbf{v}, t) \\ &= \int_{(\mathbf{v}_1, b, \phi)} \left[f_2(\mathbf{r}', \mathbf{v}', \mathbf{r}_1', \mathbf{v}_1', t) - f_2(\mathbf{r}, \mathbf{v}, \mathbf{r}_1, \mathbf{v}_1, t) \right] \mathrm{d}^3\mathbf{v}_1\, |\mathbf{v}_1 - \mathbf{v}|\, b\, \mathrm{d}b\, \mathrm{d}\phi \,, \end{aligned} \tag{30}$$

where the unprimed and primed distributions refer to the states before and after collision, respectively.

Finally, to deduce the Boltzmann equation from Eq. (30) we need a physical approximation enabling us to write f_2 and f_2' in terms of f_1 and f_1', so that (30) will reduce to an expression involving a single integro-differential equation for $f_1(\mathbf{r}, \mathbf{v}, t)$. A conventional derivation of the Boltzmann equation might be considered too heuristic and does not provide a suitable basis for accurate investigation. A better formal derivation of (30) could start out from knowledge of the N-particle joint probability density $\rho_N = \rho$ in the $6N$-dimensional Γ-space (see Eq. (1)), in which the particle velocity $\mathbf{v}$ replaces the momentum $\mathbf{p}$. As the description of a system determined by a full phase density distribution is not feasible, one could instead consider a subset of particles defining a *reduced s-particle* density function f_s. A particularly ingenious method for dealing with such a reduced density function f_s (though not pursued here) is the BBGKY hierarchy. In this formalism, f_1, f_2 and f_s are shown without proof as they will not be used hereafter (notice our way of numbering the N particles $\{\mathbf{r}, \mathbf{v}, \mathbf{r}_i, \mathbf{v}_i\}_{i=1,\ldots,N-1}$, rather than using the usual order $\{\mathbf{r}_i, \mathbf{v}_i\}_{i=1,\ldots,N}$):

$$
\begin{aligned}
f_1(\mathbf{r}, \mathbf{v}, t) &= N \int \prod_{i=1}^{N-1} \mathrm{d}^3\mathbf{r}_i \, \mathrm{d}^3\mathbf{v}_i \, \rho(\mathbf{r}, \mathbf{v}, \mathbf{r}_1, \mathbf{v}_1, \ldots, \mathbf{r}_{N-1}, \mathbf{v}_{N-1}, t), \\
f_2(\mathbf{r}, \mathbf{v}, \mathbf{r}_1, \mathbf{v}_1, t) &= N(N-1) \int \prod_{i=2}^{N-1} \mathrm{d}^3\mathbf{r}_i \, \mathrm{d}^3\mathbf{v}_i \, \rho(\mathbf{r}, \mathbf{v}, \mathbf{r}_1, \mathbf{v}_1, \ldots, \mathbf{r}_{N-1}, \mathbf{v}_{N-1}, t), \\
f_s(\mathbf{r}, \mathbf{v}, \mathbf{r}_1, \mathbf{v}_1, \ldots, \mathbf{r}_{s-1}, \mathbf{v}_{s-1}, t) & \\
&= \frac{N!}{(N-s+1)!} \int \prod_{i=s}^{N-1} \mathrm{d}^3\mathbf{r}_i \, \mathrm{d}^3\mathbf{v}_i \, \rho(\mathbf{r}, \mathbf{v}, \mathbf{r}_1, \mathbf{v}_1, \ldots, \mathbf{r}_{N-1}, \mathbf{v}_{N-1}, t) \, . \qquad (31)
\end{aligned}
$$

Even so, this way of proceeding is not fully effective in practice. The one-particle density distribution $f_1(\mathbf{r}, \mathbf{v}, t)$ in this sequence is important as it governs the evolution of the collision Boltzmann equation, provided that manageable approximate forms are available for the two-particle density distributions $f_2(\mathbf{r}, \mathbf{v}, \mathbf{r}, \mathbf{v}_1, t)$ and $f_2(\mathbf{r}', \mathbf{v}', \mathbf{r}', \mathbf{v}_1', t)$. Many attempts have been made to derive the Boltzmann equation from first principles without resorting to approximations. However, a number of assumptions come into play in all these derivations, which renders even the more formal analyses (e.g. the BBGKY hierarchy) somewhat ad hoc (see [8, 10–14]).

To find approximate closed-form solutions to Eq. (30) in terms of expressions relating $f_1(\mathbf{r}, \mathbf{v}, t)$ and $f_2(\mathbf{r}, \mathbf{v}, \mathbf{r}, \mathbf{v}_1, t)$, again consider a collision between $\mathbf{v}$- and $\mathbf{v}_1$-particles, which emerge with velocities $\mathbf{v}'$ and $\mathbf{v}_1'$ from the collision. Suppose that the $\mathbf{v}$-particle is located at $(\mathbf{r}, \mathbf{v})$ in the phase volume $\mathrm{d}^3\mathbf{r}\,\mathrm{d}^3\mathbf{v}$ and the $\mathbf{v}_1$-particle at $(\mathbf{r}, \mathbf{v}_1)$ in the phase volume $\mathrm{d}^3\mathbf{r}_1\,\mathrm{d}^3\mathbf{v}_1$. This means that collisions are local in space and that the two particles are located at the same point; since $\mathbf{r}$ and $\mathbf{r}'$ can be any points in the respective phase volume elements, we must have $\mathrm{d}^3\mathbf{r}_1 \equiv \mathrm{d}^3\mathbf{r}$. Hence

$$
f_2(\mathbf{r}, \mathbf{v}, \mathbf{r}_1, \mathbf{v}_1, t) \equiv f_2(\mathbf{r}, \mathbf{v}, \mathbf{r}, \mathbf{v}_1, t) \, .
$$

The joint two-particle density distribution f_2 is therefore *homogeneous* over the interaction domain and may be characterized by a circle of radius $\mathbf{r}_{\text{int}}$, considered to be infinitesimal relative to the mean free path of the particles. Evaluating f_2 at the same point $\mathbf{r}$ in space, regardless of the velocity, supposes that the density distribution is below some small resolution in μ-space and does not vary on scales of order $\mathbf{r}_{\text{int}}$. When the particles are sufficiently far away from each other ($|\mathbf{r}| > |\mathbf{r}_{\text{int}}|$), the interaction vanishes. When the particles enter the interaction domain ($|\mathbf{r}| \leq |\mathbf{r}_{\text{int}}|$), they experience a collision. Figures 5 and 6 illustrate the geometry of a particle-pair scattering event involving two particles of velocities $\mathbf{v}$ and $\mathbf{v}_1$, viewed from a coordinate system in which the $\mathbf{v}$-particle is at rest.

As the simplest and most drastic approximation that bypasses all the transformations related to the BBGKY hierarchy, we adopt the 'molecular chaos assumption', which postulates the statistical independence of colliding particles in the derivation of the Boltzmann collision integral. This means that the

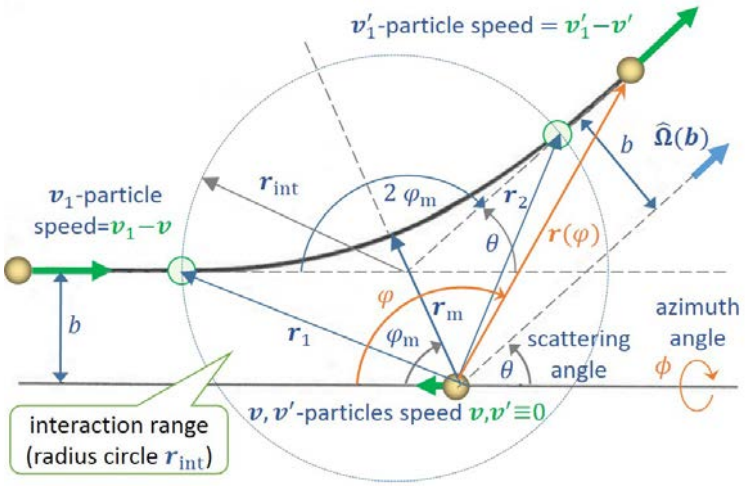

Fig. 5: Particle-pair elastic scattering: the path $\mathbf{r}(\varphi)$ of the $\mathbf{v}_1$-particle of mass m relative to the path of the $\mathbf{v}$-particle of the same mass in a frame where the origin of the $\mathbf{v}$-particle is fixed (equivalent to the centre-of-mass frame, in which the relative velocity of the $\mathbf{v}_1$-particle is $\mathbf{v}_1 - \mathbf{v}$ and that of the $\mathbf{v}$-particle is zero). The position vectors $\mathbf{r}_1$ and $\mathbf{r}_2$ mark the entry and exit points of the $\mathbf{v}_1$-particle into and out of the interaction region; $\mathbf{r}_{\rm int}$ is the interaction circle radius; θ is the scattering angle, which depends on the impact parameter b; and $\mathbf{r}_{\rm m}$ is the position of the $\mathbf{v}_1$-particle when it is at the distance of 'closest approach' from the scatterer (the $\mathbf{v}$-particle). The scattering angle θ is related to φ_m via the rule $\theta + 2\varphi_m = \pi$.

particles are assumed to be uncorrelated outside the effective range of their interaction. Therefore, their trajectories before and after a collision are rectilinear. These constraints justify the above homogeneous property, $\mathbf{r} \equiv \mathbf{r}_1$, of f_2 over the interaction range. Moreover, taking into account short-range interactions as well, the pair density distribution $f_2(\mathbf{r}, \mathbf{v}, \mathbf{r}, \mathbf{v}_1, t)$ can be approximated by the product of two single-particle density distribution functions:

$$f_2(\mathbf{r}, \mathbf{v}, \mathbf{r}, \mathbf{v}_1, t) = f_1(\mathbf{r}, \mathbf{v}, t) f_1(\mathbf{r}, \mathbf{v}_1, t) \,, \tag{32}$$

and similarly for $f_2(\mathbf{r}, \mathbf{v}', \mathbf{r}, \mathbf{v}_1', t)$, where f_2 is evaluated at the same point assuming that $\mathbf{r}' \approx \mathbf{r}$ don't vary on scales of order $\mathbf{r}_{\rm int}$.

For example, in an inter-atomic potential the collision duration $\tau_{\rm c}$ is the time over which two particles are within the effective range $\mathbf{r}_{\rm int}$ of their interaction. For particles of a sufficiently dilute gas (speed $v \approx 10^2\,{\rm m\,s^{-1}}$) with short-range interactions $\mathbf{r}_{\rm int} \approx 10^{-10}\,{\rm m}$ (typically an atomic size under standard conditions), the collision time is $\tau_{\rm c} = \mathbf{r}_{\rm int}/v \approx 10^{-12}\,{\rm s}$. From Figs. 5 and 6 we can see that the initial (relative) velocity $\mathbf{v}_1 - \mathbf{v}$ is transformed to the final velocity $\mathbf{v}_1' - \mathbf{v}'$ through the relationship between the impact parameter b and the scattering and azimuth angles (θ, ϕ). The expression for $\mathbf{v}_1'(\mathbf{b}) = \mathbf{v}_1'(\theta, \phi)$ is obtained by integration of the equations of motion. In elastic collisions, the relative velocity $|\mathbf{v}_1 - \mathbf{v}|$ (or $|\mathbf{v}_1|$) just rotates without changing its magnitude to a final direction $\mathbf{v}_1' - \mathbf{v}'$ (or $\mathbf{v}_1'$) indicated by the angles $(\theta, \phi) \equiv \hat{\mathbf{\Omega}}(b)$ (a unit vector). Equivalently, $|\mathbf{v}_1'| = |\mathbf{v}_1|$ and $\mathbf{v}_1' = |\mathbf{v}_1|\,\hat{\mathbf{\Omega}}(b)$,

Substituting (32) into (30) results in the closed-form Boltzmann equation for f_1, involving integrals and partial derivatives of the distribution function:

$$\frac{{\rm d}f_1(\mathbf{r}, \mathbf{v}, t)}{{\rm d}t} = \int_{(\mathbf{v}_1, b, \phi)} \left[f_1(\mathbf{r}, \mathbf{v}', t) f_1(\mathbf{r}, \mathbf{v}_1', t) - f_1(\mathbf{r}, \mathbf{v}, t) f_1(\mathbf{r}, \mathbf{v}_1, t) \right] {\rm d}^3\mathbf{v}_1 \, |\mathbf{v}_1 - \mathbf{v}| \, b \, {\rm d}b \, {\rm d}\phi \,.$$

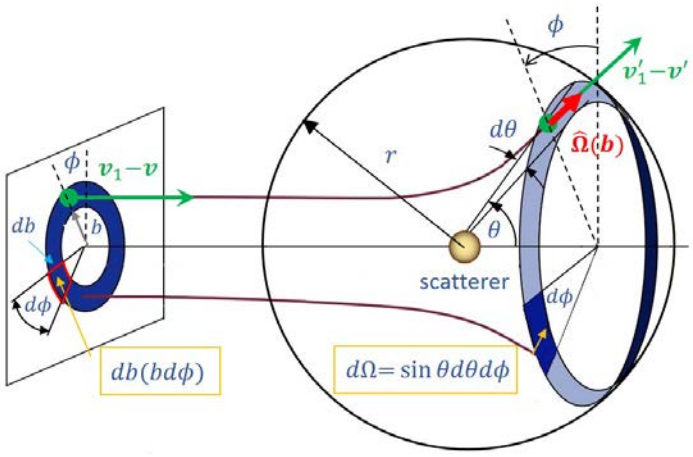

Fig. 6: Particle-pair elastic scattering (different view): particles that hit the small ring (left part of diagram) between impact parameter values b and $b+\mathrm{d}b$ are scattered by an angle between θ and $\theta+\mathrm{d}\theta$ into a larger ring on a sphere (right part of diagram), with a scatterer (the $\mathbf{v}$-particle) at rest in the centre of the sphere (i.e. $\mathbf{v}=\mathbf{v}'=0$). Note that the impact parameter $\mathbf{r}$ is equal to zero for a head-on collision. The incident $\mathbf{v}_1$-particle moves from the left in the direction of the scatterer. As in Fig. 5, the angle θ represents the scattering angle between the $\mathbf{v}_1'$-particle velocity $\mathbf{v}_1'$ and the $\mathbf{v}_1$-particle velocity $\mathbf{v}_1$; ϕ is the azimuth (rotational) angle of $\mathbf{v}_1'-\mathbf{v}'$ about the vertical axis; and $\mathrm{d}\Omega$ is the differential solid angle element of the small area in the large ring of the sphere.

Alternatively, upon expanding the total time-derivative $\mathrm{d}f_1/\mathrm{d}t$,

$$\begin{aligned}&\frac{\partial f_1(\mathbf{r},\mathbf{v},t)}{\partial t}+\mathbf{v}\cdot\nabla_r f_1(\mathbf{r},\mathbf{v},t)+\mathbf{a}\cdot\nabla_v f_1(\mathbf{r},\mathbf{v},t)\\&\quad=\int_{(\mathbf{v}_1,b,\phi)}\left[f_1(\mathbf{r},\mathbf{v}',t)f_1(\mathbf{r},\mathbf{v}_1',t)-f_1(\mathbf{r},\mathbf{v},t)f_1(\mathbf{r},\mathbf{v}_1,t)\right]\mathrm{d}^3\mathbf{v}_1\,|\mathbf{v}_1-\mathbf{v}|\,b\,\mathrm{d}b\,\mathrm{d}\phi\,.\end{aligned}\tag{33}$$

Consider a particle beam of flux (intensity) I (in units of $[\text{particle}/(\text{s m}^2)]$) incident on a scatterer located at the origin. The *differential scattering cross-section* $\sigma(\theta,\phi)$ $[\text{m}^2]$ is defined as the number of particles scattered per second per unit incident flux, at a solid angle oriented in the direction of the outgoing flux after the collision, labelled by the solid angle vector $\hat{\mathbf{\Omega}}$. Geometrically, $\sigma(\theta,\phi)$ can be understood as saying that the number of particles scattered into the solid angle element $\mathrm{d}\Omega$ per unit time is equal to the number of particles crossing an area equal to $\sigma(\theta,\phi)\,\mathrm{d}\Omega$ in the incident beam, as illustrated in Fig. 6, where the differential solid angle element of the small area in the large ring of the sphere is expressed as

$$\begin{aligned}I\sigma(\theta,\phi)\,\mathrm{d}\Omega=\;&\text{number of particles scattered per second into the solid angle element }\mathrm{d}\Omega\\&\text{oriented at }\hat{\mathbf{\Omega}}\text{ with differential solid angle}\\&\mathrm{d}\Omega=r\sin\theta\,\mathrm{d}\phi(r\,\mathrm{d}\theta)/r^2=\sin\theta\,\mathrm{d}\theta\,\mathrm{d}\phi\;\;[\text{rad}^2]\,.\end{aligned}$$

This number of particles is the number traversing the annulus element $b\,\mathrm{d}b\,\mathrm{d}\phi$, so

$$I\sigma(\theta,\phi)\,\mathrm{d}\Omega=Ib\,\mathrm{d}b\,\mathrm{d}\phi\implies\sigma(\theta,\phi)=\frac{b}{\sin\theta}\left|\frac{\mathrm{d}b}{\mathrm{d}\theta}\right|,\tag{34}$$

where the modulus sign is needed because b and θ may change in opposite directions but the cross-section $\sigma(\theta,\phi)$ is always positive. The detailed form of $\sigma(\theta,\phi)$ depends on the inter-particle potential.

Comment: $\sigma(\theta,\phi)$ can depend on the azimuth angle ϕ, but nearly all potentials are spherically symmetric so that $\sigma=\sigma(\theta)$ depends only on θ (or on the impact parameter b). Note that the alternative notation $|\mathrm{d}\sigma/\mathrm{d}\Omega|$ is often used instead of σ for the differential cross-section.

To illustrate the meaning of the differential cross-section with a simple example, consider an elastic collision involving a light point-like particle hitting a heavy hard sphere of radius r. From Fig. 7 it can be seen that the scattering angle θ is linked to the impact parameter through $b = r\sin\varphi_m \equiv r\sin[(\pi-\theta)/2]$, with $b \le r$. The differential cross-section is then calculated from (34) as

$$\begin{aligned}\sigma(\theta,\phi) &= \frac{r}{\sin\theta}\sin\left[\frac{\pi}{2}-\frac{\theta}{2}\right]\left|\frac{\mathrm{d}}{\mathrm{d}\theta}\left(r\sin\left[\frac{\pi}{2}-\frac{\theta}{2}\right]\right)\right| \\ &= \frac{r^2}{2\sin\theta}\sin\left[\frac{\pi}{2}-\frac{\theta}{2}\right]\cos\left[\frac{\pi}{2}-\frac{\theta}{2}\right] \\ &= \frac{r^2}{2\sin\theta}\left(\frac{1}{2}\sin\left[2\left(\frac{\pi}{2}-\frac{\theta}{2}\right)\right]\right) = \frac{r^2}{4\sin\theta}\sin\theta \\ \Longrightarrow\quad \sigma(\theta,\phi) &= \frac{r^2}{4}, \quad \theta = \pi - 2\arcsin\left(\frac{b}{r}\right) . \end{aligned} \tag{35}$$

In this example, the cross-section $\sigma = r^2/4$ does not depend on the scattering angle θ (nor on the azimuth angle ϕ). In particular, $\theta = \pi$ for $b = 0$ (head-on collision) and $\theta = 0$ for $b \ge r$.

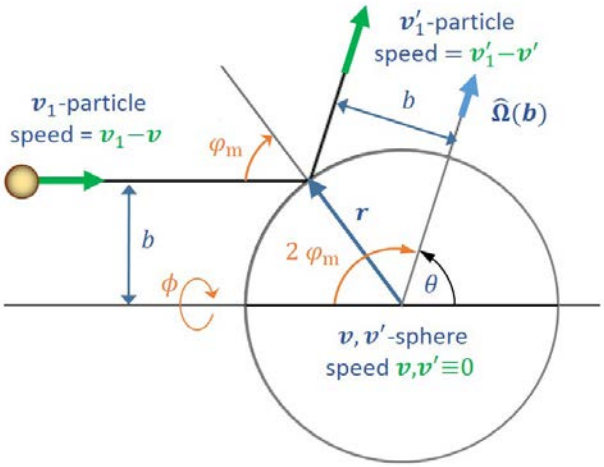

Fig. 7: Tiny elastic particle scattering from a rigid sphere. Irrespective of the impact parameter value $b \le r$, the sphere radius r is equal to the distance of 'closest approach' of the scattering sphere, and $\theta + 2\varphi_m = \pi$.

As another example, illustrated by Figs. 5 and 6, the differential scattering cross-section $\sigma(\theta,\phi)$ for the Coulomb potential $U(r)$ can be cast into the form (see e.g. [9])

$$U(r) = \frac{1}{4\pi\epsilon_0}\frac{e^2}{r}, \quad \sigma(\theta) = \frac{b_0^2}{4\sin^4(\theta/2)}, \quad b_0 = \frac{e^2}{2\pi\epsilon_0 m\,|\mathbf{v}_1-\mathbf{v}|^2} . \tag{36}$$

The equation for the scattering angle in a Coulomb potential can be written as

$$\theta = 2\arctan\left(\frac{b_0}{b}\right) \iff \tan\left(\frac{\theta}{2}\right) = \frac{b_0}{b} . \tag{37}$$

Notice that b_0 is the value of the impact parameter b for a $\pi/2$ scattering angle (not true for relativistic elastic particle collisions). Also, for $b = 0$ we have $\theta = \pi$.

Replacing $b\,\mathrm{d}b\,\mathrm{d}\phi$ by $\sigma(\theta,\phi)\,\mathrm{d}\Omega$ in Eq. (33), we obtain the following expression for the Boltzmann collision integral:

$$\begin{aligned}&\frac{\partial f_1(\mathbf{r},\mathbf{v},t)}{\partial t} + \mathbf{v}\cdot\nabla_r f_1(\mathbf{r},\mathbf{v},t) + \mathbf{a}\cdot\nabla_v f_1(\mathbf{r},\mathbf{v},t) \\ &= \int_{(\mathbf{v}_1,\theta,\phi)} \left[f_1(\mathbf{r},\mathbf{v}',t) f_1(\mathbf{r},\mathbf{v}_1',t) - f_1(\mathbf{r},\mathbf{v},t) f_1(\mathbf{r},\mathbf{v}_1,t)\right] \mathrm{d}^3\mathbf{v}_1\,|\mathbf{v}_1-\mathbf{v}|\,\sigma(\theta,\phi)\,\mathrm{d}\Omega .\end{aligned} \tag{38}$$

The external force $\mathbf{F} = m\mathbf{a}$ may also include the Lorentz force $\mathbf{F} = e(\mathbf{E} + \mathbf{v} \times \mathbf{B})$ due to externally applied fields. If the force is derived from a potential, i.e. $\mathbf{F} = -\nabla_r U(\mathbf{r})$, then (38) can be written in the following form, using $\partial/\partial\mathbf{u} \equiv \nabla_u$ ($\mathbf{u} = \mathbf{r}, \mathbf{v}$):

$$\begin{aligned}&\left[\frac{\partial}{\partial t} + \mathbf{v}\cdot\frac{\partial}{\partial \mathbf{r}} - \frac{1}{m}\frac{\partial U}{\partial \mathbf{r}}\cdot\frac{\partial}{\partial \mathbf{v}}\right] f_1(\mathbf{r},\mathbf{v},t) \\ &\quad = \int_{(\mathbf{v}_1,\,\theta,\,\phi)} \left[f_1(\mathbf{r},\mathbf{v}',t) f_1(\mathbf{r},\mathbf{v}_1',t) - f_1(\mathbf{r},\mathbf{v},t) f_1(\mathbf{r},\mathbf{v}_1,t)\right] \mathrm{d}^3\mathbf{v}_1\, |\mathbf{v}_1 - \mathbf{v}|\, \sigma(\theta,\phi)\, \mathrm{d}\Omega\,.\end{aligned} \tag{39}$$

The Boltzmann equation is a nonlinear integro-differential equation, which is not easy to solve. The terms on the left-hand side of (39) describe the motion of a single particle in an external potential, while the right-hand side consists of the collision terms. The equation can be physically interpreted as meaning that 'the probability of finding a particle of velocity $\mathbf{v}$ at position $\mathbf{r}$ suddenly changes if that particle experiences a collision with another particle of velocity $\mathbf{v}_1$'. The probability of a collision depends on the differential cross-section σ of the incident particle flux, which is proportional to $|\mathbf{v}_1 - \mathbf{v}|$, and on the joint probability of finding the two particles at $\mathbf{r}$ given their velocities, approximated by $f_1(\mathbf{r},\mathbf{v}) f_1(\mathbf{r},\mathbf{v}_1)$.

To summarize, the 'heuristic derivation' of the one-particle Boltzmann equation has required several strong assumptions, namely:

- the two-particle density distribution is homogeneous over the range of interaction;
- molecular chaos, i.e. the velocities of two colliding particles are uncorrelated;
- the range of particle interaction over the mean free path is much smaller than unity;
- the particle trajectories are rectilinear before and after collision.

2.2.1 The Maxwell–Boltzmann distribution

For gas molecules in a closed box, the modelling approach consists of establishing the equation(s) determining the evolution of the particle density function at equilibrium [8, 9, 13]. An *equilibrium* density distribution function is defined as a solution $f_1(\mathbf{r},\mathbf{v})$ of the Boltzmann equation that has no explicit time dependence and so satisfies $\partial f_1(\mathbf{r},\mathbf{v})/\partial t = 0$. Moreover, one assumes the absence of external forces, i.e. $\mathbf{a} = \mathbf{F}/m \equiv 0$, and a uniform particle distribution in space, i.e. $f_1(\mathbf{r},\mathbf{v})$ is homogeneous so that the density distribution is independent of $\mathbf{r}$ and thus $\nabla_r f_1(\mathbf{v}) = 0$. By Eq. (39), this equilibrium distribution function, denoted by $f_1^{\mathrm{eq}}(\mathbf{v})$, satisfies

$$0 = \int_{(\mathbf{v}_1,\,\theta,\,\phi)} \left[f_1^{\mathrm{eq}}(\mathbf{v}') f_1^{\mathrm{eq}}(\mathbf{v}_1') - f_1^{\mathrm{eq}}(\mathbf{v}) f_1^{\mathrm{eq}}(\mathbf{v}_1)\right] \mathrm{d}^3\mathbf{v}_1\, |\mathbf{v}_1 - \mathbf{v}|\, \sigma(\Omega)\, \mathrm{d}\Omega\,, \tag{40}$$

where $\mathbf{v}_1$ is an arbitrary velocity. It follows that $f_1^{\mathrm{eq}}(\mathbf{v})$, known as the *Maxwell–Boltzmann distribution function*, satisfies the condition

$$f_1^{\mathrm{eq}}(\mathbf{v}') f_1^{\mathrm{eq}}(\mathbf{v}_1') - f_1^{\mathrm{eq}}(\mathbf{v}) f_1^{\mathrm{eq}}(\mathbf{v}_1) = 0\,. \tag{41}$$

Taking the logarithm of (41) yields

$$\ln f_1^{\mathrm{eq}}(\mathbf{v}') + \ln f_1^{\mathrm{eq}}(\mathbf{v}_1') = \ln f_1^{\mathrm{eq}}(\mathbf{v}) + \ln f_1^{\mathrm{eq}}(\mathbf{v}_1)\,. \tag{42}$$

This equation is a summation invariant because the doublets $\{\mathbf{v},\mathbf{v}_1\}$ and $\{\mathbf{v}',\mathbf{v}_1'\}$ are the potential 'initial' and 'final' velocities of a particle-pair collision process $\{\mathbf{v},\mathbf{v}_1\} \to \{\mathbf{v}',\mathbf{v}_1'\}$. Thus, $\ln f_1^{\mathrm{eq}}(\mathbf{v})$ can be formulated by linearly mixing the invariants 'mass' m, 'momentum' $m\mathbf{v}$, and 'kinetic energy' $m|\mathbf{v}|^2/2 \equiv m\mathbf{v}^2/2$ with the constants a_0, a_2 and $\mathbf{a}_1 = a_{1,x}\hat{\mathbf{x}} + a_{1,y}\hat{\mathbf{y}} + a_{1,z}\hat{\mathbf{z}}$ in the form

$$\ln f_1^{\mathrm{eq}}(\mathbf{v}) = m\left(a_0 + \mathbf{a}_1\cdot\mathbf{v} - \frac{a_2\mathbf{v}^2}{2}\right), \tag{43}$$

where the minus sign is introduced for later convenience. This equation can be expressed in a compact form by completing the square on its right-hand side using the formula

$$ax^2 + bx + c \equiv a\left(x + \frac{b}{2a}\right)^2 + \left(c - \frac{b^2}{4a}\right) . \tag{44}$$

Letting $x \to \mathbf{v}$, $x^2 \to \mathbf{v}^2$, $a \to -a_0/2$, $b \to \mathbf{a}_1$, $c \to a_0$, the quadratic equation (43) can be written as

$$\begin{aligned}\ln f_1^{\mathrm{eq}}(\mathbf{v}) &= m\left(-\frac{a_2\mathbf{v}^2}{2} + \mathbf{a}_1\cdot\mathbf{v} + a_0\right)\\ &= -\frac{ma_2}{2}\left(\mathbf{v} - \frac{\mathbf{a}_1}{a_2}\right)^2 + m\left(a_0 + \frac{\mathbf{a}_1^2}{2a_2}\right) = -\frac{ma_2}{2}(\mathbf{v}-\mathbf{v}_0)^2 + \ln C\,,\end{aligned} \tag{45}$$

where the extra constants $\ln C = m(a_0 + \mathbf{a}_1^2/(2a_2))$ and $\mathbf{v}_0 = \mathbf{a}_1/a_2$ have been introduced to simplify the expression. Taking the exponential of $\ln f_1^{\mathrm{eq}}$ gives

$$f_1^{\mathrm{eq}}(\mathbf{v}) = C\exp\left[-\frac{1}{2}ma_2(\mathbf{v}-\mathbf{v}_0)^2\right] , \tag{46}$$

which is the Maxwell–Boltzmann equilibrium distribution function. Equation (46) contains five constant coefficients to be determined, namely C, a_2 and the three components of $\mathbf{v}_0 = v_{0,x}\hat{\mathbf{x}} + v_{0,y}\hat{\mathbf{y}} + v_{0,z}\hat{\mathbf{z}}$. These constants can be deduced from observable physical properties of the system, such as the particle density n, the average velocity $\langle\mathbf{v}\rangle$, the temperature T and the average kinetic energy $\langle m\mathbf{v}^2/2\rangle$.

For a uniformly distributed system of N particles enclosed in a box of volume V (i.e. f_1^{eq} is independent of $\mathbf{r}$), the particle density n is constant and is expressed according to the following normalization conditions:

$$N = \int_{\mathbf{v}} f_1^{\mathrm{eq}}(\mathbf{v})\,\mathrm{d}^3\mathbf{r}\,\mathrm{d}^3\mathbf{v}, \qquad n = \frac{N}{V} = \int_{\mathbf{v}} f_1^{\mathrm{eq}}(\mathbf{v})\,\mathrm{d}^3\mathbf{v}. \tag{47}$$

Performing the change of variables $\mathbf{w} = \mathbf{v} - \mathbf{v}_0$ with $\mathbf{w} = w_x\hat{\mathbf{x}} + w_y\hat{\mathbf{y}} + w_z\hat{\mathbf{z}}$, we find that

$$\begin{aligned} n &\equiv C\int_{\mathbf{w}} \exp\left[-\frac{1}{2}ma_2\mathbf{w}^2\right]\mathrm{d}^3\mathbf{w}\\ &= C\int_{-\infty}^{+\infty}\!\!\!\iiint \exp\left[-\frac{1}{2}ma_2(w_x^2+w_y^2+w_z^2)\right]\mathrm{d}w_x\,\mathrm{d}w_y\,\mathrm{d}w_z = C\left(\frac{2\pi}{ma_2}\right)^{3/2} ,\end{aligned} \tag{48}$$

so that C is determined as a function of the constant a_2,

$$C = n\left(\frac{ma_2}{2\pi}\right)^{3/2} . \tag{49}$$

Using (49) and $\mathbf{v} = \mathbf{w} + \mathbf{v}_0$, the average velocity $\langle\mathbf{v}\rangle$ is similarly evaluated as

$$\begin{aligned}\langle\mathbf{v}\rangle &= \frac{\int_{\mathbf{v}}\mathbf{v}f_1^{\mathrm{eq}}(\mathbf{v})\,\mathrm{d}^3\mathbf{v}}{\int_{\mathbf{v}} f_1^{\mathrm{eq}}(\mathbf{v})\,\mathrm{d}^3\mathbf{v}} = \left(\frac{ma_2}{2\pi}\right)^{3/2}\int_{\mathbf{v}}\mathbf{v}\exp\left[-\frac{1}{2}ma_2(\mathbf{v}-\mathbf{v}_0)^2\right]\mathrm{d}^3\mathbf{v}\\ &= \left(\frac{ma_2}{2\pi}\right)^{3/2}\int_{\mathbf{w}}\mathbf{w}\exp\left[-\frac{1}{2}ma_2\mathbf{w}^2\right]\mathrm{d}^3\mathbf{w} + \frac{C}{n}\mathbf{v}_0\int_{\mathbf{w}}\exp\left[-\frac{1}{2}ma_2\mathbf{w}^2\right]\mathrm{d}^3\mathbf{w}\\ &= \left(\frac{ma_2}{2\pi}\right)^{3/2}\int_{-\infty}^{+\infty}\!\!\!\iiint (w_x\hat{\mathbf{x}} + w_y\hat{\mathbf{y}} + w_z\hat{\mathbf{z}})\exp\left[-\frac{1}{2}ma_2\left(w_x^2+w_y^2+w_z^2\right)\right]\mathrm{d}w_x\,\mathrm{d}w_y\,\mathrm{d}w_z\end{aligned}$$

$$+\left(\frac{ma_2}{2\pi}\right)^{3/2}\mathbf{v}_0\iiint_{-\infty}^{+\infty}\exp\left[-\frac{1}{2}ma_2\left(w_x^2+w_y^2+w_z^2\right)\right]\mathrm{d}w_x\,\mathrm{d}w_y\,\mathrm{d}w_z \tag{50}$$

$$=\left(\frac{ma_2}{2\pi}\right)^{3/2}\mathbf{v}_0\left(\frac{2\pi}{ma_2}\right)^{3/2}=\mathbf{v}_0\ ,$$

where we have used the fact that the integrand $\mathbf{w}\exp[-(ma_2/2)\mathbf{w}^2]$ in (50) is an odd function of $\mathbf{w}$ so that this integral is equal to zero. Therefore

$$\mathbf{v}_0=\langle\mathbf{v}\rangle.$$

This shows that the constant $\mathbf{v}_0$ represents the mean particle velocity $\langle\mathbf{v}\rangle$. Indeed, for a stationary box containing N gas particles moving at random, there is evidently no particle translational motion as a whole, so $\mathbf{v}_0\equiv 0$.

Finally, let us calculate the average kinetic energy $\langle m\mathbf{v}^2/2\rangle$ where the 'overall particle drift' $\mathbf{v}_0$ is set to zero for convenience (i.e. there is no global particle translational motion). Symmetry considerations suggest that

$$\langle v_x^2\rangle=\langle v_y^2\rangle=\langle v_x^2\rangle\implies\langle\mathbf{v}^2\rangle\equiv\langle v_x^2+v_y^2+v_z^2\rangle=3\langle v_x^2\rangle,$$

so it suffices to compute $\langle v_x^2\rangle$ to obtain $\langle\mathbf{v}^2\rangle$. Using (49),

$$\left\langle\frac{1}{2}m\mathbf{v}^2\right\rangle=\frac{\int_{\mathbf{v}}\frac{m}{2}\mathbf{v}^2f_1^{\mathrm{eq}}(\mathbf{v})\,\mathrm{d}^3\mathbf{v}}{\int_{\mathbf{v}}f_1^{\mathrm{eq}}(\mathbf{v})\,\mathrm{d}^3\mathbf{v}}=\left(\frac{ma_2}{2\pi}\right)^{3/2}\int_{\mathbf{v}}\frac{m\mathbf{v}^2}{2}\exp\left[-\frac{1}{2}ma_2\mathbf{v}^2\right]\mathrm{d}^3\mathbf{v}$$

$$=\frac{1}{2}\left(\frac{ma_2}{2\pi}\right)^{3/2}m\iiint_{-\infty}^{+\infty}\left(v_x^2+v_y^2+v_z^2\right)\exp\left[-\frac{ma_2}{2}\left(v_x^2+v_y^2+v_z^2\right)\right]\mathrm{d}v_x\,\mathrm{d}v_y\,\mathrm{d}v_z$$

$$=\frac{1}{2}\left(\frac{ma_2}{2\pi}\right)^{3/2}m\iiint_{-\infty}^{+\infty}3v_x^2\exp\left[-\frac{ma_2}{2}\left(v_x^2+v_y^2+v_z^2\right)\right]\mathrm{d}v_x\,\mathrm{d}v_y\,\mathrm{d}v_z$$

$$=\frac{3}{2}\left(\frac{ma_2}{2\pi}\right)^{3/2}m\int_{-\infty}^{+\infty}v_x^2\exp\left[-\frac{ma_2}{2}v_x^2\right]\mathrm{d}v_x$$

$$\times\int_{-\infty}^{+\infty}\exp\left[-\frac{ma_2}{2}v_y^2\right]\mathrm{d}v_y\int_{-\infty}^{+\infty}\exp\left[-\frac{ma_2}{2}v_z^2\right]\mathrm{d}v_z$$

$$=\frac{3}{2}\left(\frac{ma_2}{2\pi}\right)^{1/2}m\int_{-\infty}^{+\infty}v_x^2\exp\left[-\frac{ma_2}{2}v_x^2\right]\mathrm{d}v_x=\frac{3}{2a_2}\ . \tag{51}$$

To quantify the constant a_2, we need to introduce some 'physics'. We use the thermodynamic definition of temperature T, 'experimentally' related to the particle kinetic energy via

$$\frac{3}{2}kT=\left\langle\frac{1}{2}m\mathbf{v}^2\right\rangle\equiv\frac{3}{2a_2}\implies a_2=\frac{1}{kT}\implies C=n\left(\frac{m}{2\pi kT}\right)^{3/2}\ , \tag{52}$$

where k is the Boltzmann constant. Substituting the constants C and a_2 into Eq. (46) and reinserting the overall particle drift constant $\mathbf{v}_0$ for completeness, the equilibrium distribution function $f_1^{\mathrm{eq}}(\mathbf{v})$ in the absence of external forcing becomes

$$f_1^{\mathrm{eq}}(\mathbf{v})=\frac{n}{(2\pi kT/m)^{3/2}}\exp\left[-\frac{m}{2kT}(\mathbf{v}-\mathbf{v}_0)^2\right]\ . \tag{53}$$

3 Intrabeam scattering

3.1 Particle-pair collisions

Intrabeam scattering (IBS), the scattering of particles within a beam, belongs to the category of processes not governed by Liouville's theorem. Other such processes include scattering on residual gas in particle accelerators and storage rings, which leads to a continuous rise in normalized emittance. A related phenomenon is the cooling of one beam by another mixed with it and travelling at the same velocity (e.g. the electron cooling of antiproton beams [15]). A characteristic feature of IBS is the rise time or damping time of the beam dimensions. In some situations IBS leads to the redistribution of partial beam emittances, which can cause undesirable beam dilution in phase space or could heat the beam as a whole (i.e. it may increase the partial beam emittances simultaneously).

Here, we follow the ingenious approach of Ya. S. Derbenev [16] and A. H. Sørensen [17] to studying the self-blowing and damping of a relativistic stored bunch caused by particle-pair collisions. In this process, the scattering between particles induces an energy exchange between transverse and longitudinal motions. Small transverse momenta are transformed into amplified longitudinal fluctuations due to the relativistic Lorentz factor in the transformation.

Comment: If the longitudinal momenta acquired during a single particle-pair collision exceed the momentum acceptance of the RF bucket that keeps the beam bunched, or if the particles hit the aperture when displaced by dispersion, the particles will get lost. This process, referred to as the *Touschek effect*, results in a finite lifetime for a bunched beam.

In greater detail, let us consider a 'simple' Coulomb collision model involving two particles (labelled 1 and 2) with initially *equal* and *opposite* momenta, $\mathbf{p}_{x_{1,2}} = \pm|\mathbf{p}_x|\hat{\mathbf{x}}$. As a result of the $\pi/2$ scattering angle, the two momenta completely transfer into longitudinal momenta (along the s-axis) parallel to the circulating beam. Equilibrium beam conditions at energies below and above the ring transition energy are assessed. In the 'laboratory frame', the transverse components of the two momenta remain unchanged from their 'beam frame' values.

The two opposite post-collision longitudinal momentum components, written as $\Delta\mathbf{p}'_{\|_{1,2}} = \pm\Delta\mathbf{p}'_{\|}$, represent the departures from the beam average momentum $\mathbf{p}_0 = |\mathbf{p}_0|\hat{\mathbf{s}} = \gamma m\mathbf{v}_0$ (in the beam frame $\bar{\mathbf{p}}_0 = |\bar{\mathbf{p}}_0|\hat{\mathbf{s}} = 0$). Viewed in the laboratory frame, $\Delta\mathbf{p}'_{\|_1}$ and $\Delta\mathbf{p}'_{\|_2}$ are both larger by a Lorentz factor $\gamma = (1 - \mathbf{v}_0^2/c^2)^{-1/2}$ than their transverse momentum components before the collision. The factor γ is related to the average beam relativistic energy $E = \gamma mc^2$ and momentum $\mathbf{p}_0 = \gamma m\mathbf{v}_0$, as shown in Fig. 8 (see also [16] and [18]). The following equation expresses the preservation of the sum of the squared momenta in the beam frame after the collision:

$$|\bar{\mathbf{p}}_{\perp_1}|^2 + |\bar{\mathbf{p}}_{\perp_2}|^2 = |\bar{\mathbf{p}}'_{\|_1}|^2 + |\bar{\mathbf{p}}'_{\|_2}|^2 \,.$$

Observe that the momentum deviations in (8) are defined in the two frames (with $|\mathbf{p}_x| = |\bar{\mathbf{p}}_x| = p_x$) as

$$\begin{aligned}
&\text{Beam frame } (\bar{\mathbf{p}}_0 = |\bar{\mathbf{p}}_0|\hat{\mathbf{s}} \stackrel{\text{def}}{=} 0): \quad && \bar{\mathbf{p}}_{\perp_{1,2}} = \bar{\mathbf{p}}_{x_{1,2}} = \mp|\bar{\mathbf{p}}_x|\hat{\mathbf{x}}\,, \\
& && \bar{\mathbf{p}}'_{\|_{1,2}} = \bar{\mathbf{p}}'_{s_{1,2}} = \pm|\bar{\mathbf{p}}_x|\hat{\mathbf{s}}\,; \\
&\text{Laboratory frame } (\mathbf{p}_0 = \gamma m\mathbf{v}_0): \quad && \Delta\mathbf{p}_{\perp_{1,2}} \stackrel{\text{def}}{=} \mathbf{p}_{\perp_{1,2}} = \mathbf{p}_{s_{1,2}} = \mp|\mathbf{p}_x|\hat{\mathbf{x}}\,, \\
& && \Delta\mathbf{p}'_{\|_{1,2}} \stackrel{\text{def}}{=} \mathbf{p}'_{\|_{1,2}} = \mathbf{p}'_{s_{1,2}} = \pm\gamma|\mathbf{p}_x|\hat{\mathbf{s}}\,.
\end{aligned} \tag{54}$$

The horizontal single-particle emittance relates to the Courant–Snyder invariant (see Eq. (6)), where α_x, β_x and γ_x are the Twiss parameters of the lattice, D_x is the momentum dispersion function and $x' = |\mathbf{p}_x|/|\mathbf{p}_0| = p_x/p_0$:

$$\varepsilon_x = \gamma_x x_\beta^2 + 2\alpha_x x_\beta x'_\beta + \beta_x x'^2_\beta = \frac{1+\alpha_x^2}{\beta_x} x_\beta^2 - \beta'_x x_\beta x'_\beta + \beta_x x'^2_\beta \,, \qquad x_\beta = x - D_x\frac{\Delta p}{p_0} \,. \tag{55}$$

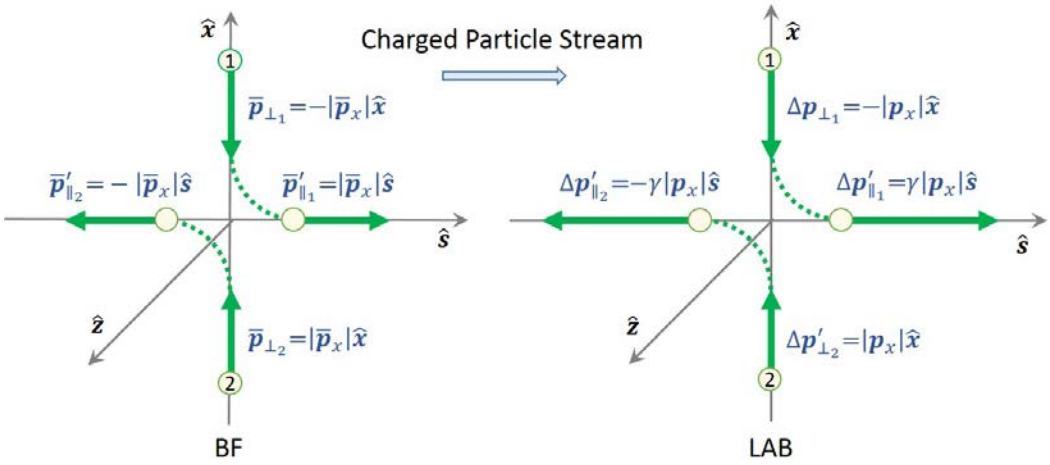

Fig. 8: Particle-pair elastic Coulomb scattering between two particles with momenta $\mathbf{p}_{x,1,2} \equiv \mathbf{p}_{\perp,1,2}$ before collision when viewed in the laboratory frame (LAB), or $\bar{\mathbf{p}}_{\perp,1,2}$ if viewed in the beam frame (BF). After collision the particles' initial momenta become longitudinal, $\pm\mathbf{p}'_{\parallel,1,2}$. A bar on top of a momentum indicates the beam frame, and a prime denotes momentum after collision. The post-collision momenta $\Delta\mathbf{p}'_{\parallel_{1,2}}$ are just the momentum deviations from the average velocity $\mathbf{p}_0$ of the particle stream.

Now, neglecting the derivatives of the lattice parameters β_x and D_x yields $\beta'_x = D'_x = 0$, and the emittance reduces to

$$\varepsilon_x = \frac{1}{\beta_x}\left(x_\beta^2 + \beta_x^2 x_\beta'^2\right) . \tag{56}$$

Assume that the particle interaction point $x \equiv x_{1,2}$ stays constant during the collision time and that the scattering angles $x'_{1,2} = p_{x_{1,2}}/|\mathbf{p}_0|$ vary instantaneously with the momentum change. Then, the kinematic picture of the particle collision can be cast in terms of the betatron amplitude x_β and its derivative x'_β as follows:

$$\begin{aligned} &\text{Before collision:} \quad x_{\beta_{1,2}} \equiv x, && x'_{\beta_{1,2}} = \frac{p_{x_{1,2}}}{p_0} = \pm\frac{p_x}{p_0}. \\ &\text{After collision:} \quad x_{\beta_{1,2}} \equiv x_{1,2} - D_x\frac{\Delta p}{p_0} = x \mp D_x\gamma\frac{p_x}{p_0}, && x'_{1,2} = x'_{\beta_{1,2}} = 0 . \end{aligned} \tag{57}$$

In the above we have used the relations

$$\Delta\mathbf{p}'_{s_{1,2}} = \Delta\mathbf{p}'_{\parallel_{1,2}} = \pm\gamma|\mathbf{p}_{\perp_{1,2}}|\hat{\mathbf{x}} = \pm\gamma|\mathbf{p}_{x_{1,2}}|\hat{\mathbf{x}} = \pm\gamma|\mathbf{p}_x|\hat{\mathbf{x}}, \tag{58}$$

$$D_x\frac{|\Delta\mathbf{p}'_{s_{1,2}}|}{|\mathbf{p}_0|} = \pm\gamma D_x\frac{|\mathbf{p}_x|}{|\mathbf{p}_0|} . \tag{59}$$

Using Eqs. (55)–(59), we can evaluate the change in the sum of emittances of the two colliding particles:

$$\begin{aligned} \beta_x\Delta(\varepsilon_{x_1} + \varepsilon_{x_2}) = \Delta\varepsilon_{x_1} + \Delta\varepsilon_{x_2} &= \left(\varepsilon_{x_1}^{\text{aftcoll}} - \varepsilon_{x_1}^{\text{befcoll}}\right) + \left(\varepsilon_{x_2}^{\text{aftcoll}} - \varepsilon_{x_2}^{\text{befcoll}}\right) \\ &= \left\{\left[\left(x_1 - D_x\gamma\frac{p_{x_1}}{p_0}\right)^2 + 0\right] - \left[x_1^2 + \beta_x^2\left(\frac{p_{x_1}}{p_0}\right)^2\right]\right\} \\ &\quad + \left\{\left[\left(x_2 - D_x\gamma\frac{p_{x_2}}{p_0}\right)^2 + 0\right] - \left[x_2^2 + \beta_x^2\left(\frac{p_{x_2}}{p_0}\right)^2\right]\right\} \end{aligned}$$

$$
\begin{aligned}
&= \left\{ \left[\left(x - D_x \gamma \frac{p_x}{p_0} \right)^2 \right] - \left[x^2 + \beta_x^2 \left(\frac{p_x}{p_0} \right)^2 \right] \right\} \\
&\quad + \left\{ \left[\left(x + D_x \gamma \frac{p_x}{p_0} \right)^2 \right] - \left[x_2^2 + \beta_x^2 \left(-\frac{p_x}{p_0} \right)^2 \right] \right\} \\
&= \left\{ -2x D_x \gamma \frac{p_x}{p_0} + \left(\frac{p_x}{p_0} \right)^2 \left(D_x^2 \gamma^2 - \beta_x^2 \right) \right\} \\
&\quad + \left\{ 2x D_x \gamma \frac{p_x}{p_0} + \left(\frac{p_x}{p_0} \right)^2 \left(D_x^2 \gamma^2 - \beta_x^2 \right) \right\} \\
&= 2 \left(\frac{p_x}{p_0} \right)^2 \left(D_x^2 \gamma^2 - \beta_x^2 \right) , \qquad (60)
\end{aligned}
$$

where $x_1 = x_2 \equiv x$ and $\Delta(\varepsilon_{x_1} + \varepsilon_{x_2})$ symbolically represents the sum of the two particles' emittance variations before and after the collision. Hence

$$
\Delta(\varepsilon_{x_1} + \varepsilon_{x_2}) = \frac{2}{\beta_x} \left(\frac{p_x}{p_0} \right)^2 \left(D_x^2 \gamma^2 - \beta_x^2 \right) = 2 \beta_x \gamma^2 \left(\frac{p_x}{p_0} \right)^2 \left(\frac{D_x^2}{\beta_x^2} - \frac{1}{\gamma^2} \right) . \qquad (61)
$$

The following approximations for the betatron and momentum dispersion functions, referred to as the *smooth focusing approximation*, can be written in the form

$$
\langle \beta_x \rangle \approx \frac{R}{Q_x}, \quad \langle D_x \rangle \approx \frac{\langle \beta_x \rangle}{Q_x} \quad \Longrightarrow \quad \frac{D_x^2}{\beta_x^2} \approx \frac{\langle D_x \rangle^2}{\langle \beta_x \rangle^2} \approx \frac{1}{Q_x^2} . \qquad (62)
$$

Here, R is the mean ring radius and Q_x is the horizontal tune. Introducing the *momentum compaction factor* α_p with associated *transition energy* $\gamma_t mc^2$ and *slip factor* η_t, plus ring curvature radius ρ, we get (see e.g. [18, 19])

$$
\begin{gathered}
\gamma_t \overset{\text{def}}{=} \frac{1}{\sqrt{\alpha_p}}, \qquad \eta_t \overset{\text{def}}{=} \frac{1}{\gamma_t^2} - \frac{1}{\gamma^2}, \\
\alpha_p = \frac{1}{2\pi R} \oint \frac{D_x(s)}{\rho(s)} \, \mathrm{d}s = \left\langle \frac{D_x(s)}{\rho(s)} \right\rangle = \frac{1}{\gamma_t^2} \quad \Longrightarrow \quad \left\langle \frac{D_x(s)}{\rho(s)} \right\rangle \approx \frac{\langle D_x \rangle}{R} \approx \frac{1}{Q_x^2} \approx \frac{1}{\gamma_t^2} . \qquad (63)
\end{gathered}
$$

Note that the contribution to the integral in (63) vanishes in the straight section of the lattice where $\rho(s) \to \infty$. The transition energy is therefore the energy for which the slip factor vanishes. Combining Eq. (61) with the smooth approximations (62) and (63), the change in the sum of the particle emittances becomes

$$
\begin{aligned}
\Delta(\varepsilon_{x_1} + \varepsilon_{x_2}) &= 2 \beta_x \gamma^2 \left(\frac{p_x}{p_0} \right)^2 \left(\frac{\langle D_x \rangle^2}{\langle \beta_x \rangle^2} - \frac{1}{\gamma^2} \right) = 2 \beta_x \gamma^2 \left(\frac{p_x}{p_0} \right)^2 \left(\frac{1}{\gamma_t^2} - \frac{1}{\gamma^2} \right) \\
&= 2 \beta_x \gamma^2 \left(\frac{p_x}{p_0} \right)^2 \eta_t . \qquad (64)
\end{aligned}
$$

In summary:

- Above the transition ($\gamma > \gamma_t$, $\eta_t > 0$): the collisions lead to increased oscillation amplitudes, giving rise to horizontal emittance growth, so that the beam cannot reach an equilibrium.
- Below the transition ($\gamma < \gamma_t$, $\eta_t < 0$): the collisions lead to decreased oscillation amplitudes, giving rise to horizontal emittance reduction, and so a beam equilibrium can exist.

3.2 The original Piwinski IBS model

3.2.1 Introduction

Intrabeam scattering in *weak-focusing* or *smooth ring* lattices can be related to scattering of gas molecules in a closed box, where the walls behave like quadrupole focusing forces and the RF voltage keeps the particles together. The scattering of the molecules leads to the Maxwell–Boltzmann distribution (53) of the three velocity components (v_x, v_z, v_s), where m is the molecule mass, T the temperature, k the Boltzmann's constant, n the volume density of the gas and f_1 the density distribution

$$f_1(v_x, v_z, v_s) = \frac{1}{(2\pi kT/m)^{3/2}} \exp\left[-m(v_x^2 + v_z^2 + v_s^2)/(2kT)\right] \ . \tag{65}$$

The original coordinates $\mathbf{v} = v_x\hat{\mathbf{x}} + v_y\hat{\mathbf{y}} + v_z\hat{\mathbf{z}}$ of Eq. (53) have been transformed to the curvilinear coordinate system $v_x\hat{\mathbf{x}} + v_z\hat{\mathbf{z}} + v_s\hat{\mathbf{s}}$, often used to describe particle motion in synchrotrons, where s is the arc length along the reference orbit. The difference between IBS and scattering of gas molecules enclosed in a box is due to the curvature of the ring orbit.

Orbit curvature

- The curvature of the reference orbit produces a *dispersion*, so that a sudden change of energy will change the betatron amplitudes and initiate a *synchro-betatron* oscillation coupling.
- The curvature also gives rise to the *negative mass instability*; that is, when a particle accelerates above transition it becomes slower and behaves like a particle with negative mass, and so an equilibrium of particles above the transition energy cannot exist. Additional comment: In a particle accelerator the *transition energy* $\gamma_t^2 mc^2$ is attained once $\gamma^2 = \gamma_t^2 \equiv \alpha_p^{-1} = (\mathrm{d}p/p)/(\mathrm{d}R/R)$, where the last term of this formula is the ratio of the relative momentum change to the relative orbit radius change.

Above transition

- The IBS effect is to increase the three bunch dimensions; that is, there is a continuous emittance increase in both the transverse and the longitudinal directions.
- For instance, in the LHC at 7 TeV, although $\gamma = 7461 \gg \gamma_t \approx 53.8$ ($\eta_t \approx 3.4{\times}10^{-4}$), the undesirable growth of the bunch emittances caused by IBS is counterbalanced by the *synchrotron radiation damping* effect.

Below transition

- An equilibrium particle distribution between the partial transverse and longitudinal emittances can exist, provided the conditions for the *smooth focusing approximation* hold, i.e. for weak-focusing accelerators and storage rings or for sufficiently smooth lattices. If these conditions do not hold, an equilibrium particle distribution may not exist.
- For example, in the strong-focusing compact ring ELENA, to decelerate at 100 keV and cool the antiprotons sent by the Antiproton Decelerator to give dense beams, a redistribution of partial emittances due to IBS is anticipated, even though $\gamma \approx 1.0 \ll \gamma_t \approx 1.9$ ($\eta_t \approx -0.72$).

3.2.2 Core intrabeam scattering model

The mathematics of IBS is rather complicated. Calculation of the growth rates in each degree of freedom involves integration and averaging procedures that cannot be undertaken entirely analytically and may need to be finished by computer. At present, various IBS computer codes are available which implement the different models developed so far. The inputs are the lattice parameters of the accelerator or storage ring (Twiss parameters, momentum dispersion function and its derivative, etc.) and the beam characteristics (e.g. bunched or coasting beam, number of circulating particles, momentum spread and emittances).

The main outputs are the rise/damping times (or growth/damping rates) for the horizontal, vertical and longitudinal emittances and the momentum spread.

Here we follow the approach of A. Piwinski [1,20] to work out in some detail the growth or decay rates of the beam dimensions due to the IBS effect. The strategy can be outlined in six steps as follows.

Step 1: Transform the momenta of the two colliding particles from the laboratory frame to the beam frame.

Step 2: Calculate the changes in momenta due to an elastic collision.

Step 3: Transform the momenta back to the laboratory frame.

Step 4: Relate the changes in momenta to changes in transverse and longitudinal emittances.

Step 5: Average over the scattering angle distribution using the classical Rutherford cross-section.

Step 6: Average over the distributions of the particle momenta and positions within a bunch.

Steps* 1–3: *Momentum kinematics

In line with Piwinski's approach, the relative momentum changes $\delta\mathbf{p}_{1,2}/|\mathbf{p}|$ from the average particle momentum $\mathbf{p}$ after a collision between two particles (labelled 1 and 2) can be obtained from the first three steps listed above (which is a fairly lengthy task). For brevity, we will omit some details of the calculations.

First of all, the partial longitudinal, horizontal and vertical particle momenta $(p_{s_{1,2}}, p_{x_{1,2}}, p_{z_{1,2}})$ before the collision can be represented in the (s, x, z) coordinate system of the laboratory (or rest) frame (LAB) attached to the reference orbit of the storage ring (supposing that $p_{s_{1,2}} \approx p_{1,2}$):

$$\mathbf{p}_{1,2} = p_{s_{1,2}}\hat{\mathbf{s}} + p_{x_{1,2}}\hat{\mathbf{x}} + p_{z_{1,2}}\hat{\mathbf{z}} = p_{s_{1,2}}\big(\hat{\mathbf{s}} + x'_{1,2}\hat{\mathbf{x}} + z'_{1,2}\hat{\mathbf{z}}\big) \approx p_{1,2}\big(\hat{\mathbf{s}} + x'_{1,2}\hat{\mathbf{x}} + z'_{1,2}\hat{\mathbf{z}}\big)\ , \tag{66}$$

where $x'_{1,2} = p_{x_{1,2}}/p_{s_{1,2}}$ and $z'_{1,2} = p_{z_{1,2}}/p_{s_{1,2}}$ are the betatron angles and $\hat{\mathbf{s}}$, $\hat{\mathbf{x}}$ and $\hat{\mathbf{z}}$ are unit vectors parallel to the s, x and z coordinate axes. Then, an extra coordinate system with axes (u, v, w) oriented along the unit vectors $(\hat{\mathbf{u}}, \hat{\mathbf{v}}, \hat{\mathbf{z}})$ is defined in the LAB frame for an ensuing Lorentz transformation parallel to $\mathbf{p}_1 + \mathbf{p}_2$ longitudinally, to $\mathbf{p}_1 \times \mathbf{p}_2$ horizontally and to $(\mathbf{p}_1 + \mathbf{p}_2) \times (\mathbf{p}_1 \times \mathbf{p}_2)$ vertically:

$$\hat{\mathbf{u}} = \frac{\mathbf{p}_1 + \mathbf{p}_2}{|\mathbf{p}_1 + \mathbf{p}_2|}, \quad \hat{\mathbf{v}} = \frac{\mathbf{p}_1 \times \mathbf{p}_2}{|\mathbf{p}_1 \times \mathbf{p}_2|}, \quad \hat{\mathbf{w}} = \hat{\mathbf{u}} \times \hat{\mathbf{v}}\ . \tag{67}$$

The particle momenta can then be represented in this coordinate system as

$$\mathbf{p}_{1,2} = p_{s_{1,2}}\big(\cos\alpha_{1,2}\hat{\mathbf{u}} + 0\,\hat{\mathbf{v}} \pm \sin\alpha_{1,2}\hat{\mathbf{w}}\big) \approx p_{1,2}\big(\cos\alpha_{1,2}\hat{\mathbf{u}} + 0\,\hat{\mathbf{v}} \pm \sin\alpha_{1,2}\hat{\mathbf{w}}\big)\ , \tag{68}$$

where $\alpha_{1,2}$ are the angles between the vectors $\mathbf{p}_1 + \mathbf{p}_2$ and $\mathbf{p}_{1,2}$ (see Fig. 9).

Comment: ***Momentum-Energy Lorentz Transformation.*** Let a particle moving at velocity $V_u\hat{\mathbf{u}} \stackrel{\text{def}}{=} \beta_u c\,\hat{\mathbf{u}}$ along the u-axis in the LAB frame (u, v) and at $\bar{V}_u\hat{\bar{\mathbf{u}}} \stackrel{\text{def}}{=} \bar{\beta}_u c\,\hat{\bar{\mathbf{u}}}$ in the CM frame $(\bar{u}, \bar{v})$ (overbars refer to the CM system). The relative velocity parallel to the u-axis between the two inertial frames is denoted $V_r\hat{\mathbf{u}} \stackrel{\text{def}}{=} \beta_r c\,\hat{\mathbf{u}}$. The subscript on the β's and γ's mean $\beta(V_u), \gamma(V_u)$ or $\beta(V_r), \gamma(V_r)$ (the relative frame 'velocity' $V_r\hat{\mathbf{u}}$). The total energy and momentum in the LAB frame are $E = m\gamma_u c^2$ and $p_u = m\gamma_u\beta_u c \equiv E\beta_u/c$, with $\gamma_u = \big(1-\beta_u^2\big)^{-1/2}$. The factor $\bar{\gamma}_u$ stated in term of γ_u and γ_r is needful to compute energy $\bar{E} = m\gamma_{\bar{u}}c^2$ and momentum $\bar{p}_u = m\gamma_{\bar{u}}\beta_{\bar{u}}c$. Using the formula for the additions of velocities $\bar{\beta}_u = (\beta_u - \beta_r)/(1-\beta_u\beta_r)$, we compute $\gamma_{\bar{u}} = \gamma_u\gamma_r(1-\beta_u\beta_r)$. So, the Lorentz transformations from the LAB to the CM frame (and vice versa) on the u- and v-directions $V_v\hat{\mathbf{v}} \stackrel{\text{def}}{=} \beta_v c\,\hat{\mathbf{v}}$ are (cf. [21]):

$$\{\bar{p}_u = \gamma_{\rm r}(p_u - \beta_{\rm r}E/c), \bar{E}/c = \gamma_{\rm r}(E/c - \beta_{\rm r}\,p_u)\}, \quad \{p_u = (\gamma_{\rm r}\,\bar{p}_u + \beta_{\rm r}\bar{E}/c), E/c = \gamma_{\rm r}(\bar{E}/c - \beta_{\rm r}\,\bar{p}_u)\}$$
$$\{\bar{p}_v = p_v, \bar{E}/c = E/c\}, \quad \{p_v = \bar{p}_v, E/c = \bar{E}/c\}$$

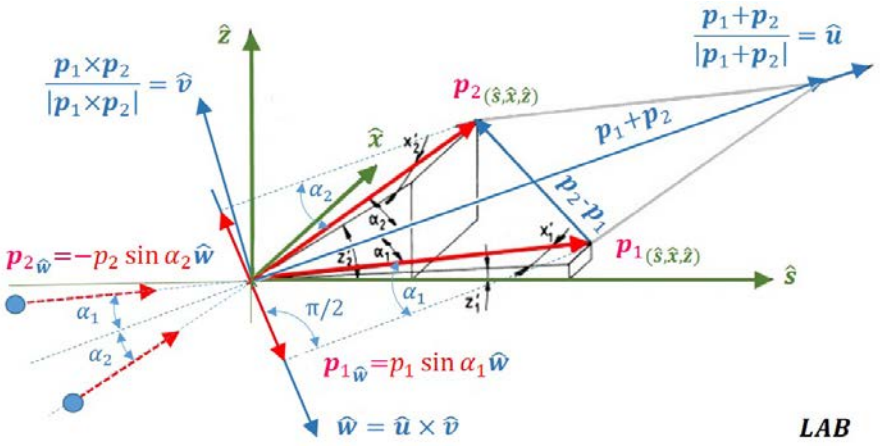

Fig. 9: Relationship between the rest coordinate system $(\hat{\mathbf{s}},\hat{\mathbf{x}},\hat{\mathbf{z}})$ (i.e. LAB frame) and the overlaid $(\hat{\mathbf{u}},\hat{\mathbf{v}},\hat{\mathbf{w}})$ coordinate system aligned on the centre-of-mass motion. Geometrically we have $\mathbf{p}_{1_{\hat{\mathbf{w}}},2_{\hat{\mathbf{w}}}}=\pm p_{1,2}\sin\alpha_{1,2}\hat{\mathbf{w}}$, $\mathbf{p}_{1_{\hat{\mathbf{u}}},2_{\hat{\mathbf{u}}}}=p_{1,2}\cos\alpha_{1,2}\hat{\mathbf{u}}$ and $\mathbf{p}_{1_{\hat{\mathbf{v}}},2_{\hat{\mathbf{v}}}}=0$, since $\hat{\mathbf{v}}$ is perpendicular to the plane containing $\mathbf{p}_{1,2}$. Also, $\mathbf{p}_1\cdot\mathbf{p}_2=p_1p_2\cos[\alpha_1+\alpha_2]$ and $p_1\sin\alpha_1=p_2\sin\alpha_2$ (cf. Piwinski [1]).

We now perform the Lorentz transformations along the u-axis parallel to the sum of the two momenta in Fig. 9, $\mathbf{p}_u\overset{\text{def}}{=}\mathbf{p}_1+\mathbf{p}_2$, and the sum of the two energies, $E_u\overset{\text{def}}{=}E_1+E_2$. The velocity of the CM frame $(\hat{\mathbf{u}},\hat{\bar{\mathbf{v}}},\hat{\bar{\mathbf{w}}})$ relative to the LAB frame $(\hat{\mathbf{s}},\hat{\mathbf{x}},\hat{\mathbf{z}})$ is β_r, with Lorentz factor γ_r, and $\beta_{1,2}c$ and $\gamma_{1,2}$ are the velocities and Lorentz factors of $\mathbf{p}_{1,2}$ in the LAB frame. Hence, the momentum-energy Lorentz transformation parallel to the u-axis gives the momentum in the CM frame, with the help of Eq. (68):

$$\begin{aligned}\bar{\mathbf{p}}_{1,2_{\hat{\mathbf{u}}}}&=\gamma_\mathrm{r}\left(|\mathbf{p}_{1,2_{\hat{\mathbf{u}}}}|-\beta_\mathrm{r}\frac{E_{1,2}}{c}\right)\hat{\bar{\mathbf{u}}}=\gamma_\mathrm{r}\left(|\mathbf{p}_{1,2_{\hat{\mathbf{u}}}}|-\beta_\mathrm{r}\frac{|\mathbf{p}_{1,2}|}{\beta_{1,2}}\right)\hat{\bar{\mathbf{u}}}\\&=\gamma_\mathrm{r}\left(|\mathbf{p}_{1,2}|\cos\alpha_{1,2}-\beta_\mathrm{r}\frac{|\mathbf{p}_{1,2}|}{\beta_{1,2}}\right)\hat{\bar{\mathbf{u}}}=p_{1,2}\gamma_\mathrm{r}\left(\cos\alpha_{1,2}-\frac{\beta_\mathrm{r}}{\beta_{1,2}}\right)\hat{\bar{\mathbf{u}}}\,,\end{aligned}\tag{69}$$

where the subscript $\hat{\bar{\mathbf{u}}}$ on the left-hand side refers to the component $\bar{\mathbf{p}}_{1,2}$ along the $\bar{u}$-axis. The relative velocity β_r of the CM frame is fixed by the necessity that $\bar{\mathbf{p}}_1+\bar{\mathbf{p}}_2=0$ (cf. Piwinski [22] Appendix A1). Using Eq. (69) and with $|\mathbf{p}_{1,2}|=m\gamma_{1,2}\beta_{1,2}c$ for the two LAB frame particles one get:

$$\begin{aligned}&|\bar{\mathbf{p}}_{1_{\hat{\mathbf{u}}}}+\bar{\mathbf{p}}_{2_{\hat{\mathbf{u}}}}|=m\gamma_r c(-\beta_r(\gamma_1+\gamma_2)+\beta_1\gamma_1\cos\alpha_1+\beta_2\gamma_2\cos\alpha_2)\equiv 0,\quad\text{solving for }\beta_\mathrm{r}\text{ gives:}\\&\beta_\mathrm{r}=\frac{\beta_1\gamma_1\cos\alpha_1+\beta_2\gamma_2\cos\alpha_2}{\gamma_1+\gamma_2}\equiv\frac{|\mathbf{p}_1+\mathbf{p}_2|c}{E_1+E_2},\ \ \gamma_\mathrm{r}=\left(1-\beta_\mathrm{r}^2\right)^{-1/2}=\left(1+\frac{|\mathbf{p}_1+\mathbf{p}_2|^2c^2}{(E_1+E_2)^2}\right)^{-1/2},\\&\gamma_\mathrm{r}^2=\left(1-\beta_\mathrm{r}^2\right)^{-1}=\frac{1}{2}\frac{(\gamma_1+\gamma_2)^2}{1+\gamma_1\gamma_2-\beta_1\gamma_1\beta_2\gamma_2\cos[\alpha_1+\alpha_2]}\approx\frac{\gamma^2}{1+\gamma^2-\beta^2\gamma^2(1-2\alpha^2)}=\frac{\gamma^2}{1+\beta^2\gamma^2\alpha^2}\,.\end{aligned}\tag{70}$$

which in turn yields the approximate relative velocity of the CM frame $\beta_\mathrm{r}=\sqrt{\gamma_\mathrm{r}^2-1}/\gamma_\mathrm{r}\approx\beta(1-\alpha^2/2)$. Also $E_{1,2}=mc^2\gamma_{1,2}$, $p_{1,2}c=mc^2\beta_{1,2}\gamma_{1,2}$, $\cos[\alpha_1+\alpha_2]=\cos 2\alpha$, $\mathbf{p}_1\cdot\mathbf{p}_2=p_1p_2\cos 2\alpha$, $\beta^2\gamma^2=\gamma^2-1$, assuming $p_{s_{1,2}}\approx p_{1,2}$, $x'_{1,2}\approx p_{x_{1,2}}/p\ll 1$, $z'_{1,2}\approx p_{z_{1,2}}/p\ll 1$, and $\alpha_1\approx\alpha_2\approx\alpha$, see Eq. (75), and since:

$$\begin{aligned}&\mathbf{p}_1+\mathbf{p}_2=\left(p_1\cos\alpha_1+p_2\cos\alpha_2\right)\hat{\mathbf{u}}+\left(p_1\sin\alpha_1-p_2\sin\alpha_2\right)\hat{\mathbf{w}}=\left(p_1\cos\alpha_1+p_2\cos\alpha_2\right)\hat{\mathbf{u}}\text{ (Fig. 9)},\\&|\mathbf{p}_1|\sin\alpha_1=|\mathbf{p}_2|\sin\alpha_2,\ \ |\mathbf{p}_1+\mathbf{p}_2|=mc\left(\beta_1\gamma_1\cos\alpha_1+\beta_2\gamma_2\cos\alpha_2\right),\ \ E_1+E_2=mc^2(\gamma_1+\gamma_2).\end{aligned}$$

Completing Eq. (69) with the Lorentz transformation on the w-axis using Eq. (68), the component on the $\bar{v}$-axis being null, and adding the Lorentz transformation for the energy, we get the three momenta and the energy expressed in the CM frame $(\hat{\bar{\mathbf{u}}},\hat{\bar{\mathbf{v}}},\hat{\bar{\mathbf{w}}})$ (Eq. (71) will be set in a more operable form below):

$$\bar{\mathbf{p}}_{1,2}=p_{1,2}\left[\gamma_\mathrm{r}\left(\cos\alpha_{1,2}-\frac{\beta_\mathrm{r}}{\beta_{1,2}}\right)\hat{\bar{\mathbf{u}}}+0\,\hat{\bar{\mathbf{v}}}\pm\sin\alpha_{1,2}\hat{\bar{\mathbf{w}}}\right],\ \ \bar{E}_{1,2}=\gamma_\mathrm{r}\left(1-\beta_\mathrm{r}\beta_{1,2}\cos\alpha_{1,2}\right)=\frac{E_1+E_2}{2\gamma_\mathrm{r}}.\tag{71}$$

By symmetry, the changes in momenta of the two colliding particles have the same absolute values but opposite signs in the CM frame, their directions are described by the two angles $\bar{\psi}$ and $\bar{\phi}$ (see Fig. 10).

$$\bar{\mathbf{p}}'_{1,2} = \pm\Big[\big(\bar{p}_{\bar{w}}\sin\bar{\psi}\cos\bar{\phi} + \bar{p}_{\bar{u}}\cos\bar{\psi}\big)\hat{\bar{\mathbf{u}}} + \bar{p}\sin\bar{\psi}\sin\bar{\phi}\,\hat{\bar{\mathbf{v}}} + \big(\bar{p}_{\bar{w}}\cos\bar{\psi} - \bar{p}_{\bar{u}}\sin\bar{\psi}\cos\bar{\phi}\big)\hat{\bar{\mathbf{w}}}\Big] \ . \quad (72)$$

Let us summarize this 'gymnastic' back and forth between the rest and centre-of-mass frames:

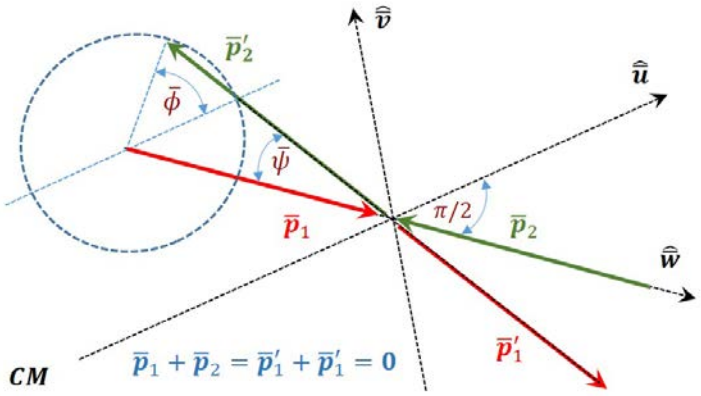

Fig. 10: Changes of momenta in a particle-pair collision in the centre-of-mass coordinate system (Ref. [1])

Before collision (Fig. 9)

(a) LAB frame coordinate system $(\hat{\mathbf{s}}, \hat{\mathbf{x}}, \hat{\mathbf{z}})$: the three momenta of the two particles are given in (66),

$$\mathbf{p}_{1,2} = p_{s_{1,2}}\hat{\mathbf{s}} + p_{x_{1,2}}\hat{\mathbf{x}} + p_{z_{1,2}}\hat{\mathbf{z}} \approx p_{1,2}\big(\hat{\mathbf{s}} + x'_{1,2}\hat{\mathbf{x}} + z'_{1,2}\hat{\mathbf{z}}\big) \ .$$

(b) LAB frame $(\hat{\mathbf{u}}, \hat{\mathbf{v}}, \hat{\mathbf{w}})$: the three momenta of the two particles reduce to two momenta, which can be written using the angles $\alpha_{1,2}$ between the u-axis and the particle momenta as (68),

$$\mathbf{p}_{1,2} = p_{1,2}\big(\cos\alpha_{1,2}\hat{\mathbf{u}} + 0\,\hat{\mathbf{v}} \pm \sin\alpha_{1,2}\hat{\mathbf{w}}\big) \ .$$

(c) CM frame $(\hat{\bar{\mathbf{u}}}, \hat{\bar{\mathbf{v}}}, \hat{\bar{\mathbf{w}}})$: the two particle momenta in the CM frame calculated by way of a Lorentz transformation parallel to the u-axis can be cast into the form (71) ,

$$\bar{\mathbf{p}}_{1,2} = p_{1,2}\left[\gamma_{\mathrm{r}}\left(\cos\alpha_{1,2} - \frac{\beta_{\mathrm{r}}}{\beta_{1,2}}\right)\hat{\bar{\mathbf{u}}} + 0\,\hat{\bar{\mathbf{v}}} \pm \sin\alpha_{1,2}\hat{\bar{\mathbf{w}}}\right] \ .$$

After collision (Fig. 10)

(a) CM frame $(\hat{\bar{\mathbf{u}}}, \hat{\bar{\mathbf{v}}}, \hat{\bar{\mathbf{w}}})$: the two particle momenta are rotated by the axial and azimuthal scattering angles $(\bar{\psi}, \bar{\phi})$; they are stated in (72),

$$\bar{\mathbf{p}}'_{1,2} = \pm\Big[\big(\bar{p}_{\bar{w}}\sin\bar{\psi}\cos\bar{\phi} + \bar{p}_{\bar{u}}\cos\bar{\psi}\big)\hat{\bar{\mathbf{u}}} + \bar{p}\sin\bar{\psi}\sin\bar{\phi}\,\hat{\bar{\mathbf{v}}} + \big(\bar{p}_{\bar{w}}\cos\bar{\psi} - \bar{p}_{\bar{u}}\sin\bar{\psi}\cos\bar{\phi}\big)\hat{\bar{\mathbf{w}}}\Big] \ .$$

(b) LAB frame $(\hat{\mathbf{u}}, \hat{\mathbf{v}}, \hat{\mathbf{w}})$: the two momenta are transformed back to the laboratory coordinate system after the collision; they can be expressed as

$$\begin{aligned}\mathbf{p}'_{1,2} = p_{1,2}\Bigg\{&\gamma_{\mathrm{r}}\left[\pm\sin\bar{\psi}\cos\bar{\phi}\sin\alpha_{1,2} + \cos\bar{\psi}\gamma_{\mathrm{r}}\left(\cos\alpha_{1,2} - \frac{\beta_{\mathrm{r}}}{\beta_{1,2}}\right)\right]\hat{\mathbf{u}} \\ &+ \left[\pm\sin\bar{\psi}\sin\bar{\phi}\frac{p}{p_{1,2}} - \sin\bar{\psi}\cos\bar{\phi}\left(\cos\alpha_{1,2} - \frac{\beta_{\mathrm{r}}}{\beta_{1,2}}\right)\right]\hat{\mathbf{v}} + \big[\cos\bar{\phi}\sin\alpha_{1,2}\big]\,\hat{\mathbf{w}}\Bigg\} \ . \quad (73)\end{aligned}$$

Therefore, for the two particles colliding with each other, the change in the particle momenta $\delta\mathbf{p}_{1,2}$ in the laboratory frame $(\hat{\mathbf{u}}, \hat{\mathbf{v}}, \hat{\mathbf{w}})$ is obtained immediately by subtracting (68) from (73). The result is

$$\begin{aligned}\delta\mathbf{p}_{1,2} &= \mathbf{p}'_{1,2} - \mathbf{p}_{1,2} \\ &= p_{1,2}\Bigg\{\gamma_{\mathrm{r}}\left[\pm\sin\bar{\psi}\cos\bar{\phi}\sin\alpha_{1,2} + (\cos\bar{\psi}-1)\gamma_{\mathrm{r}}\left(\cos\alpha_{1,2} - \frac{\beta_{\mathrm{r}}}{\beta_{1,2}}\right)\right]\hat{\mathbf{u}} \\ &\quad \pm\left[\sin\bar{\psi}\sin\bar{\phi}\frac{p}{p_{1,2}}\right]\hat{\mathbf{v}} - \left[\sin\bar{\psi}\cos\bar{\phi}\left(\cos\alpha_{1,2} - \frac{\beta_{\mathrm{r}}}{\beta_{1,2}}\right) \pm (\cos\bar{\phi}-1)\sin\alpha_{1,2}\right]\hat{\mathbf{w}}\Bigg\}\,. \quad (74)\end{aligned}$$

More approximations are needed to progress further. Let us introduce the three angles ξ, θ and ζ, used as integration variables for the averaging process over the particle distribution inside the bunch. It is assumed that, in the LAB frame, the angle between the two colliding particle momenta is small, and that the derivatives $x'_{1,2}, z'_{1,2}$ of $x_{1,2}, z_{1,2}$ with respect to the longitudinal axis are equal to the small angles the particles make with this s-axis, that is $p_{s_{1,2}} \approx p_{1,2}$, $x'_{1,2} \ll 1$ and $z'_{1,2} \ll 1$, which implies $\alpha_1 \approx \alpha_2 \approx \alpha$ as seen above (cf. also Fig. 9).

$$\begin{gathered}\gamma\xi = \frac{p_1 - p_2}{p}, \quad \theta = \frac{p_{x_1} - p_{x_2}}{p} \equiv x'_1 - x'_2, \quad \zeta = \frac{p_{z_1} - p_{z_2}}{p} \equiv z'_1 - z'_2\,, \\ 2\alpha = \alpha_1 + \alpha_2 = \sqrt{(x'_1 - x'_2)^2 + (z'_1 - z'_2)^2} = \sqrt{\theta^2 + \zeta^2}\,.\end{gathered} \quad (75)$$

Comment: The first expression in (75) can also be written as $\gamma\xi = [(p_1 - p) - (p_2 - p)]/p = \Delta p_1/p - \Delta p_2/p$.

Using Eqs. (70) and (75) with the above approximations and expanding the cosine and sine functions in power series to second-order, Eq. (71) simplifies (see [6, 22] for more details) supposing that $\gamma^2\alpha^2 \ll 1$, where $p = |\mathbf{p}|$ is the average momentum value of all particles in the bunch. One obtain

$$\begin{aligned}\bar{\mathbf{p}}_{1,2} &= \pm\frac{p}{2}\left[\xi\sqrt{1+\beta^2\gamma^2\alpha^2}\hat{\tilde{\mathbf{u}}} + 0\hat{\tilde{\mathbf{v}}} + 2\alpha\hat{\tilde{\mathbf{w}}}\right] \\ &\approx \pm\frac{p}{2}\left[\xi\hat{\tilde{\mathbf{u}}} + 0\hat{\tilde{\mathbf{v}}} + 2\alpha\hat{\tilde{\mathbf{w}}}\right] \approx \pm\frac{p}{2}\left[\frac{p_1 - p_2}{\gamma p}\hat{\tilde{\mathbf{u}}} + 0\hat{\tilde{\mathbf{v}}} + 2\alpha\hat{\tilde{\mathbf{w}}}\right]. \quad (76)\end{aligned}$$

Finally, it remains to formulate the change of momenta $\delta\mathbf{p}_{1,2}$ for the two colliding particles (74) in the laboratory frame $(\hat{\mathbf{s}}, \hat{\mathbf{x}}, \hat{\mathbf{z}})$ of the storage ring coordinate system. After some manipulations the result can be written in the form (see Piwinski [1])

$$\begin{aligned}\frac{\delta\mathbf{p}_{1,2}}{|\mathbf{p}|} = \frac{\mathbf{p}'_{1,2} - \mathbf{p}_{1,2}}{|\mathbf{p}|} &= \frac{\delta p_{s_{1,2}}}{p}\hat{\mathbf{s}} + \frac{\delta p_{x_{1,2}}}{p}\hat{\mathbf{x}} + \frac{\delta p_{z_{1,2}}}{p}\hat{\mathbf{z}} = \frac{1}{2}\left[2\gamma\alpha\cos\bar{\phi}\sin\bar{\psi} + \gamma\xi(\cos\bar{\psi}-1)\right]\hat{\mathbf{s}} \\ &\quad + \frac{1}{2}\left[\left(\zeta\sqrt{1+\frac{\xi^2}{4\alpha^2}}\sin\bar{\phi} - \frac{\xi\theta}{2\alpha}\cos\bar{\phi}\right)\sin\bar{\psi} + \theta(\cos\bar{\psi}-1)\right]\hat{\mathbf{x}} \\ &\quad + \frac{1}{2}\left[\left(\theta\sqrt{1+\frac{\xi^2}{4\alpha^2}}\sin\bar{\phi} - \frac{\xi\zeta}{2\alpha}\cos\bar{\phi}\right)\sin\bar{\psi} + \zeta(\cos\bar{\psi}-1)\right]\hat{\mathbf{z}}\,. \quad (77)\end{aligned}$$

Equation (77) captures the essence of the intrabeam collision process.

Step* 4: *Emittance change induced by momentum change

The change in the particle momenta after collision leads to a parallel change in the particle invariants, namely the longitudinal and transverse emittances. These changes can be calculated by supposing that the transverse particle positions are not altered during the interaction time (assumed to be short enough). From now on we focus the analysis of *bunched beams*. The radial particle movement from the reference closed orbit is the sum of the betatron motion x_β and the momentum deviation contribution from the

product of the momentum dispersion function $D_{x,z}$ and the relative momentum deviation $\Delta p/p$. To simplify the notation, we assume that the reference orbit lies in the plane containing the s- and x-axes; that is, no orbit curvature takes place in the vertical direction z, so that $D_z(s) \equiv 0$. Then

$$x = x_\beta + D_x \frac{\Delta p}{p}, \quad z = z_\beta \quad \text{and} \quad x' \equiv \frac{p_x}{p} = x'_\beta - D'_x \frac{\Delta p}{p}, \quad z' \equiv \frac{p_z}{p} = z'_\beta \,. \tag{78}$$

The invariants of the motion are the single-particle *transverse emittances* $\varepsilon_{x,z}$ (identified with the *Courant–Snyder invariant*) and the *longitudinal invariant* H for a bunched beam:

$$\varepsilon_x = \gamma_x x_\beta^2 + 2\alpha_x x_\beta x'_\beta + \beta_x x'^2_\beta \quad \text{and} \quad H = \left(\frac{\Delta p}{p}\right)^2 + \frac{1}{\Omega^2}\left[\frac{\mathrm{d}}{\mathrm{d}t}\left(\frac{\Delta p}{p}\right)\right]^2 , \tag{79}$$

where α_x, β_x and γ_x are the *Twiss parameters*, with $\beta_x\gamma_x - \alpha_x^2 = 1$ and $2\alpha_x = -\beta'_x$, and Ω is the *synchrotron frequency*.

The change $\delta\varepsilon_x$ in the invariant ε_x after collision is given by

$$\delta\varepsilon_x = \gamma_x\big(2x_\beta\delta x_\beta + \delta x_\beta^2\big) + 2\alpha_x\big(x'_\beta\delta x_\beta + x_\beta\delta x'_\beta + \delta x_\beta\delta x'_\beta\big) + \beta_x\big(2x'_\beta\delta x'_\beta + \delta x'^2_\beta\big) \,. \tag{80}$$

Replace x with z to get $\delta\varepsilon_z$.

It has already been assumed that the ring lattice is vertically free of dispersion, i.e. $D_z = D'_z = 0$. Suppose also that $x_{1,2}$ and $z_{1,2}$ stay constant during the short collision time, so that only $x'_{1,2}$ and $z'_{1,2}$ vary with the change in momentum. Now $\delta(\Delta p/p) = \delta p/p$, as the average (or reference) momentum $p_s = |\mathbf{p}_s|$ remains constant if the beam is not accelerated.

Comment: Indeed, $\delta(\Delta p/p) = \delta[(p - p_s)/p_s] = \delta p/p_s - \delta p_s/p_s = \delta p/p_s \approx \delta p/p$ as p_s is constant. Defining $\eta = \Delta p/p$ gives $\delta\eta \approx \delta p/p$.

So the variations δx_β, $\delta x'_\beta$ and $\delta z'_\beta$ can be formulated in terms of the betatron amplitudes as

$$\delta x_\beta = -D_x\frac{\delta p}{p}, \qquad \delta x'_\beta = \frac{\delta p_x}{p} - D'_x\frac{\delta p}{p}, \qquad \delta z'_\beta = \frac{\delta p_z}{p} \,, \tag{81}$$

where, for instance, we have used the 'trick'

$$\delta x = \delta x_\beta + D_x\frac{\Delta p}{p} = \delta x_\beta + D_x\delta\left[\frac{\Delta p}{p}\right] = \delta x_\beta + D_x\frac{\delta p}{p} \equiv 0 \implies \delta x_\beta = -D_x\frac{\delta p}{p} \,.$$

the changes $\delta\varepsilon_{x,z}$ and δH of $\varepsilon_{x,z}$ and H can be written in the form

$$\begin{aligned}\frac{\delta\varepsilon_x}{\beta_x} &= -\frac{2}{\beta_x}\Big[x_\beta(\gamma_x D_x + \alpha_x D'_x) + x'_\beta\tilde{D}_x\Big]\frac{\delta p}{p} \\ &\quad + \frac{D_x^2 + \tilde{D}_x^2}{\beta_x^2}\left(\frac{\delta p}{p}\right)^2 + 2\left(x'_\beta + \frac{\alpha_x}{\beta_x}x_\beta\right)\frac{\delta p_x}{p} + \left(\frac{\delta p_x}{p}\right)^2 - \frac{2\tilde{D}_x}{\beta_x}\frac{\delta p}{p}\frac{\delta p_x}{p} \,, \end{aligned} \tag{82}$$

$$\frac{\delta\varepsilon_z}{\beta_z} = 2\left(z'_\beta + \frac{\alpha_z}{\beta_z}z_\beta\right)\frac{\delta p_z}{p} + \left(\frac{\delta p_z}{p}\right)^2, \qquad \delta H = 2\frac{\Delta p}{p}\frac{\delta p}{p} + \left(\frac{\delta p}{p}\right)^2 \,, \tag{83}$$

where $\tilde{D}_x = \alpha_x D_x + \beta_x D'_x$ and we have neglected possible time variation of the synchrotron frequency during the collision.

Comment: Likewise, assuming that $\mathrm{d}\eta/\mathrm{d}t = 0$ at the collision time, we have $H \equiv \eta^2$ and $\delta H = (\eta + \delta\eta)^2 - \eta^2 = 2\eta\delta\eta + (\delta\eta)^2 = 2\eta\delta p/p + (\delta p/p)^2$ as $\delta\eta \equiv \delta(\Delta p/p) \approx \delta p/p$.

In the presence of radial dispersion, the momentum change δp of the particle during the collision leads to a change in the horizontal emittance given by Eq. (82). In what follows, the shorthand $\eta_{1,2} \stackrel{\text{def}}{=} \Delta p_{1,2}/p_{1,2}$ or $\eta = \Delta p/p$ will be used.

Step* 5: *Averaging over the scattering angles

The variation of the beam phase space volume can be calculated by averaging the change of the particle invariants over all the collisions in accordance with the particle distribution function. Piwinski defined the time-derivative $\mathrm{d}\langle\varepsilon_x\rangle/\mathrm{d}\bar{t}$ of the average radial emittance $\langle\varepsilon_x\rangle$ in the CM frame for all particles by means of a stepwise integration process.

Stated in detail (see [1, 3]): "To calculate the mean value of the emittance and momentum deviation change for one particle we have to average with respect to the second particle betatron angles and momentum deviations. Thus, to derive the overall mean value of the emittance and momentum deviation change for all particles we have to average further with respect to all betatron angles, momentum deviations and positions of the first particle. This means that we have to integrate over all phase space betatron coordinates, momentum spread values and azimuthal locations of two interacting particles, by means of a probability density function P (in the rest frame) for the betatron amplitudes and angles, the momentum deviations and the azimuthal positions of the interacting particles. This is done by integrating $\bar{P}$ (in the CM frame) over the particle bunch phase space volume $\bar{V}$ with respect to the differential phase space volume element $\mathrm{d}\bar{V}$:

$$\left\langle \frac{\mathrm{d}}{\mathrm{d}\bar{t}} \frac{\langle\varepsilon_{x_1}\rangle}{\beta_x} \right\rangle = \int_{\bar{V}} 2c\bar{\beta}\bar{P}\,\mathrm{d}\bar{V} \int_{\bar{\psi}_{\min}}^{\pi} \mathrm{d}\bar{\psi} \int_0^{2\pi} \mathrm{d}\bar{\phi}\,\bar{\sigma}(\bar{\psi}) \frac{\delta\varepsilon_{x_1}}{\beta_x} \sin\bar{\psi}, \tag{84}$$

where the outer brackets $\langle\,\cdot\,\rangle$ denote the average value over the lattice parameters of the ring. Here $\bar{\sigma}(\psi)$ is the differential Coulomb scattering cross-section for the scattering into a solid angle element $\mathrm{d}\bar{\Omega}(\bar{\psi},\bar{\phi})$ in the CM frame, $\mathrm{d}\bar{t}$ and $\mathrm{d}t$ are the *proper time* intervals in the CM and rest LAB frames, such that $\mathrm{d}t = \gamma\,\mathrm{d}\bar{t}$, c is the speed of light, and $2c\bar{\beta}$ is the relative velocity of two interacting particles (labelled 1 and 2) with velocities $\bar{\mathbf{v}}_1 + \bar{\mathbf{v}}_2 = 0$ in the CM frame. The probability density function P is defined by a product of 12 variables and can be formulated in the LAB frame as

$$P_{12\text{var}} = P_{\eta s}(\eta_1, s_1) P_{\eta s}(\eta_2, s_2) P_{x_\beta x'_\beta}(x_{\beta_1}, x'_{\beta_1}) P_{x_\beta x'_\beta}(x_{\beta_2}, x'_{\beta_2}) P_{zz'}(z_1, z'_1) P_{zz'}(z_2, z'_2)\,,$$

and the two-particle infinitesimal phase space volume element is

$$\mathrm{d}V_{12\text{var}} = \mathrm{d}\eta_1\,\mathrm{d}s_1\,\mathrm{d}\eta_2\,\mathrm{d}s_2\,\mathrm{d}x_{\beta_1}\,\mathrm{d}x'_{\beta_1}\,\mathrm{d}x_{\beta_2}\,\mathrm{d}x'_{\beta_2}\,\mathrm{d}z_1\,\mathrm{d}z'_1\,\mathrm{d}z_2\,\mathrm{d}z'_2\,. \tag{85}$$

Of these 12 partial joint probability density functions, three are dependent, since during the time of the interaction the positions of the particles are supposed to remain unchanged on account of the short collision duration (equivalently, this follows from the assumption that the two colliding particles have the same position). So, the variables $s_{1,2}$, $x_{\beta_{1,2}}$ and $z_{1,2}$ satisfy the following conditions if $D_z = 0$:

$$s_1 = s_2, \qquad x_{\beta_1} + D_x\eta_1 \equiv x_{\beta_2} + D_x\eta_2, \qquad z_1 = z_{\beta_1} \equiv z_2 = z_{\beta_2}\,. \tag{86}$$

Then $P_{12\text{var}}$ and $\mathrm{d}V_{12\text{var}}$ can be reduced to 9 variables

$$P = P_\eta(\eta_1) P_\eta(\eta_2) P_s(s_1) P_{x_\beta}(x_{\beta_1}) P_{x'_\beta}(x'_{\beta_1}) P_{x'_\beta}(x'_{\beta_2}) P_z(z_1) P_{z'}(z'_1) P_{z'}(z'_2)\,, \tag{87}$$

$$\mathrm{d}V = \mathrm{d}\eta_1\,\mathrm{d}\eta_2\,\mathrm{d}s_1\,\mathrm{d}x_{\beta_1}\,\mathrm{d}x'_{\beta_1}\,\mathrm{d}x'_{\beta_2}\,\mathrm{d}z_1\,\mathrm{d}z'_1\,\mathrm{d}z'_2\,. \tag{88}$$

We now investigate the distribution of the scattering angle $\bar{\psi}$ resulting from the Coulomb interaction of two non-relativistic ions (with $\bar{\beta} \ll 1$) of charge Z and atomic mass A in the CM frame, for which we can use the 'classical' *Rutherford differential cross-section* formula:

$$\bar{\sigma}(\bar{\psi}) = \left(\frac{AmZ^2e^2}{4\pi\epsilon_0|\bar{\mathbf{p}}_2 - \bar{\mathbf{p}}_1|^2}\right)^2 \frac{1}{\sin^4[\bar{\psi}/2]} = \left(\frac{Z^2 r_0 mc^2}{2\bar{T}}\right)^2 \frac{1}{\sin^4[\bar{\psi}/2]} = \left(\frac{Z^2}{A}\frac{r_0}{4\bar{\beta}^2}\right)^2 \frac{1}{\sin^4[\bar{\psi}/2]}\,, \tag{89}$$

where $\bar{T}=|\bar{\mathbf{p}}_2-\bar{\mathbf{p}}_1|^2/2Am=2Am\bar{\beta}^2c^2$ is the kinetic energy of the ion, $2Am\bar{\beta}c$ is the relative momentum of the two colliding ions, with $\bar{\mathbf{p}}_1+\bar{\mathbf{p}}_2=0$ in the CM frame as the collision is elastic, and

$$r_0=\frac{e^2}{4\pi\epsilon_0 mc^2}\quad\text{and}\quad r_{\rm i}=\frac{r_0Z^2}{A} \tag{90}$$

are the *classical proton radius* and *classical ion radius*, respectively.

With the assumptions $p_{s_{1,2}}\approx p_{1,2}$, $(p_1-p_2)/p\ll 1$, $p_{x_{1,2}}/p=x'_{1,2}\ll 1$ and $p_{z_{1,2}}/p=z'_{1,2}\ll 1$ (see Eq. (75) in which $2\alpha\equiv\sqrt{\theta^2+\zeta^2}$), Eq. (76) can be rewritten in the following way to show the connection between the particle velocities in the CM and LAB systems.

$$\bar{\mathbf{p}}_{1,2}=m\bar{\gamma}_{1,2}\bar{\beta}_{1,2}c\approx\pm\frac{p}{2}\left[\xi\hat{\bar{\mathbf{u}}}+0\hat{\bar{\mathbf{v}}}+2\alpha\hat{\bar{\mathbf{w}}}\right]=\pm\frac{m\gamma\beta c}{2}\left[\xi\hat{\bar{\mathbf{u}}}+0\hat{\bar{\mathbf{v}}}+2\alpha\hat{\bar{\mathbf{w}}}\right]=\pm\frac{m\gamma\beta c}{2}\left[\xi\hat{\bar{\mathbf{u}}}+0\hat{\bar{\mathbf{v}}}+\sqrt{\theta^2+\zeta^2}\hat{\bar{\mathbf{w}}}\right]$$
$$\Longrightarrow\quad|\bar{\mathbf{p}}_{1,2}|^2\approx(m\bar{\gamma}_{1,2}\bar{\beta}_{1,2}c)^2\approx\frac{m^2\gamma^2\beta^2c}{4}(\alpha^2+\theta^2+\zeta^2)\,. \tag{91}$$

Moreover, assuming non-relativistic particle velocities in the CM frame, i.e. $\bar{\beta}\ll 1$, $\bar{\gamma}\approx 1$, then with (91)

$$\bar{\beta}\approx\frac{\beta\gamma}{2}\sqrt{\xi^2+\alpha^2}=\frac{\beta\gamma}{2}\sqrt{\xi^2+\theta^2+\zeta^2}=\frac{\beta\gamma}{2}\sqrt{\left(\frac{p_1-p_2}{\gamma p}\right)^2+\left(x'_1-x'_2\right)^2+\left(z'_1-z'_2\right)^2}\,. \tag{92}$$

The integrations required to calculate Eq. (84) can be done as follows, where the next integral I_{x_1}, needed to evaluate part of the mean time-derivative of $\langle\varepsilon_{x_1}\rangle/\beta_x$ is computed by replacing $\delta p/p$ and $\delta p_x/p$ with their expressions in terms of the parameters $\alpha,\xi,\theta,\bar{\phi}$ and $\bar{\psi}$ (77). Integrating $\delta\varepsilon_{x_1}/\beta_x$ over the azimuthal and scattering angle $\bar{\psi}$ and $\bar{\phi}$ using the *Mathematica* program gives, upon expanding the scattering integrals into first order series development in $\bar{\psi}_{\rm min}$, using the Eqs. (94)–(95) below to approximate $\bar{\psi}_{\rm min}/2\approx r_{\rm i}/(2\bar{\beta}^2\bar{b}_{\rm max})$, we find that

$$\begin{aligned}
I_{x_1}&\equiv\int_{\bar{\psi}_{\rm min}}^{\pi}\mathrm{d}\bar{\psi}\int_0^{2\pi}\mathrm{d}\bar{\phi}\,\bar{\sigma}(\bar{\psi})\frac{\delta\varepsilon_{x_1}}{\beta_x}\sin\bar{\psi}\\
&=-\frac{\pi r_{\rm i}^2}{8\bar{\beta}^4}\left\{\xi^2+\zeta^2-2\theta^2+\frac{D_x^2+\tilde{D}_x^2}{\beta_x^2}\gamma^2\left(\zeta^2+\theta^2-2\xi^2\right)+\frac{6\tilde{D}_x}{\beta_x}\gamma\theta\xi\right\}\\
&+\frac{\pi r_{\rm i}^2}{4\bar{\beta}^4}\left\{\frac{4x_{\beta_1}}{\beta_x}\left(\gamma_xD_x\gamma\xi+\alpha_x(D'_x\gamma\xi-\theta)\right)+4x'_{\beta_1}\left(\frac{\tilde{D}_x\gamma\xi}{\beta_x}-\theta\right)+\xi^2+\zeta^2\right.\\
&\qquad\left.+\frac{D_x^2+\tilde{D}_x^2}{\beta_x^2}\gamma^2\left(\zeta^2+\theta^2\right)+\frac{2\tilde{D}_x}{\beta_x}\gamma\xi\theta\right\}\ln\left[\frac{2}{\bar{\psi}_{\rm min}}\right].
\end{aligned} \tag{93}$$

Notice that the smallest scattering angle $\bar{\psi}_{\rm min}$ is defined by the maximum *impact parameter* $\bar{b}_{\rm max}$, as shown in Eqs. (36) and (37) for a classical Coulomb scattering process,

$$\tan\left[\frac{\bar{\psi}_{\rm min}}{2}\right]\approx\frac{r_{\rm i}}{2\bar{\beta}^2\bar{b}_{\rm max}}\,. \tag{94}$$

Also, the maximum impact parameter $\bar{b}_{\rm max}$ gives a cut-off angle for the scattering angle ψ, it is often defined as the half the beam diameter or beam height $2\sigma_z$ since $D_z=0$.

Comment: From Eq. (36) we write, for $A=Z=1$ and with Eq. (90), $b_0=e^2/2\pi\epsilon_0 m\,|\bar{\mathbf{v}}_1-\bar{\mathbf{v}}|^2=e^2/2\pi\epsilon_0 m|2\bar{\mathbf{v}}|^2=e^2/4\pi\epsilon_0 2m\bar{\beta}^2c^2=r_0/2\bar{\beta}^2$, supposing that $\bar{\mathbf{v}}_1=-\bar{\mathbf{v}}$. Hence, by means of Eq. (37), we get $\tan[\bar{\psi}_{\rm min}/2]=r_0/2\bar{\beta}^2\bar{b}_{\rm max}$.

To obtain manageable results, we assume that $\bar{\psi}_{\text{min}} \ll 1$ (i.e. $\tan[\bar{\psi}_{\text{min}}/2] \ll 1$), so that

$$2\bar{\beta}^2\bar{b}_{\text{max}}/r_i \gg 1\,. \tag{95}$$

The two brackets in (93) have comparable small values as the angles ξ, θ and $\zeta \ll 1$; however the first bracket is negligible compared to the second one because it is multiplied by the *Coulomb logarithm* (97) (with usual values between 10 and 20).

$$\begin{aligned} I_{x_1} &\equiv \int_{\bar{\psi}_{\text{min}}}^{\pi} \mathrm{d}\bar{\psi} \int_0^{2\pi} \mathrm{d}\bar{\phi}\, \bar{\sigma}(\bar{\psi}) \frac{\delta\varepsilon_{x_1}}{\beta_x} \sin\bar{\psi} \\ &= \frac{\pi r_{\text{i}}^2}{4\bar{\beta}^4} \Bigg\{ \frac{4x_{\beta_1}}{\beta_x}\big(\gamma_x D_x \gamma\xi + \alpha_x(D'_x\gamma\xi - \theta)\big) + 4x'_{\beta_1}\left(\frac{\tilde{D}_x\gamma\xi}{\beta_x} - \theta\right) + \xi^2 + \zeta^2 \\ &\qquad + \frac{D_x^2 + \tilde{D}_x^2}{\beta_x^2}\gamma^2\big(\zeta^2 + \theta^2\big) + \frac{2\tilde{D}_x}{\beta_x}\gamma\xi\theta \Bigg\} \ln\left[\frac{2\bar{\beta}^2\bar{b}_{\text{max}}}{r_{\text{i}}}\right]. \end{aligned} \tag{96}$$

The logarithm factor in (96) is the so-called Coulomb logarithm $\bar{C}_{\log}$ defined in the CM system (see e.g. [2, 23]) as

$$\bar{C}_{\log} \equiv \ln\left[\frac{2\bar{\beta}^2\bar{b}_{\text{max}}}{r_{\text{i}}}\right] = \ln\left[\frac{2}{\bar{\psi}_{\text{min}}}\right]\,. \tag{97}$$

Comment: Observe that $C_{\log} \neq \bar{C}_{\log}$ because β in the rest frame is not equal to $\bar{\beta}$ in the CM frame as shown in Eq. (92).

Alternative definitions of the Coulomb logarithm are proposed, for example in [18]. However, its logarithmic dependence means that it changes slowly over a large range of the elements involved in its definition. In summary:

The other integrals I_{z_1} and I_{s_1} for the vertical and longitudinal momenta can be worked out in a similar way, assuming no vertical dispersion ($D_z = D'_z = 0$, with $\alpha_z \neq 0$). Combined, they yield the transverse and longitudinal scattering integrals (in which δH in Eq. 83 is now rewritten as $\delta H \approx 2\eta\delta p_s/p + (\delta p_s/p)^2$ since $\delta p \approx \delta p_s$, where $\eta = \Delta p/p$)

$$\begin{pmatrix} I_{s_1} \\ I_{x_1} \\ I_{z_1} \end{pmatrix} \equiv \int_{\bar{\psi}_{\text{min}}}^{\pi} \mathrm{d}\bar{\psi} \int_0^{2\pi} \mathrm{d}\bar{\phi}\, \sin\bar{\psi}\, \bar{\sigma}(\bar{\psi}) \begin{Bmatrix} \delta H_1/\gamma^2 \\ \delta\varepsilon_{x_1}/\beta_x \\ \delta\varepsilon_{z_1}/\beta_z \end{Bmatrix} = \frac{\pi r_{\text{i}}^2}{4\bar{\beta}^4} \ln\left[\frac{2\bar{\beta}^2\bar{b}_{\text{max}}}{r_{\text{i}}}\right] \tag{98}$$

$$\times \begin{Bmatrix} -\dfrac{4\eta_1}{\gamma}\xi + \theta^2 + \zeta^2 \\ \dfrac{4x_{\beta_1}}{\beta_x}\big(\gamma_x D_x\gamma\xi + \alpha_x(D'_x\gamma\xi - \theta)\big) + 4x'_{\beta_1}\Big(\frac{\tilde{D}_x\gamma\xi}{\beta_x} - \theta\Big) + \xi^2 + \zeta^2 + \frac{D_x^2+\tilde{D}_x^2}{\beta_x^2}\gamma^2\big(\zeta^2+\theta^2\big) + \dfrac{2\tilde{D}_x}{\beta_x}\gamma\xi\theta \\ -\dfrac{4\alpha_z z_1}{\beta_z}\zeta - 4z'_1\zeta + \xi^2 + \theta^2 \end{Bmatrix}.$$

In the centre of mass system, the derivatives $\mathrm{d}/\mathrm{d}s$ are reduced by the factor γ due to the Lorentz contraction along the longitudinal direction s, the transverse beam sizes and the relative momentum spread remain unchanged, the impact parameter $\bar{b}_{\text{max}} = b_{\text{max}}$ since it is perpendicular to the s-axis, the bunch length becomes $\bar{\sigma}_s = \gamma\sigma_s$

$$\begin{aligned} \bar{P} &= P/\gamma\,, \quad \mathrm{d}\bar{\mathrm{t}} = \mathrm{d}\mathrm{t}/\gamma \quad \text{and} \quad \bar{\sigma}_{x'_\beta} = \sigma_{x'_\beta}/\gamma \quad \bar{\sigma}'_z = \sigma'_z/\gamma\,, \\ \bar{\sigma}_{x_\beta} &= \sigma_{x_\beta}\,, \quad \bar{\sigma}_z = \sigma_z \quad \text{and} \quad \bar{\sigma}_{x'_\beta} = \sigma_{x'_\beta}/\gamma \quad \bar{\sigma}'_z = \sigma'_z/\gamma\,, \end{aligned} \tag{99}$$

$$\bar{\sigma}_\eta \;= \sigma_\eta \;, \qquad \bar{\sigma}_s \;= \gamma\sigma_s.$$

In accordance with Piwinski [6] - [20] the relative velocity between two colliding particles in the centre of mass system is $2\bar{\beta}c$. Thus, using the Rutherford differential cross-section $\bar{\sigma}(\bar{\psi})$ the likelihood of a collision per unit time and solid angle element $\mathrm{d}\bar{\Omega}(\bar{\psi},\bar{\phi})$, denoted $\bar{P}_{\text{scat}}$ is determined by the particle density distribution in phase space $\bar{P}$. We can write

$$\bar{P}_{\text{scat}} = 2\bar{\beta}c\,\bar{P}\,\bar{\sigma}(\bar{\psi}) \quad \text{with} \quad \bar{\sigma}(\bar{\psi})\mathrm{d}\bar{\Omega} = \left(\frac{r_{\text{i}}}{4\bar{\beta}^2\sin^2[\bar{\psi}/2]}\right)^2 \sin\bar{\psi}\mathrm{d}\bar{\psi}\mathrm{d}\bar{\phi}\;. \tag{100}$$

The phase space density distribution $\bar{P}$ is given by P/γ, P being defined in LAB frame; also, the transformation of the time step $\mathrm{d}\bar{\mathrm{t}} = \mathrm{d}t/\gamma$ in LAB frame produces another factor γ. It follows that Eq. (84) for the change per unit time of the mean values $\langle H\rangle/\gamma^2$ and $\langle\varepsilon_{x,z}\rangle/\beta_{x,z}$, averaged over all particles, integrating P over the phase space volume element dV introduced in Eqs. (87)–(88) can be cast into the form, with Eq. (98):

$$\left\langle \frac{\mathrm{d}}{\mathrm{d}t}\begin{bmatrix}\langle H_1\rangle/\gamma^2\\ \langle\varepsilon_{x_1}\rangle/\beta_x\\ \langle\varepsilon_{z_1}\rangle/\beta_z\end{bmatrix}\right\rangle = \int_V \frac{2\bar{\beta}cP}{\gamma^2}\begin{pmatrix}I_{s_1}\\ I_{x_1}\\ I_{z_1}\end{pmatrix}\mathrm{d}V\;. \tag{101}$$

Equation (101) is stated in the LAB frame except for β. It will be fully converted back to the laboratory system, with $\bar{\beta}$ replaced by its approximation $\beta\gamma\sqrt{\xi^2+\theta^2+\zeta^2}/2$ (Eq. (92)) after a suitable change of variables in P.

Step* 6: *Averaging over the particle momenta and positions

Computation of the mean change of the invariants $\varepsilon_{x,z}$ and H of all particles due to the multiple particle collisions requires averaging the above three integrals for the colliding particles over the joint density distribution P, where the 12 variables are reduced to nine $(\eta, s, \xi, x_\beta, x'_\beta, \theta, z, z', \zeta)$, as three of them are dependent; see Eq. (86). The mapping to the following new variables transformation P into $\mathcal{P}$ is

$$P(\eta_1,\eta_2,s_1,x_{\beta_1},x'_{\beta_1},x'_{\beta_2},z_1,z'_1,z'_2) \;\longmapsto\; \mathcal{P}(\eta,\xi,s,x_\beta,x'_\beta,\theta,z,z',\zeta)\;, \tag{102}$$

where the three angles ξ, θ and ζ have been introduced. Let us make the variable substitution (in conformity with Eq. (75)), taking into account that $D'_x \neq 0$:

$$\begin{aligned} x_{\beta_{1,2}} &= x_\beta \mp \frac{D_x\gamma\xi}{2}\;, & \eta_{1,2} &= \eta \pm \frac{\gamma\xi}{2}\;,\\ x'_{\beta_{1,2}} &= x'_\beta \pm \frac{\theta - D'_x\gamma\xi}{2}\;, & z'_{1,2} &= z' \pm \frac{\zeta}{2}\;,\\ x_{1,2} &= x\;, & z_{1,2} &= z\;, \qquad s_{1,2}= s. \end{aligned} \tag{103}$$

Hence, the phase space volume element $\mathrm{d}V$ (88) can be expressed in terms of these new variables via the 9×9 Jacobian matrix J of the transformation (103).

$$\begin{aligned} J &= \begin{pmatrix} \partial\eta_1/\partial\eta & \partial\eta_2/\partial\eta & \cdots & x'_{\beta_1}/\partial\eta & x'_{\beta_2}/\partial\eta & \cdots & z'_{\beta_1}/\partial\eta & z'_{\beta_2}/\partial\eta\\ \partial\eta_1/\partial\xi & \partial\eta_2/\partial\xi & \cdots & x'_{\beta_1}/\partial\xi & x'_{\beta_2}/\partial\xi & \cdots & z'_{\beta_1}/\partial\xi & z'_{\beta_2}/\partial\xi\\ \vdots & \vdots & \ddots & \vdots & \ddots & \vdots & & \\ \partial\eta_1/\partial\zeta & \partial\eta_2/\partial\zeta & \cdots & x'_{\beta_1}/\partial\zeta & x'_{\beta_2}/\partial\zeta & \cdots & z'_{\beta_1}/\partial\zeta & z'_{\beta_2}/\partial\zeta \end{pmatrix}\\ &= \begin{pmatrix} 1 & 1 & \cdots & 0 & 0 & \cdots & 0 & 0\\ \gamma/2 & -\gamma/2 & \cdots & -D'_x\gamma/2 & D'_x\gamma/2 & \cdots & 0 & 0\\ \vdots & \vdots & \ddots & \vdots & \vdots & \ddots & \vdots & \vdots\\ 0 & 0 & \cdots & 0 & 0 & \cdots & 1/2 & -1/2 \end{pmatrix}, \end{aligned} \tag{104}$$

The absolute value of the determinant of J is easily found to be $|\det \mathrm{J}| = \gamma$, the density distribution and the phase space volume element in the new variables being labelled $\mathcal{P}$ (102) and $\mathrm{d}\mathcal{V}$. The relation between the new and the initial phase volume elements is related to the transformation of multiple integrals by

$$\int_V P \,\mathrm{d}V = \int_{\mathcal{V}} |\det \mathrm{J}\,| \mathcal{P} \,\mathrm{d}\mathcal{V} \tag{105}$$

with $\mathrm{d}\mathcal{V} = \mathrm{d}\eta \,\mathrm{d}\xi \,\mathrm{d}s \,\mathrm{d}x_\beta \,\mathrm{d}x'_\beta \,\mathrm{d}\theta \,\mathrm{d}z \,\mathrm{d}z' \,\mathrm{d}\zeta$ and $\mathrm{d}V = \mathrm{d}\eta_1 \,\mathrm{d}\eta_2 \,\mathrm{d}s_1 \,\mathrm{d}x_{\beta_1} \,\mathrm{d}x'_{\beta_1} \,\mathrm{d}x'_{\beta_2} \,\mathrm{d}z_1 \,\mathrm{d}z'_1 \,\mathrm{d}z'_2$.

Hence, the change per unit time of the three averaged invariants (101) can be rewritten using (105), taking γ for $|\det \mathrm{J}|$

$$\left\langle \frac{\mathrm{d}}{\mathrm{d}t} \begin{bmatrix} \langle H\rangle/\gamma^2 \\ \langle \varepsilon_x\rangle/\beta_x \\ \langle \varepsilon_z\rangle/\beta_z \end{bmatrix} \right\rangle = \int_{\mathcal{V}} \frac{2\bar{\beta} c \mathcal{P}}{\gamma} \begin{pmatrix} I_{s_1} \\ I_{x_1} \\ I_{z_1} \end{pmatrix} \mathrm{d}\mathcal{V} \,. \tag{106}$$

Let us consider I_{x_1} in Eq. (98) and replace the variables x_{β_1} and x'_{β_1} in the bracket by the relevant new variables (103) into Eq. (106). We obtain

$$\begin{aligned} \left\langle \frac{\mathrm{d}}{\mathrm{d}t} \frac{\langle \varepsilon_x\rangle}{\beta_x} \right\rangle &= \frac{\pi c r_\mathrm{i}^2}{2} \int_{\mathcal{V}} \frac{\mathrm{d}\mathcal{V}}{\bar{\beta}^3 \gamma} \mathcal{P}\big(\eta, s, \xi, x_\beta, x'_\beta, \theta, z, z', \zeta\big) \ln\left[\frac{2\bar{\beta}^2 \bar{b}_{\max}}{r_\mathrm{i}}\right] \\ &\times \left\{ \xi^2 + \zeta^2 - 2\theta^2 + \frac{D_x^2 + \tilde{D}_x^2}{\beta_x^2} \gamma^2 \big(\zeta^2 + \theta^2\big) - \frac{2\gamma_x D_x^2}{\beta_x} \gamma^2 \xi^2 - \frac{2D'_x}{\beta_x} \big(\alpha_x D_x + \tilde{D}_x\big) \gamma^2 \xi^2 + \frac{4\tilde{D}_x}{\beta_x} \gamma (x'_\beta + \theta) \xi \right. \\ &\left. - \frac{4\gamma}{\beta_x} (\alpha_x x_\beta + \beta_x x'_\beta) \theta + \frac{2D_x}{\beta_x} \gamma (2\gamma_x x_\beta + \alpha_x \theta) \xi + \frac{4D'_x}{\beta_x} \gamma \alpha_x x_\beta \xi + 2D'_x \gamma \theta \xi \right\} . \end{aligned} \tag{107}$$

By construction the probability density law $\mathcal{P}$ is clearly symmetrical with respect to the angles ξ, θ and ζ, so the integrals vanish for the linear terms in ξ, θ and ζ of the integrands. Consequently, keeping only the factors ξ^2, θ^2 and ζ^2, Eq. (107) reduces to the expression to

$$\begin{aligned} \left\langle \frac{\mathrm{d}}{\mathrm{d}t} \frac{\langle \varepsilon_x\rangle}{\beta_x} \right\rangle &= \frac{\pi c r_\mathrm{i}^2}{2} \int_{\mathcal{V}} \frac{\mathrm{d}\mathcal{V}}{\bar{\beta}^3 \gamma} \mathcal{P}\big(\eta, s, \xi, x_\beta, x'_\beta, \theta, z, z', \zeta\big) \ln\left[\frac{2\bar{\beta}^2 \bar{b}_{\max}}{r_\mathrm{i}}\right] \\ &\times \left\{ \xi^2 + \zeta^2 - 2\theta^2 + \frac{D_x^2 + \tilde{D}_x^2}{\beta_x^2} \gamma^2 \big(\zeta^2 + \theta^2\big) - \frac{2\gamma_x D_x^2}{\beta_x} \gamma^2 \xi^2 - \frac{2D'_x}{\beta_x} (\alpha_x D_x + \tilde{D}_x) \gamma^2 \xi^2 \right\} . \end{aligned} \tag{108}$$

Comment: Using Eq. (102), the symmetry of $\mathcal{P}$ means that $\mathcal{P}(\eta, -\xi, s, x_\beta, x'_\beta, -\theta, z, z', -\zeta) \longmapsto P(\eta_2, \eta_1, s_1, x_{\beta_1}, x'_{\beta_2}, x'_{\beta_1}, z_1, z'_2, z'_1)$ where the order of the variables $\{\eta_1, \eta_2\}$, $\{x'_{\beta_1}, x'_{\beta_2}\}$ and $\{z'_1, z'_2\}$ in P permutes without changing the probability law.

Proceeding similarly with I_{s_1} and I_{z_1} in (98) and by inserting the upgrade terms into Eq. (107) yields:

$$\begin{aligned} \left\langle \frac{\mathrm{d}}{\mathrm{d}t} \begin{bmatrix} \langle H\rangle/\gamma^2 \\ \langle \varepsilon_x\rangle/\beta_x \\ \langle \varepsilon_z\rangle/\beta_z \end{bmatrix} \right\rangle &= \frac{\pi c r_\mathrm{i}^2}{2} \int_{\mathcal{V}} \frac{\mathrm{d}\mathcal{V}}{\bar{\beta}^3 \gamma} \mathcal{P}\big(\eta, s, \xi, x_\beta, x'_\beta, \theta, z, z', \zeta\big) \ln\left[\frac{2\bar{\beta}^2 \bar{b}_{\max}}{r_\mathrm{i}}\right] \\ &\times \left\{ \begin{array}{c} \theta^2 + \zeta^2 - 2\xi^2 \\ \xi^2 + \zeta^2 - 2\theta^2 + \dfrac{D_x^2 + \tilde{D}_x^2}{\beta_x^2} \gamma^2 \big(\zeta^2 + \theta^2\big) - \dfrac{2\gamma_x D_x^2}{\beta_x} \gamma^2 \xi^2 - \dfrac{2D'_x}{\beta_x} (\alpha_x D_x + \tilde{D}_x) \gamma^2 \xi^2 \\ \xi^2 + \theta^2 - 2\zeta^2 \end{array} \right\} . \end{aligned} \tag{109}$$

This formula for the mean change of the invariants $\varepsilon_{x,z}$ and H makes no a priori assumption about the density distribution P ($\mathcal{P}$) of the particles within the bunch. So in principle the integral can be calculated for arbitrary distribution functions. However, since 'Gaussian integration' is quite easily

performed, many analytical IBS models are based on the assumption that all the betatron amplitudes and angles, as well as the momentum deviations and the coordinates of the synchrotron motion (for bunched beams), follow Gaussian distributions.

Consequently, at this stage we assume that all the variables follow Gaussian probability laws. We then introduce bi-Gaussian formulations of the betatron amplitude and angle distributions, $P_{x_\beta x'_\beta}(x_{\beta_{1,2}}, x'_{\beta_{1,2}})$ and $P_{zz'}(z_{1,2}, z'_{1,2})$, along with the momentum and bunch-length deviation distributions $P_{\eta s}(\eta_{1,2}, s_{1,2})$. The density distributions, in which $u = x, z$ stands for both horizontal and vertical betatron motions, can be expressed as (see [24])

$$P_{u_\beta u'_\beta}(u_\beta, u'_\beta) = \frac{\sqrt{1+\alpha_u^2}}{2\sigma_{u_\beta}\sigma'_{u_\beta}} \exp\left[-Q\left(u_\beta, u'_\beta\right)\right] , \tag{110}$$

$$Q\left(u_\beta, u'_\beta\right) = \frac{1+\alpha_u^2}{2}\left[\frac{u_\beta^2}{\sigma_{u_\beta}^2} + \frac{2u_\beta u'_\beta \alpha_u}{\sigma_{u_\beta}\sigma_{u'_\beta}\sqrt{1+\alpha_u^2}} + \frac{u'^2_\beta}{\sigma_{u'_\beta}^2}\right] ,$$

$$P_{\eta s}(\eta, s) = P_\eta(\eta) P_s(s) = \frac{1}{2\pi\sigma_\eta\sigma_s} \exp\left[-\frac{\eta^2}{2\sigma_\eta^2} - \frac{(s-s_0)^2}{2\sigma_s^2}\right] . \tag{111}$$

In standard Gaussian notation, σ_{x_β} and $\sigma_{x'_\beta}$ are the r.m.s. beam size $\sqrt{\langle x^2\rangle}$ and angular spread $\sqrt{\langle x'^2\rangle}$, respectively, and similarly for the vertical betatron motion z, for which $z = z_\beta$ and $z' = z'_\beta$ by Eq. (78). Likewise σ_η is the momentum spread $\sqrt{\langle\eta^2\rangle}$, and σ_s is the r.m.s. bunch length $\sqrt{\langle s^2\rangle}$, with $\Delta s = s - s_0$ being the synchrotron coordinates, i.e. the position relative to the synchronous particle. The quadratic form $Q =$ constant is a tilted ellipse with correlation coefficient $\rho_x = \alpha_x/\sqrt{1+\alpha_x^2}$. The above probability distributions P must be well-matched to the Courant–Snyder invariant $\varepsilon_x = \gamma_x x_\beta^2 + 2\alpha_x x_\beta x'_\beta + \beta_x x'^2_\beta$. Using the related betatron amplitude and angle r.m.s. values σ_{x_β} and $\sigma_{x'_\beta} = \sigma_{x_\beta}\sqrt{\gamma_x/\beta_x}$, the probability $P_{x_\beta x'_\beta}$ can be rewritten as

$$P_{x_\beta x'_\beta}(x_\beta, x'_\beta) = \frac{\beta_x}{2\sigma_{x_\beta}^2} \exp\left[-\frac{\beta_x}{2\sigma_{x_\beta}^2}\left(\gamma_x x_\beta^2 + 2\alpha_x x_\beta x'_\beta + \beta_x x'^2_\beta\right)\right] . \tag{112}$$

or using the emittance ε_x in place of the variables position and angle x_β, x'_β

$$P_{\varepsilon_x}(\varepsilon_x) = \frac{\beta_x}{2\sigma_{x_\beta}^2} \exp\left[-\frac{\beta_x\varepsilon_x}{2\sigma_{x_\beta}^2}\right] \iff P_{\varepsilon_x}(\varepsilon_x) = \frac{1}{\langle\varepsilon_x\rangle} \exp\left[-\frac{\varepsilon_x}{\langle\varepsilon_x\rangle}\right] . \tag{113}$$

Here, the emittance describes the phase space area used by the beam; that is, for a phase space area covering a fraction F_{ε_x} of a Gaussian beam with r.m.s. value σ_{x_β}, the emittance at F_{ε_x} % of particles is

$$\varepsilon_x = -\frac{2\sigma_{x_\beta}^2}{\beta_x}\ln(1-F_{\varepsilon_x}) \quad \text{or} \quad F_{\varepsilon_x}(\varepsilon_x) = 1 - \exp\left[-\frac{\beta_x\varepsilon_x}{2\sigma_{x_\beta}^2}\right] \quad \text{with} \quad 0 < F_{\varepsilon_x} \le 1 . \tag{114}$$

$F_{\varepsilon_x}(\varepsilon_x)$ is the cumulative probability function and its derivative is the probability $P_{\varepsilon_x}(\varepsilon_x) = \mathrm{d}F/\mathrm{d}t$ (113). The second moment of $P_\eta(\eta)$ and the mean value of $P_{\varepsilon_x}(\varepsilon_x)$ are:

$$\langle\eta^2\rangle = \int_{-\infty}^{\infty} \eta^2 P_\eta(\eta)\mathrm{d}\eta = \sigma_\eta^2 \ \text{ and } \ \langle\varepsilon_x\rangle = \int_0^\infty \varepsilon_x P_{\varepsilon_x}(\varepsilon_x)\mathrm{d}\varepsilon_x = \frac{2\sigma_{x_\beta}^2}{\beta_x} \implies$$

$$\langle x_\beta^2\rangle \equiv \sigma_{x_\beta}^2 = \frac{\beta_x\langle\varepsilon_x\rangle}{2} \ \text{ and } \ \langle x'^2_\beta\rangle \equiv \sigma_{x'_\beta}^2 = \frac{\gamma_x\langle\varepsilon_x\rangle}{2} \implies \frac{\sigma_{x'_\beta}}{\sigma_{x_\beta}} = \sqrt{\frac{\gamma_x}{\beta_x}} = \frac{1}{\beta_x} \ \text{ if } \ \alpha_x = 0. \tag{115}$$

The last two formulae in (115) are obtained looking at Fig. 11, which shows beam boundaries at $\pm\sqrt{6}\sigma_{x_\beta}$ and $\pm\sqrt{6}\sigma_{x'_\beta}$. In analogy, the boundaries for $\langle\varepsilon_x\rangle$ would be at $\pm\sigma_{x_\beta} = \pm\sqrt{\beta_x\langle\varepsilon_x\rangle/2}$ and $\pm\sigma_{x'_\beta} = \pm\sqrt{\gamma_x\langle\varepsilon_x\rangle/2}$, yielding $\sigma_{x'_\beta}^2 = \gamma_x\langle\varepsilon_x\rangle/2$.

Figure 11 depicts the area occupied by the distribution in phase space, which parameterizes an elliptical contour surrounding a given fraction of the beam. Thus, a larger ellipse containing, say, 95% of the particles in the bunch has envelope boundaries at $\pm\sqrt{6}\sigma_{x_\beta}=\pm\sqrt{\beta_x\varepsilon_x}$ and $\pm\sqrt{6}\sigma_{x'_\beta}=\pm\sqrt{\gamma_x\varepsilon_x}$. For instance, the emittances at $F_{\varepsilon_x}=(39,\,87,\,95)\%$ of particles in phase space are $\varepsilon_x=(1,\,4,\,6)\,\sigma^2_{x_\beta}/\beta_x$. The emittance at 39% is the r.m.s. emittance, labelled $\varepsilon_{x_{\rm rms}}$.

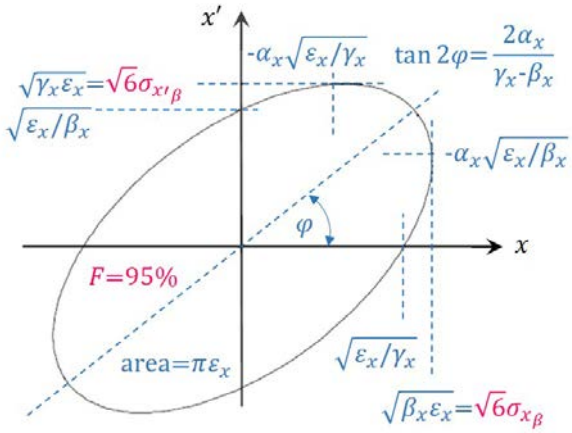

Fig. 11: Extrema, intercepts and slope of the phase space ellipse enclosing $F_{x_\beta x'_\beta}$ % of particles characterized by the Twiss parameters. The area bounded by the ellipse is equal to $\pi\varepsilon_x$.

Comment: Besides ε_x, which bounds a fraction F_{ε_x} of particles in phase space, an alternative well known emittance concept is defined as $\varepsilon_x^{\rm proj}$ ('projected emittance'), whose beam width contains a fraction $F_{\varepsilon_x}^{\rm proj}$ of particles projected onto a betatron amplitude axis. Unlike F_{ε_x} for ε_x, the beam fraction $F_{\varepsilon_x}^{\rm proj}$, for instance $\varepsilon_x^{\rm proj}=(1,\,4,\,6)\,\sigma^2_{x_\beta}/\beta_x$ is equal to $F_{\varepsilon_x}^{\rm proj}=(68,\,95,\,99)\%$. Actually, emittance measurements using beam profile monitors, like wire-scanners and gas ionization monitors, measure projected transverse beam distributions through 'integration' over the angles x', from whence σ_x and $\varepsilon_x^{\rm proj}$ are derived. On the other end, beam destructive type devices, such as scrapers, ongoing decrease of beam intensity by moving blades into the beam. This process delivers the transverse beam size versus the fraction of remaining intensity and, by differentiation, the betatron beam amplitude distribution. Therefore, emittance ε_x are by nature of the process expressed in term of the enclosed fraction of particles.

Summing up for the r.m.s. emittances derived from phase space and projected beam densities one gets (see also (115))

$$F_{\varepsilon_{x_{\rm rms}}}=F_{\varepsilon_{x_{\rm rms}}}\big(\varepsilon_{x_{\rm rms}}=\sigma^2_{x_\beta}/\beta_x\big)=1-\exp\big[-\frac{1}{2}\big]=0.39\quad\text{with}\quad\langle\varepsilon_{x_{\rm rms}}\rangle=\frac{2\sigma^2_{x_\beta}}{\beta_x}\neq\varepsilon_{x_{\rm rms}}=\frac{\sigma^2_{x_\beta}}{\beta_x}\,,$$

$$F^{\rm proj}_{\varepsilon_{x_{\rm rms}}}=F^{\rm proj}_{\varepsilon_{x_{\rm rms}}}\left(\varepsilon^{\rm proj}_{x_{\rm rms}}=\frac{\sigma^2_{x_\beta}}{\beta_x}\right)=\int_{-\sigma_{x_\beta}}^{\sigma_{x_\beta}}P^{\rm proj}_{x_\beta}(x_\beta)\mathrm{d}x_\beta=0.68\ \text{ where }\ P^{\rm proj}_{x_\beta}(x_\beta)=\frac{1}{\sqrt{2\pi}\,\sigma_{x_\beta}}\exp\Big[-\frac{x^2_\beta}{2\sigma^2_{x_\beta}}\Big],$$

$$\langle x^2_\beta\rangle=\int_{-\infty}^{\infty}x^2_\beta P^{\rm proj}_{x_\beta}(x_\beta)\mathrm{d}x_\beta=\sigma^2_{x_\beta}\ \Longrightarrow\ \langle\varepsilon^{\rm proj}_{x_{\rm rms}}\rangle=\frac{\langle x^2_\beta\rangle}{\beta_x}=\frac{\sigma^2_{x_\beta}}{\beta_x}\equiv\varepsilon^{\rm proj}_{x_{\rm rms}}\neq\langle\varepsilon_{x_{\rm rms}}\rangle\,. \tag{116}$$

Figure 12 shows the reference orbit of a synchrotron accelerator or storage ring system, referred to as the rest frame. The coordinate system attached to the rotating vector $\mathbf{r}_0(s)$ is referred to as the centre-of-mass frame, even though it is not an inertial system moving at constant velocity along a straight line.

To simplify and clarify the formalism, from now on we neglect the derivatives of the dispersion and transverse betatron functions (the vertical dispersion was earlier assumed to be null) that is:

$$D'_{x,z}=0,\quad\beta'_{x,z}=-2\alpha_{x,z}=0\ \Longrightarrow\ \tilde{D}_{x,z}=\alpha_{x,z}D_{x,z}+\beta_{x,z}D'_{x,z}=0,\quad\gamma_{x,z}=1/\beta_{x,z}\,. \tag{117}$$

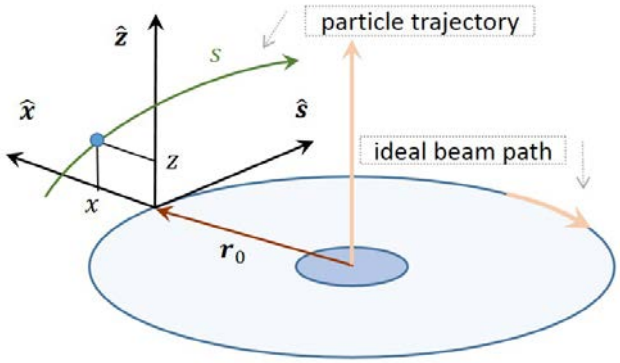

Fig. 12: Curvilinear Frenet–Serret coordinate system for particle motion in accelerator and storage rings: $\mathbf{r}(s) = \mathbf{r}_0(s) + x(s)\hat{\mathbf{x}} + z(s)\hat{\mathbf{z}}$, with $\hat{\mathbf{s}} = \frac{\mathrm{d}\mathbf{r}_0}{\mathrm{d}s} \big/ \left|\frac{\mathrm{d}\mathbf{r}_0}{\mathrm{d}s}\right|$ and $\hat{\mathbf{z}} = \hat{\mathbf{s}} \times \hat{\mathbf{x}}$.

Using the change of variables (103), in which $x'_{\beta_{1,2}}$ reduces to $x'_\beta \pm \theta/2$ since $D'_x = 0$, the Gaussian density distributions (110) and (111) can be rewritten in terms of the nine variables $\eta, s, \xi, x_\beta, x'_\beta, \theta, z, z', \zeta$ as (swapping from P to $\mathcal{P}$)

$$\mathcal{P}_{x_\beta x'_\beta}\left(x_\beta \mp \frac{D_x\gamma\xi}{2},\, x'_\beta \pm \frac{\theta}{2}\right), \quad \mathcal{P}_{zz'}\left(z,\, z' \pm \frac{\zeta}{2}\right), \quad \mathcal{P}_\eta\left(\eta \pm \frac{\gamma\xi}{2}\right), \quad \mathcal{P}_s^2(s)\,. \tag{118}$$

Consequently the transformation mapping P into $\mathcal{P}$ (Eq. 102) of the density distributions $P_{x_\beta x'_\beta}(x_\beta, x'_\beta)$, $P_{zz'}(z, z')$ and $P_{\eta s}(\eta, s)$, Eqs. (110) and (111), which are now separable since $\alpha_{x,z} = 0$, can thus be rephrased (remembering that two particles are involved and that (78) apply) as

$$P_\eta(\eta_1, \eta_2) = P_\eta(\eta_1)P_\eta(\eta_2) \mapsto \mathcal{P}_\eta\left(\eta + \frac{\gamma\xi}{2}\right)\mathcal{P}_\eta\left(\eta - \frac{\gamma\xi}{2}\right), \tag{119}$$

$$P_s(s_1, s_2) = P_s(s_1)P_s(s_2) \mapsto \mathcal{P}_s(s)\mathcal{P}_s(s) = \mathcal{P}_s^2(s), \tag{120}$$

$$P_{x_\beta}(x_{\beta_1}, x_{\beta_2}) = P_{x_\beta}(x_{\beta_1})P_{x_\beta}(x_{\beta_2}) \mapsto \mathcal{P}_{x_\beta}\left(x_\beta - \frac{D_x\gamma\xi}{2}\right)\mathcal{P}_{x_\beta}\left(x_\beta + \frac{D_x\gamma\xi}{2}\right), \tag{121}$$

$$P_{x'_\beta}(x'_{\beta_1}, x'_{\beta_2}) = P_{x'_\beta}(x'_{\beta_1})P_{x'_\beta}(x'_{\beta_2}) \mapsto \mathcal{P}_{x'_\beta}\left(x'_\beta + \frac{\theta}{2}\right)\mathcal{P}_{x'_\beta}\left(z'_\beta - \frac{\theta}{2}\right), \tag{122}$$

$$P_z(z_1, z_2) = P_z(z_1)P_z(z_2) \mapsto \mathcal{P}_z^2(z), \tag{123}$$

$$P_{z'}(z'_1, z'_2) = P_{z'}(z'_1)P_{z'}(z'_2) \mapsto \mathcal{P}_{z'}\left(z' + \frac{\zeta}{2}\right)\mathcal{P}_{z'}\left(z'_\beta - \frac{\zeta}{2}\right)\,. \tag{124}$$

The Gaussian integrals over the six variables $\eta, s, x_\beta, x'_\beta, z, z'$ can be made by means of *Mathematica*. Some calculation details of the density distribution integrals are shown for (119) and (120), which are representative of the other four integrals. Substituting the η-exp part of (111) into (119) and integrating over the momentum deviation range $\{-\infty, \infty\}$ gives,

$$\begin{aligned}
&\int_{-\infty}^{\infty} \mathrm{d}\eta\, P_\eta\Big(\eta + \frac{\gamma\xi}{2}\Big)\mathcal{P}_\eta\Big(\eta - \frac{\gamma\xi}{2}\Big) \\
&\quad = \frac{1}{2\pi\sigma_\eta^2}\int_{-\infty}^{\infty} \mathrm{d}\eta\, \exp\left[-\frac{1}{2\sigma_\eta^2}\Big(\eta + \frac{\gamma\xi}{2}\Big)^2 - \frac{1}{2\sigma_\eta^2}\Big(\eta - \frac{\gamma\xi}{2}\Big)^2\right] \\
&\quad = \frac{1}{2\pi\sigma_\eta^2}\int_{-\infty}^{\infty} \mathrm{d}\eta\, \exp\left[-\frac{1}{2\sigma_\eta^2}\left(2\eta^2 + \frac{\gamma^2\xi^2}{2}\right)\right] \\
&\quad = \frac{1}{2\pi\sigma_\eta^2}\, \exp\left[-\frac{\gamma^2\xi^2}{4\sigma_\eta^2}\right]\int_{-\infty}^{\infty} \mathrm{d}\eta\, \exp\left[-\frac{\eta^2}{\sigma_\eta^2}\right]
\end{aligned}$$

$$= \frac{1}{2\pi\sigma_\eta^2}\exp\left[-\frac{\gamma^2\xi^2}{4\sigma_\eta^2}\right]\sqrt{\pi}\sigma_\eta = \frac{1}{2\sqrt{\pi}\sigma_\eta}\exp\left[-\frac{\gamma^2\xi^2}{4\sigma_\eta^2}\right] . \tag{125}$$

Likewise, substituting the s-exp part of (111) into (120) and integrating gives

$$\int_{-\infty}^{\infty}\mathrm{d}s\,\mathcal{P}_s^2(s) = \frac{1}{2\pi\sigma_s^2}\int_{-\infty}^{\infty}\mathrm{d}s\exp\left[-\frac{(s-s_0)^2}{2\sigma_s^2}\right]\exp\left[-\frac{(s-s_0)^2}{2\sigma_s^2}\right] = \frac{1}{2\sqrt{\pi}\sigma_s} . \tag{126}$$

Hence, the particle density distribution $\mathcal{P}$ is the product of the six terms obtained after integrating the six density distributions (right part of Eqs. (119) to (124)) with respect to the variables $\eta, s, x_\beta, x'_\beta, z, z'$, times N_b, the number of particles per bunch is

$$\begin{aligned}\mathcal{P}(\xi,\theta,\zeta) &= N_b\prod_{u=\eta,s,x_\beta}^{x'_\beta,z,z'}\int_{-\infty}^{\infty}\mathrm{d}u\,\mathcal{P}_u\Big(u\pm\frac{\gamma\lambda_u}{2}\Big)\mathcal{P}_u\Big(u\mp\frac{\gamma\lambda_u}{2}\Big)\\ &= N_b\,\frac{\exp\Big[-\frac{\gamma^2\xi^2}{4}\Big(\frac{1}{\sigma_\eta^2}+\frac{D_x^2}{\sigma_{x_\beta}^2}\Big)-\frac{\theta^2}{4\sigma_{x'_\beta}^2}-\frac{\zeta^2}{4\sigma_{z'}^2}\Big]}{64\pi^3\sigma_{x_\beta}\sigma_{x'_\beta}\sigma_z\sigma_{z'}\sigma_\eta\sigma_s} .\end{aligned} \tag{127}$$

where λ_u stands for either ξ, 0, $D_x\xi$, θ, or ζ. At present $\mathcal{P}$ is reduced to the variables ξ, θ, ζ.

To complete the transformation back to the laboratory system, $\bar\beta$ must be replaced by its LAB frame approximation $\beta\gamma\sqrt{\xi^2+\theta^2+\zeta^2}/2)$. Let us define the Piwinski IBS constant $\mathcal{A}_\mathrm{P}$ as

$$\mathcal{A}_\mathrm{P} = \frac{cr_\mathrm{i}^2N_b}{64\pi^2\beta^3\gamma^4\sigma_{x_\beta}\sigma_{x'_\beta}\sigma_z\sigma_{z'}\sigma_\eta\sigma_s} = \frac{cr_\mathrm{i}^2N_b}{64\pi^2\beta^3\gamma^4\varepsilon_x\varepsilon_z\varepsilon_s} , \quad \text{wherein} \tag{128}$$

$$\sigma_x^2=\sigma_{x_\beta}^2+D_x^2\sigma_\eta^2 , \;\; \sigma_z^2=\sigma_{z_\beta}^2 , \;\; \sigma_{x_\beta,z_\beta}^2=\beta_{x,z}\varepsilon_{x,z} , \;\; \sigma_{x'_\beta,z'_\beta}^2=\frac{\varepsilon_{x,z}}{\beta_{x,z}} , \;\; \sigma_{x_\beta,z_\beta}\sigma_{x'_\beta,z'_\beta}=\varepsilon_{x,z} , \;\; \sigma_\eta\sigma_s=\varepsilon_s .$$

Now, using (92) and (127) the full set of Eq. (109), in which the factors $D'_{x,z}$ and $\alpha_{x,z}$ have to be removed because or the additional assumption $D'_{x,z}=\beta'_{x,z}=0$, can be easily rearranged as

$$\begin{aligned}\left\langle\begin{pmatrix}\frac{\mathrm{d}}{\mathrm{d}t}\frac{\langle H\rangle}{\gamma^2}\\ \frac{\mathrm{d}}{\mathrm{d}t}\frac{\langle\varepsilon_x\rangle}{\beta_x}\\ \frac{\mathrm{d}}{\mathrm{d}t}\frac{\langle\varepsilon_z\rangle}{\beta_z}\end{pmatrix}\right\rangle &= 4\mathcal{A}_\mathrm{P}\iiint_{-\infty}^{\infty}\frac{\mathrm{d}\xi\,\mathrm{d}\theta\,\mathrm{d}\zeta}{(\xi^2+\theta^2+\zeta^2)^{3/2}}\exp\left[-\frac{\gamma^2\xi^2}{4}\left(\frac{1}{\sigma_\eta^2}+\frac{D_x^2}{\sigma_{x_\beta}^2}\right)-\frac{\theta^2}{4\sigma_{x'_\beta}^2}-\frac{\zeta^2}{4\sigma_{z'_\beta}^2}\right]\\ &\times\begin{Bmatrix}\theta^2+\zeta^2-2\xi^2\\ \xi^2+\zeta^2-2\theta^2+\frac{D_x^2}{\beta_x^2}\gamma^2\big(\zeta^2+\theta^2-2\xi^2\big)\\ \xi^2+\theta^2-2\zeta^2\end{Bmatrix}\ln\left[\frac{q^2}{4}\big(\xi^2+\theta^2+\zeta^2\big)\right] .\end{aligned} \tag{129}$$

in which the parameter q is introduced for convenience

$$q = \beta\gamma\sqrt{\frac{2b_\mathrm{max}}{r_\mathrm{i}}} \approx 2\beta\gamma\sqrt{\frac{\sigma_z}{r_\mathrm{i}}} , \quad \text{with} \quad b_\mathrm{max}\overset{\mathrm{def}}{=}2\sigma_z , \quad \text{(half beam or bunch height)} . \tag{130}$$

Comment: The Coulomb logarithm C_log in the rest frame is 'hidden' inside Eq. (129) since $\ln\big[\frac{q^2}{4}\big(\xi^2+\theta^2+\zeta^2\big)\big] = C_\mathrm{log}+\ln\big[\frac{\gamma^2}{4}\big(\xi^2+\theta^2+\zeta^2\big)\big]$, with $C_\mathrm{log}=\ln\big[\frac{2\beta^2b_\mathrm{max}}{r_\mathrm{i}}\big]$; see (97).

Discussion on an invariant

In the simplest circumstances, intrabeam scattering of particles in a bunched beam may cause dilution of the beam in phase space, leading to continuous growth of the momentum spread and/or growth of one or both transverse emittances. The importance of the transition energy is briefly revisited here in the light of the invariants.

The behaviour of the beam can be described via a global invariant which can be arranged in a form close to the sum of the mean value of the change in emittance $\langle \varepsilon_{x,z} \rangle$ and the change in momentum deviation $\langle H \rangle$ over the collisions of all particles, as discussed above. Then, multiplying the top momentum deviation change term $\frac{\mathrm{d}}{\mathrm{d}t}\big[\langle H \rangle / \gamma^2\big]$ in the left part of Eq. (129) by the factor $(1-\gamma^2 D_x^2/\beta_x^2)$ and adding it to the emittance change middle and bottom terms $\frac{\mathrm{d}}{\mathrm{d}t}\big[\langle \varepsilon_{x,z} \rangle \beta_{x,z}\big]$ gives a result equal to zero:

$$\frac{\mathrm{d}}{\mathrm{d}t}\left[\langle H \rangle \left(\frac{1}{\gamma^2} - \frac{D_x^2}{\beta_x^2}\right) + \frac{\langle \varepsilon_x \rangle}{\beta_x} + \frac{\langle \varepsilon_z \rangle}{\beta_z}\right] = 0 \,. \tag{131}$$

Unfortunately, the quantity acted on by the derivative operator $\mathrm{d}/\mathrm{d}t$ is not an invariant, because the ratio D_x/β_x varies along the ring lattice (i.e. it depends on the longitudinal or azimuthal coordinate s along the lattice). However, the smooth focusing approximation holds for a weak-focusing or smooth lattice. So, from the betatron and dispersion functions, the momentum compaction factor and the transition energy factor, we have

$$\langle \beta_{x,z} \rangle \equiv \frac{R}{Q_{x,z}}, \quad \langle D_x \rangle \equiv \frac{R}{Q_{x,z}^2}, \quad \alpha_p = \frac{\langle D_{x,z}(s) \rangle}{\rho(s)} = \frac{1}{\gamma_t^2} \equiv \frac{\langle D_{x,z} \rangle}{R} = Q_{x,z}^{-2} \implies \left\langle \frac{D_{x,z}}{\beta_{x,z}} \right\rangle \equiv \frac{1}{\gamma_t^2} \,.$$

(where $\langle \cdot \rangle$ denotes an average over the lattice). After straightforward integration with respect to t (with the integrand now being a constant), we get the invariant

$$\langle H \rangle \left(\frac{1}{\gamma^2} - \frac{1}{\gamma_t^2}\right) + \frac{\langle \varepsilon_x \rangle}{\beta_x} + \frac{\langle \varepsilon_z \rangle}{\beta_z} = \text{constant} \,, \tag{132}$$

where $\eta_t = \gamma_t^{-2} - \gamma^{-2}$ is the *slip factor*.

Above transition energy ($\eta_t \geq 0$)

- The coefficient of $\langle H \rangle$ in (132) is negative and the total oscillation energy can increase as long as it does not exceed other limitations. Therefore no equilibrium distribution can exist.

Below transition energy ($\eta_t < 0$)

- The sum of the three positive invariants, and hence of the three oscillation energies, is bounded (i.e. the IBS emittance growth is constrained). So the emittances are redistributed in all three phase planes, holding the whole phase space invariant; the particle density distribution P is stable, and an equilibrium exists (like the situation of gas molecules in a closed box where the focusing forces are produced by the wall of the box).

Growth rates calculation (neglecting $\alpha_{x,z}$ and $D'_{x,z}$)

In his original model of 1974 [1], Piwinski derived expressions for the variations in the transverse oscillation amplitudes (similarly the square root of the transverse emittances) and momentum spread per unit time caused by a scattering event, using the *smooth focusing approximation* in which only the mean values of the lattice functions are considered; see Eq. (62). In addition, as seen earlier, the variations of the betatron and dispersion functions are neglected and a zero vertical dispersion function along the ring lattice is assumed, namely

$$\langle \beta_x \rangle = \frac{R}{Q_x} \,, \quad \langle D_x \rangle = \frac{R}{Q_x^2} \,, \quad \beta'_{x,z} = -2\alpha_{x,z} = 0 \quad D'_{x,z} = 0 \,, \quad \tilde{D}_x = \alpha_x D_x + \beta_x D'_x = 0 \,, \quad D_z = 0 \,, \tag{133}$$

where R is the mean radius of the ring and $Q_{x,z}$ are the transverse betatron tunes.

The longitudinal, horizontal and vertical growth times $\tau_{\eta,x,z}^{-1}$ are given by

$$\frac{1}{\tau_\eta}=\frac{1}{\sigma_\eta}\frac{d\sigma_\eta}{dt}=\frac{1}{2\sigma_\eta^2}\frac{d\sigma_\eta^2}{dt}=\frac{1}{2\langle\eta^2\rangle}\frac{d\langle\eta^2\rangle}{dt}=\frac{1}{2\langle H\rangle}\frac{d\langle H\rangle}{dt}\quad\overset{\text{sol.}}{\Longrightarrow}\quad\langle H\rangle=\langle H_0\rangle\exp\Big[\frac{2t}{\tau_\eta}\Big]\,,\tag{134}$$
$$\frac{1}{\tau_x}=\frac{1}{\sigma_{x_\beta}}\frac{d\sigma_{x_\beta}}{dt}=\frac{1}{2\sigma_{x_\beta}^2}\frac{d\sigma_{x_\beta}^2}{dt}=\frac{1}{2\langle x_\beta^2\rangle}\frac{d\langle x_\beta^2\rangle}{dt}=\frac{1}{2\langle\varepsilon_x\rangle}\frac{d\langle\varepsilon_x\rangle}{dt}\quad\overset{\text{sol.}}{\Longrightarrow}\quad\langle\varepsilon_x\rangle=\langle\varepsilon_{x_0}\rangle\exp\Big[\frac{2\,t}{\tau_\eta}\Big]\,.$$

where σ_η is the r.m.s. relative momentum spread, H_0 and ε_{x_0} are the natural relative momentum spread squared and equilibrium transverse emittance in the absence of IBS.

At this place, the projected r.m.s. emittance onto the x-axis $\langle\varepsilon_{x_{\rm rms}}^{\rm proj}\rangle=\sigma_{x_\beta}^2/\beta_x$ $\big($equal to $\varepsilon_{x_{\rm rms}}^{\rm proj}\big)$ is chosen rather than the emittance defined by (116), that is $\langle\varepsilon_{x_{\rm rms}}\rangle=2\sigma_{x_\beta}^2/\beta_x$ $\big($not equal to $\varepsilon_{x_{\rm rms}}\big)$, idem for $\langle\varepsilon_{z_{\rm rms}}\rangle$, and using $\sigma_\eta^2=\langle\eta^2\rangle$ for the relative momentum deviation squared. From now on we drop the flags 'proj' and 'rms' from the emittance notation.

Comment: The IBS growth times depend of the instantaneous beam emittance and momentum deviation values. So, it is necessary to use an iterative procedure to compute the growth times and derive the evolution of the emittances and momentum deviation. The IBS growth rates are defined by (134), where τ_η and $\tau_{x,z}$ are the longitudinal and transverse IBS growth times of the relative momentum spread squared H and transverse emittances ε_{x_0,z_0}. Adding 'synchrotron radiation damping'(SRD) effect with damping times $\tau_{\eta_{\rm srd}}$, $\tau_{x_{\rm srd}}$ and $\tau_{z_{\rm srd}}$ to IBS effect, the quantities $H=\eta^2$ and $\varepsilon_{x,z}$ will evolve in accordance with [30] as:

$$\frac{{\rm d}H}{dt}=-\frac{2}{\tau_{\eta_{\rm srd}}}\big(H-H_0\big)+\frac{2}{\tau_\eta}H\qquad\frac{{\rm d}\varepsilon_{x,z}}{dt}=-\frac{2}{\tau_{x_{\rm srd},z_{\rm srd}}}\big(\varepsilon_{x,z}-\varepsilon_{x_0,z_0}\big)+\frac{2}{\tau_{x,z}}\varepsilon_{x,z}\,.\tag{135}$$

Equilibrium emittances $\varepsilon_{x_{\rm eq},z_{\rm eq}}$ and $H_{\eta_{\rm eq}}$ are reached once ${\rm d}\varepsilon_{x,z}/{\rm d}t=0$ and ${\rm d}H/{\rm d}t=0$. One find

$$H_{\eta_{\rm eq}}=\frac{\tau_\eta}{\tau_\eta-\tau_{\eta_{\rm srd}}}H_0\qquad\varepsilon_{x_{\rm eq},z_{\rm eq}}=\frac{\tau_{x,z}}{\tau_{x,z}-\tau_{x_{\rm srd},z_{\rm srd}}}\varepsilon_{x_0,z_0}\,.\tag{136}$$

As said above, iterative computations are required simultaneously in longitudinal and transverse planes to get the equilibrium.

Warning! The form and the units of the first column of Eq. (129), (e.g. $\beta_x^{-1}{\rm d}\langle\varepsilon_x\rangle/{\rm d}t$ in [rad^2]) do not fit those of Eq. (134) where $1/\tau_{\eta,x,z}$ is in [s^{-1}], as shown below. Therefore, the following quantities, introduced for suitability, (the last two are in [rad^{-2}]) will be added to the last column of (138) below for compatibility

$$\frac{(1-d^2)\,q^2}{c^2}=\frac{\gamma^2}{\sigma_\eta^2}\qquad\frac{a^2q^2}{c^2}=\frac{1}{\sigma_{x'_\beta}^2}\qquad\frac{b^2q^2}{c^2}=\frac{1}{\sigma_{z'_\beta}^2}\,,\tag{137}$$

For example, considering τ_x^{-1} and ε_x, we compute $(2\langle\varepsilon_x\rangle)^{-1}{\rm d}\langle\varepsilon_x\rangle/{\rm d}t=(2\sigma_{x_\beta}^2)^{-1}{\rm d}\langle\varepsilon_x\rangle/{\rm d}t=(2\sigma_{x'_\beta}^2\beta_x)^{-1}{\rm d}\langle\varepsilon_x\rangle/{\rm d}t=(a^2q^2/2\,c^2)^{-1}{\rm d}\langle\varepsilon_x/\beta_x\rangle/{\rm d}t$ (with $\alpha_x=0$) using (115)–(137); similarly for $\tau_{z,\eta}^{-1}$, we find

$$\begin{pmatrix}\frac{1}{\tau_\eta}\\ \frac{1}{\tau_x}\\ \frac{1}{\tau_z}\end{pmatrix}=\begin{pmatrix}\frac{1}{2\sigma_\eta^2}\frac{{\rm d}\sigma_\eta^2}{{\rm d}t}\\ \frac{1}{2\sigma_{x_\beta}^2}\frac{{\rm d}\sigma_{x_\beta}^2}{{\rm d}t}\\ \frac{1}{2\sigma_{z_\beta}^2}\frac{{\rm d}\sigma_{z_\beta}^2}{{\rm d}t}\end{pmatrix}=\begin{pmatrix}\frac{1}{2\langle H\rangle}\frac{d\langle H\rangle}{dt}\\ \frac{1}{2\langle\varepsilon_x\rangle}\frac{d\langle\varepsilon_x\rangle}{dt}\\ \frac{1}{2\langle\varepsilon_z\rangle}\frac{d\langle\varepsilon_z\rangle}{dt}\end{pmatrix}=\frac{q^2}{2\,c^2}\begin{pmatrix}(1-d^2)\frac{\rm d}{{\rm d}t}\frac{\langle H\rangle}{\gamma^2}\\ a^2\quad\frac{\rm d}{{\rm d}t}\frac{\langle\varepsilon_x\rangle}{\beta_x}\\ b^2\quad\frac{\rm d}{{\rm d}t}\frac{\langle\varepsilon_z\rangle}{\beta_z}\end{pmatrix}\neq\begin{pmatrix}\frac{\rm d}{{\rm d}t}\frac{\langle H\rangle}{\gamma^2}\\ \frac{\rm d}{{\rm d}t}\frac{\langle\varepsilon_x\rangle}{\beta_x}\\ \frac{\rm d}{{\rm d}t}\frac{\langle\varepsilon_z\rangle}{\beta_z}\end{pmatrix}\,.\tag{138}$$

where for $D_z = 0$ (see also Eq. (130)),

$$a = \frac{\sigma_h}{\gamma\sigma_{x'_\beta}}, \quad b = \frac{\sigma_h}{\gamma\sigma_{z'_\beta}}, \quad c = q\sigma_h = \Big(\beta\gamma\sqrt{\frac{2b_{\max}}{r_{\rm i}}}\Big)\sigma_h, \quad q = \gamma\exp\Big[\frac{C_{\log}}{2}\Big] \quad d^2 = 1 - \frac{\sigma_h^2}{\sigma_\eta^2}\,, \tag{139}$$

$$\frac{1}{\sigma_h^2} = \left(\frac{1}{\sigma_\eta^2} + \frac{D_x^2}{\sigma_{x_\beta}^2}\right) \iff \sigma_h = \frac{\sigma_\eta\sigma_{x_\beta}}{\sigma_x}$$

or equivalently

$$a = \frac{\beta_x\sigma_\eta}{\gamma\sigma_x}, \quad b = \frac{\beta_z\sigma_\eta}{\gamma\sigma_x}, \quad c = \frac{\sigma_\eta\sigma_{x_\beta}}{\sigma_x}\exp\Big[\frac{C_{\log}}{2}\Big] \quad d = \frac{D_x\sigma_\eta}{\sigma_x}\,, \tag{140}$$

The remaining three integrals over ξ, θ, ζ in Eq. (129) still need to be computed to get the mean change of the invariants $\langle\varepsilon_{x,z}\rangle$ and $\langle H\rangle = \eta^2$ due to the multiple collisions of the bunch particles circulating along the lattice. To this end, a first change of variables $(\xi, \theta, \zeta) \to (u, v, w)$ is made as a first step toward the integration over the 'angles' ξ, θ and ζ; that is,

$$\big(2u = q\xi,\ 2v = q\theta,\ 2w = q\zeta\big) \implies u^2 + v^2 + w^2 = \frac{q^2}{4}(\xi^2 + \theta^2 + \zeta^2)\,. \tag{141}$$

The aim of these approximations and changes of variables is to derive an 'almost closed-form' and manageable IBS formula for estimation of the rise times of the mean oscillation amplitudes, which determine the bunch dimensions caused by the effects of IBS. Hence, in the framework of the Piwinski model, the growth rates are calculated in accordance with Eq. (129) reformulated using the new set of variables (u, v, w).

This gives, converting in Eq. (129) the expressions $\gamma^2(1/\sigma_\eta^2 + D_x^2/\sigma_{x_\beta}^2)$ into q^2/c^2 and $\gamma^2 D_x^2/\beta_x^2$ into d^2/a^2 using (139) and (140)

$$\begin{pmatrix} \frac{1}{\tau_\eta} \\ \frac{1}{\tau_x} \\ \frac{1}{\tau_z} \end{pmatrix} = \left\langle \frac{q^2}{2\,c^2} \begin{pmatrix} (1-d^2)\,\frac{\mathrm{d}}{\mathrm{d}t}\frac{\langle H\rangle}{\gamma^2} \\ a^2 \quad \frac{\mathrm{d}}{\mathrm{d}t}\frac{\langle\varepsilon_x\rangle}{\beta_x} \\ b^2 \quad \frac{\mathrm{d}}{\mathrm{d}t}\frac{\langle\varepsilon_z\rangle}{\beta_z} \end{pmatrix} \right\rangle = \frac{8\mathcal{A}_{\rm P}}{c^2}\iiint_{-\infty}^{\infty}\exp\Big[-\frac{1}{c^2}\big(u^2 + a^2v^2 + b^2w^2\big)\Big]$$

$$\times\,\frac{\ln[u^2+v^2+w^2]}{\big(u^2+v^2+w^2\big)^{3/2}} \left\{ \begin{matrix} (1-d^2)(-2u^2+v^2+w^2) \\ a^2\big((u^2-2v^2+w^2) + \big(\frac{d}{a}\big)^2(-2u^2+v^2+w^2)\big) \\ b^2(u^2+v^2-2w^2) \end{matrix} \right\} \mathrm{d}u\,\mathrm{d}v\,\mathrm{d}w\,, \tag{142}$$

Eq. (142) is then further transformed to a triple integral in spherical-like coordinates $(u, v, w) \to (\sqrt{r}, \mu, \nu)$ with

$$\big(u = \sqrt{r}\sin\mu\cos\nu,\ v = \sqrt{r}\sin\mu\sin\nu,\ w = \sqrt{r}\cos\mu\big) \implies u^2 + v^2 + w^2 = r\,, \tag{143}$$

which readily gives, using *Mathematica*

$$\begin{pmatrix} \tau_\eta^{-1} \\ \tau_x^{-1} \\ \tau_z^{-1} \end{pmatrix} = \frac{\mathcal{A}_{\rm P}}{c^2}\int_0^\infty \mathrm{d}r \int_0^\pi \mathrm{d}\mu \int_0^{2\pi} \mathrm{d}\nu\,\sin[\mu]\exp[-rD(\mu,\nu)]\ln[r]$$

$$\times \left\{ \begin{matrix} (1-d^2)\Big[\cos^2[\mu] - \frac{1}{2}(1 + 3\cos[2\nu]\sin^2[\mu])\Big] \\ \big(a^2+d^2\big)\big(1+3\cos[2\mu]\big) + 6\big(a^2-d^2\big)\cos[2\nu]\sin^2[\mu] \\ -2\,b^2\big(1+3\cos[2\mu]\big) \end{matrix} \right\}\,, \tag{144}$$

where

$$D(\mu,\nu)=\frac{1}{c^2}\Big(b^2\cos^2[\mu]+\sin^2[\mu]\big(\cos^2[\nu]+a^2\sin^2[\nu]\big)\Big)\,. \tag{145}$$

Therefore, introducing the following three functions:

$$g_1[\mu,\nu]=1-3\sin^2[\mu]\cos^2[\nu]\quad g_2[\mu,\nu]=1-3\sin^2[\mu]\sin^2[\nu]\quad g_3[\mu,\nu]=1-3\cos^2[\mu]\,, \tag{146}$$

Eq. (144) can be cast in the compact form, in which the outer bracket $\langle\,\cdot\,\rangle$ averages over the lattice parameters,

$$\begin{pmatrix}\tau_\eta^{-1}\\ \tau_x^{-1}\\ \tau_z^{-1}\end{pmatrix}=\left\langle\frac{q^2}{2\,c^2}\begin{bmatrix}(1-d^2)\\ a^2\\ b^2\end{bmatrix}\frac{\mathrm{d}}{\mathrm{d}t}\begin{bmatrix}\langle H\rangle/\gamma^2\\ \langle\varepsilon_x\rangle/\beta_x\\ \langle\varepsilon_z\rangle/\beta_z\end{bmatrix}\right\rangle=\frac{\mathcal{A}_{\mathrm{P}}}{c^2}\int_0^\infty\mathrm{d}r\int_0^\pi\mathrm{d}\mu\int_0^{2\pi}\mathrm{d}\nu$$
$$\times\,\sin[\mu]\exp[-rD(\mu,\nu)]\ln[r]\begin{Bmatrix}(1-d^2)\,g_1[\mu,\nu]\\ a^2g_2[\mu,\nu]+d^2g_1[\mu,\nu]\\ b^2g_3[\mu,\nu]\big)\end{Bmatrix}\,. \tag{147}$$

Now, let us define the 'scattering function' by means of the triple integrals

$$f(a,b,c)=2\int_0^\pi\mathrm{d}\mu\int_0^{2\pi}\mathrm{d}\nu\,\sin[\mu]\,(1-3\cos^2[\mu])\int_0^\infty\mathrm{d}\rho\,\log[c^2\rho]\exp\Big[-\rho\,D_0(\mu,\nu)\Big] \tag{148}$$

where a new variable $\rho=r/c^2$ is introduced, a,b,c being defined in (139) and

$$D_0(\mu,\nu)=\Big(\sin^2[\mu]\big(a^2\cos^2[\nu]+b^2\sin^2[\nu]\big)+\cos^2[\mu]\Big)\,. \tag{149}$$

Notice that $D_0(\mu,\nu)\neq D(\mu,\nu)$. The function $\mathrm{f(a,b,c)}$ cannot be evaluated in closed form over the three variables, but the single integral over ρ can be solved analytically (e.g. by *Mathematica*):

$$\int_0^\infty\mathrm{d}\rho\log[c^2\rho]\exp\big[-\rho\,D_0(\mu,\nu)\big]=\frac{2\log c-C_{\text{Euler}}-\log\big[D_0(\mu,\nu)\big]}{D_0(\mu,\nu)}\,, \tag{150}$$

where $C_{\text{Euler}}=0.5772$ is Euler's constant. Thus, (148) reduces to the double integral

$$f(a,b,c)=2\int_0^\pi\mathrm{d}\mu\int_0^{2\pi}\mathrm{d}\nu\,\sin[\mu]\,\big(1-3\cos^2[\mu]\big)\,\frac{2\log c-C_{\text{Euler}}-\log\big[D_0(\mu,\nu)\big]}{D_0(\mu,\nu)}\,, \tag{151}$$

From (139) we obtain $2\log c=C_{\log}+2\log[\gamma\sigma_h]\approx C_{\log}$ assuming that $C_{\log}\gg\log[\gamma\sigma_h]$. This approximation sounds fine as usually $10\lesssim C_{\log}\lesssim 20$ $\big($e.g. 7 Tev LHC: $\gamma=7000$, $\sigma_\eta\approx10^{-4}$, $C_{\log}\approx20$, and taking $\sigma_h\approx\sigma_\eta$ we get $\log[c^2]\approx C_{\log}\gg\log\big[\gamma^2\sigma_\eta^2\big]=-0.7\big)$.

Following Evans and Zotter approach [25], the scattering function (151) is first transformed by a change of variables ($x=\cos\mu$, $y=2\,\nu$), using the periodicity of π and symmetry about $\pi/2$ of $\cos^2[\nu]$ and $\sin^2[\nu]$ (as also μ) which allows to replace the limit π of μ by $\pi/2$ and 2π of ν by $\pi/2$ and then to multiply the integral by an additional factor 8. Therefore, since $\mathrm{d}\mu\,\mathrm{d}\nu=-(2\,\sin[\mu])^{-1}\mathrm{d}x\,\mathrm{d}y$, and with the new limits of integration ($0\leq\mu\leq\pi/2\rightarrow1\leq x\leq0$) and ($0\leq\nu\leq\pi/2\rightarrow0\leq y\leq\pi$), the scattering function (151) becomes :

$$f(a,b,c)=8\int_0^1\mathrm{d}x\int_0^\pi\mathrm{d}y\,\big(1-3\cos^2[\mu]\big)\,\frac{2\log c-C_{\text{Euler}}-\log\big[D_0(\mu,\nu)\big]}{D_0(\mu,\nu)}\,. \tag{152}$$

Finally, Eq. (152) can be reduced to the single integral representation, see [25] and [28], [3], [24]:

$$f(a,b,c) = 8\pi \int_0^1 \left(2\,\ln\left[\frac{\tilde{C}}{2}\left\{\frac{1}{\sqrt{P(x)}} + \frac{1}{\sqrt{Q(x)}}\right\}\right] - C_{\text{Euler}}\right) \frac{1-3x^2}{\sqrt{P(x)Q(x)}}\,\mathrm{d}x, \tag{153}$$

$$\text{with} \quad P(x) = a^2 + (1-a^2)x^2, \quad Q(x) = b^2 + (1-b^2)x^2, \quad \tilde{C} = \log[c^2] - C_{\text{Euler}}\,.$$

The function $f(a,b,c)$ is the 'new scattering function' (see [25] for a full, clear and detailed derivation). Except for a few cases, its calculation requires numerical integration.

After some more work the IBS growth rates for bunched beams can be cast into the compact form that suits Eq. (147)

$$\begin{pmatrix} \dfrac{1}{\tau_\eta} \\ \dfrac{1}{\tau_x} \\ \dfrac{1}{\tau_z} \end{pmatrix} = \mathcal{A}_{\text{P}} \begin{pmatrix} \dfrac{\sigma_{x_\beta}^2}{\sigma_x^2}\, f(a,b,c) \\ f\left(\dfrac{1}{a}, \dfrac{b}{a}, \dfrac{c}{a}\right) + \dfrac{D_x^2\sigma_\eta^2}{\sigma_{x_\beta}^2} f(a,b,c) \\ f\left(\dfrac{1}{b}, \dfrac{a}{b}, \dfrac{c}{b}\right) \end{pmatrix}. \tag{154}$$

where $\sigma_{x_\beta}^2/\sigma_x^2 = 1 - D_x^2\sigma_\eta^2/\sigma_x^2 = 1 - d^2 \equiv \sigma_h^2/\sigma_\eta^2$ according to (139) and (140). Either Eq. (148) or Eq. (153) can be used for $f(a,b,c)$ but it is faster to evaluate the growth rates with the single integral. See the appendix A for a proof of the equivalence between the two formulations (147) and (154).

3.3 The Bjorken–Mtingwa IBS model

3.3.1 Beam phase space density and emittance

A Gaussian probability distribution is taken to characterize the density of the beam in the six-dimensional phase space $\{\mathbf{r}, \mathbf{p}\}$, with $\mathbf{r} = (x, z, s)$ and $\mathbf{p} = (p_x, p_z, p_s)$, where x, z and s stand for the horizontal, vertical and longitudinal directions. The model is formulated as follows (see [2]), in connection with the work of Piwinski [1] (see also [26] for a more recent and enlightening discussion of the topic):

$$\begin{gathered} P(\mathbf{r},\mathbf{p}) = \frac{N_b}{\Gamma}\exp\big[-S(\mathbf{r},\mathbf{p})\big], \qquad \Gamma = \int \mathrm{d}^3\mathbf{r}\,\mathrm{d}^3\mathbf{p}\exp\big[-S(\mathbf{r},\mathbf{p})\big], \\ S(\mathbf{r},\mathbf{p}) = \frac{1}{2}\sum_{i,j=1}^{3}\Big(A_{ij}\delta p_i\delta p_j + 2B_{ij}\delta p_i\delta r_j + C_{ij}\delta r_i\delta r_j\Big) = S^{(x)} + S^{(z)} + S^{(s)}\,, \end{gathered} \tag{155}$$

where $P(\mathbf{r},\mathbf{p})$ is the phase space density of the beam containing N_b particles, Γ is the phase space 'volume' of the beam and $S(\mathbf{r},\mathbf{p})$ represents the nature of the Gaussian particle beam probability distribution, with $\delta\mathbf{r}$ and $\delta\mathbf{p}$ denoting the position and momentum from the reference values $\mathbf{r}$ and $\mathbf{p}$. Upon working out the coefficients A_{ij}, B_{ij} and C_{ij}, the expression for $S(\mathbf{r},\mathbf{p})$ can be written as

$$\begin{gathered} S(\mathbf{r},\mathbf{p}) = S^{(x)} + S^{(z)} + S^{(s)}, \\ S^{(x)} = \frac{\beta_x}{2\sigma_{x_\beta}^2}\big(\gamma_x x_\beta^2 + 2\alpha_x x_\beta x'_\beta + \beta_x x'^2_\beta\big), \quad S^{(z)} = \frac{\beta_z}{2\sigma_{z_\beta}^2}\big(\gamma_z z_\beta^2 + 2\alpha_z z_\beta z'_\beta + \beta_z z'^2_\beta\big), \\ S^{(s)} = \frac{\eta^2}{2\sigma_\eta^2} + \frac{(s-s_0)^2}{2\sigma_s^2}\,, \end{gathered} \tag{156}$$

where $\alpha_{x,z}$, $\beta_{x,z}$ and $\gamma_{x,z}$ are the Twiss parameters, $\varepsilon_{x,z}$ are the r.m.s. transverse beam emittances, ε_s is the r.m.s. longitudinal beam emittance, σ_η is the r.m.s beam momentum spread, σ_s is the r.m.s. beam

length, and $\sigma_{x,z}$ are the r.m.s. beam width and height. Moreover,

$$\varepsilon_x = \frac{\sigma_{x_\beta}^2}{\beta x}\,, \quad \varepsilon_z = \frac{\sigma_{z_\beta}^2}{\beta z}\,, \quad \varepsilon_s = \sigma_\eta \sigma_s\,, \quad x_\beta = x - D_x\eta\,, \qquad (157)$$
$$z_\beta = z - D_z\eta\,, \quad x'_\beta = x' - D'_x\eta\,, \quad z'_\beta = z' - D'_z\eta$$

where

$$x' = \frac{\Delta p_x}{p}, \quad z' = \frac{\Delta p_z}{p}, \quad \eta = \frac{\Delta p}{p}\,.$$

From now on the Heaviside–Lorentz (HL) units $\epsilon_0 = \hbar = c = 1$ will be used instead of the SI units kg, m, s etc. (with a few exceptions). To convert back to SI units, we must restore the missing factors $\epsilon_0, \hbar$ and c.

Comment: Since $\hbar \stackrel{\text{def}}{=} h/2\pi = 1.054 \times 10^{-34}\,\text{J s}$, in HL units the value of the Planck constant is $h = 2\pi$. Referring to the footnote associated with Eq. (1), the number of 'single-particle states' in the momentum volume $\mathrm{d}^3\mathbf{p}$ is $\mathrm{d}^3\mathbf{p}/h^3$, which in HL units is $\mathrm{d}^3\mathbf{p}/(2\pi)^3$.

3.3.2 Two-body scattering

The Bjorken and Mtingwa approach to IBS modelling is based on the *S-matrix*, which is a time-evolution operator relating the transition from an *initial* (quantum) state $|i\rangle$ to a *final* state $|f\rangle$ of a physical system undergoing a scattering process; the matrix elements of S are inner products denoted by $\langle f|S|i\rangle$.

Comment: The S-matrix is proportional to the *amplitude* $\mathcal{M}$, which represents the physics of the process [31]: $S \propto (2\pi)^4\delta^4(p_f - p_i)\mathcal{M}$ (which we take for granted at this stage), where p_f and p_i are the 4-momenta of the outgoing and incoming states. The δ-function enforces the momentum conservation of the process.

The squared modulus $|\langle f|S|i\rangle|^2$ is interpreted as a *transition probability* $\mathcal{P}$ for a transition from an initial state to a final one. See the appendix B for more details about this topic. Bjorken's formalism provides new insight into the other theories; in particular, the IBS calculations allow for the case of *strong-focusing* lattices.

In a two-body scattering process, particles 1 and 2 with 4-momenta $p^\mu_{1,2}$ (written in brief as $p_{1,2} \stackrel{\text{def}}{=} p^\mu_{1,2}$), i.e. with energy–momentum 4-vectors $p^\mu_{1,2}$, interact with each other to give the following two 4-momenta after collision: $p'_{1,2} \stackrel{\text{def}}{=} p'^\mu_{1,2}$; cf. Eq. (160). The vectors $\mathbf{p}_{1,2}$ are the usual 3-momenta (e.g. $\mathbf{p}_1 + \mathbf{p}_2 \to \mathbf{p}'_1 + \mathbf{p}'_2$ for 3-momenta and $p_1 + p_2 \to p'_1 + p'_2$ for 4-momenta). The *transition rate* for the two-particle scattering process, or equivalently the number of scattering events per unit time, is given by Eq. (2.3) in [2]; see also Eq. (7.42bis) in [32]:

$$\frac{\mathrm{d}\mathcal{P}}{\mathrm{d}t} = \frac{1}{2}\int \mathrm{d}^3\mathbf{r}\frac{\mathrm{d}^3\mathbf{p}_1}{\gamma_1}\frac{\mathrm{d}^3\mathbf{p}_2}{\gamma_2}\,P(\mathbf{r},\mathbf{p}_1)\,P(\mathbf{r},\mathbf{p}_2)\big|\mathcal{M}\big|^2\,\frac{\mathrm{d}^3\mathbf{p}'_1}{\gamma'_1}\,\frac{\mathrm{d}^3\mathbf{p}'_2}{\gamma'_2}\,\frac{\delta^4(p'_1+p'_2-p_1-p_2)}{(2\pi)^2}\,, \qquad (158)$$

where $\gamma_{1,2} = E_{1,2}/m$, with m being the mass of the two particles (assumed to be the same) and $E_{1,2}$ their energies (in HL units), and $\mathcal{M}$ is the Lorentz-invariant Coulomb scattering amplitude.

The transition rate $\mathrm{d}\mathcal{P}/\mathrm{d}t$ caused by a two-particle scattering process, (158), can be reformulated by introducing the exponent $S(\mathbf{r},\mathbf{p})$ of the Gaussian beam phase space distribution $P(\mathbf{r},\mathbf{p})$ in (155), to calculate the rate of change of the emittances ε_u (with $u = x, z, s$); this yields (cf. [2, 33])

$$\begin{aligned}\frac{\mathrm{d}\varepsilon_u}{\mathrm{d}t} = \frac{N_b}{2\Gamma^2}\int \mathrm{d}^3\mathbf{r}\,\frac{\mathrm{d}^3\mathbf{p}_1}{\gamma_1}\,\frac{\mathrm{d}^3\mathbf{p}_2}{\gamma_2}\,\exp\big[-S(\mathbf{r},\mathbf{p}_1)\big]\exp\big[-S(\mathbf{r},\mathbf{p}_2)\big] \\ \times\,\big|\mathcal{M}\big|^2\big(\varepsilon_u(\mathbf{p}'_1)-\varepsilon_u(\mathbf{p}_1)+\varepsilon_u(\mathbf{p}'_2)-\varepsilon_u(\mathbf{p}_2)\big)\,\frac{\mathrm{d}^3\mathbf{p}'_1}{\gamma'_1}\,\frac{\mathrm{d}^3\mathbf{p}'_2}{\gamma'_2}\,\frac{\delta^4(p'_1+p'_2-p_1-p_2)}{(2\pi)^2}\,.\end{aligned} \qquad (159)$$

The goal is now to compute the scattering amplitude $\mathcal{M}$ for a Coulomb interaction between two particles. This will be done by means of the *Feynman rules*, using the *Feynman diagram* representation of a simple scattering process.

Comment: Feynman diagrams are graphical representations of interactions according to a set of rules that allow us to calculate the matrix elements and amplitude $\mathcal{M}$ of a given interaction. With this approach, the scattering cross-sections, decay rates, transition probabilities etc. can be calculated via a function, called the *propagator*, which represents the transfer of momentum from one particle to another. Propagators are obtained by following the prescriptions of the Feynman rules.

Computation of $\mathcal{M}$ for a simplified process is sketched in the following. Let r^μ denote a contravariant vector, which, together with the corresponding covariant vector $r_\mu \stackrel{\text{def}}{=} g_{\mu\nu} r^\nu$, makes the product $g_{\mu\nu} r_\mu r_\nu$ invariant with respect to the Lorentz transform (with $g_{11} = 1$, $g_{22} = g_{33} = g_{44} = -1$, and $g_{\mu\neq\nu} = 0$).

Comment: The metric is 4-momentum^2 = energy^2 − 3-momentum^2 (in HL units), where 4-momenta are written as p and 3-momenta as $\mathbf{p}$ (boldface).

Then we can write (briefly reintroducing $c = 3 \times 10^8 \,\mathrm{m\,s^{-1}}$ in place of its HL value $c = 1$)

$$
\begin{gathered}
r \stackrel{\text{def}}{=} r^\mu \equiv (ct, \mathbf{r}) = (ct, x, z, s), \qquad p \stackrel{\text{def}}{=} p^\mu \equiv \left(\frac{E}{c},\, \mathbf{p}\right) = \left(\frac{E}{c},\, p_x,\, p_z,\, p_s\right), \\
p_1 \cdot p_2 \stackrel{\text{def}}{=} p_1^\mu p_{2_\mu} \equiv \frac{E_1 E_2}{c} - \mathbf{p}_1 \cdot \mathbf{p}_2, \quad p^2 \stackrel{\text{def}}{=} p^\mu p_\mu \equiv \frac{E^2}{c^2} - \mathbf{p}^2 = m^2 c^2, \\
r \cdot p \stackrel{\text{def}}{=} r^\mu p_\mu \equiv tE = \mathbf{r} \cdot \mathbf{p}.
\end{gathered}
\tag{160}
$$

The fourth formula in (160) is the well-known squared 3-momentum $|\mathbf{p}|^2 c^2 = E^2 - m^2 c^4$. With the help of these definitions, the integral of the Dirac delta-functions in (158) expresses the conservation of the 4-momentum:

$$
\int \cdots \delta^4(p_1 + p_2' - p_1' - p_2)\, \mathrm{d}p_1\, \mathrm{d}p_2\, \mathrm{d}p_1\, \mathrm{d}p_1'\, \mathrm{d}p_2' \,.
$$

Here the intention is to sketch the techniques involved in analysing the interactions of charged particles. The approach is a kind of makeshift job based on several approximations, such as non-relativistic elastic scattering in the centre-of-mass frame and the assumption of 'structureless' particles. This allows us to regard proton–proton and electron–electron collisions as being on the same footing. (evidently protons, with spin $1/2$, subject to IBS electromagnetic forces within a circulating beam have nothing to do with high-energy head-on collisions between protons circulating in opposite directions and experiencing chromodynamic quark–quark interactions, with spin $1/2$, mediated by the exchange of gluons, with spin 1.)

Let us consider a Coulomb scattering between two electrons of mass m via the exchange of a virtual photon driving the electromagnetic force, as described by quantum electrodynamics (QED). To quantify this scattering process with the minimal amount of formalism, we drastically simplify the computations of the tricky QED mathematics for the 'real-life' four-body process $\mathrm{e}^- + \mathrm{e}^- \to \mathrm{e}^- + \mathrm{e}^-$ with electrons of spin $1/2$ and a massless photon of spin 1 (carrying the electromagnetic force). Instead, we use a 'toy model' which does not handle particles with spin (cf. [34]). Thus, spinless and point-like charged particles with spinless and massless bosons are used to mimic protons and photons.

Figure 13 illustrates the elastic scattering process $\mathbf{p}_1 + \mathbf{p}_2 \to \mathbf{p}_1' + \mathbf{p}_2'$ in the centre-of-mass frame of two particles, say electrons. Unlike a classical Rutherford Coulomb scattering process, for a QED scattering process, referred to as Møller scattering, the force between two electrons results from the exchange of *virtual photons* (i.e. photons that cannot be directly observed) located at two vertices. Figure 14 depicts a two-electron scattering process described using a Feynman diagram. The two electrons enter from the left of the diagram, exchange a photon and then move away to the right of the

diagram. The nature of the interaction is described by relativistic quantum electrodynamic theory (see e.g. [31, 32, 34, 35]).

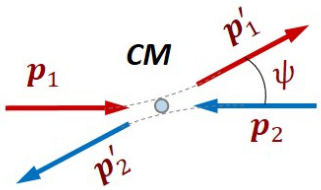

Fig. 13: Kinematics of two-particle scattering in the centre-of-mass system, with scattering angle ψ and 4-momentum $p_{1,2} = (E_{1,2}, \pm\mathbf{p}_{1,2})$; similarly for $p'_{1,2}$ after the collision.

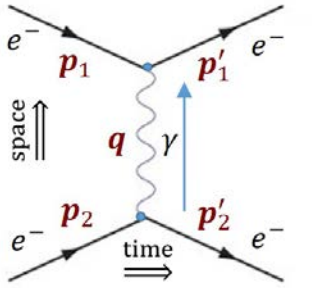

Fig. 14: Feynman diagram for electron–electron scattering in QED; 'time' flows from left to right, the left-hand side of the diagram is the initial state, the right-hand side is the final state, and the wavy line in the middle belongs to neither the initial nor the final state—it shows 'how the interaction happened'. The intermediate photon γ is 'virtual'.

In the framework of the toy model, the electrons are reduced to spin-0 'particles' with mass m, the four *external* lines in the Feynman diagram are associated with the particle 4-momenta p_1, p_2 and p'_1, p'_2 before and after the collision. The photon becomes a spin-0 and zero-mass 'particle', with one *internal* wavy line associated with the internal 4-momentum labelled $\mathbf{q}$.

The amplitude $\mathcal{M}$ for the scattering process is worked out using the Feynman diagram in Fig. 14 together with the Feynman rules. The steps of the Feynman prescriptions for toy models are sketched without proof.

1. **Notation:** Label the incoming and outgoing external 4-momenta p_1, p_2, p'_1, p'_2 and the internal 4-momentum q (with $p_{1,2} \stackrel{\text{def}}{=} p^\mu_{1,2}$ and $q \stackrel{\text{def}}{=} q^\mu$ as above).
2. **Vertex factor:** The two vertices contribute two factors of $-\mathrm{i}g$, where $\mathrm{i} = \sqrt{-1}$. Multiplying these two factors together yields $-g^2$. Note that the coupling constant g in QED specifies the interaction strength between electrons and photons and is related to the *fine structure constant* α through $g = \sqrt{4\pi\alpha}$. In SI units $\alpha = e^2/(4\pi\epsilon_0\hbar c) = 1/137$, and in HL units $\alpha = e^2/(4\pi)$.
3. **Propagator:** The single internal wavy line contributes a factor of $f(q) = \mathrm{i}/(|q|^2 - m_i^2) \equiv \mathrm{i}/|q|^2$ because of the spinlessness and zero mass ($m_i = 0$) of the internal 'boson' (the mimicked photon). Note that a propagator $f(q)$ is associated with the internal wavy line in the Feynman diagram and represents the transfer, or propagation, of momentum from one electron e^- to the other during the interaction time, via a virtual photon γ.
4. **Energy–momentum conservation:** For the two vertices, introduce two Dirac delta-functions $(2\pi)^4\delta^4(p_2 - p'_2 - q)$ and $(2\pi)^4\delta^4(p_1 + q - p'_1)$ and multiply them together. The scattering amplitude is expressed as the product of the coupling constant g and the propagator $f(q)$, namely $\mathcal{M} = gf(q)$. Note that this prescription enforces the conservation of energy and momentum at each vertex, because the delta-functions are zero when the sum of the incoming 4-momenta and that of the outgoing 4-momenta are the same.
5. **Integration over internal 4-momenta:** Then integrate the delta-functions for the unique internal 4-momentum q over the variables $\mathrm{d}^4q/(2\pi)^4$.

Steps 1–5 give the amplitude approximation for non-relativistic scattering of spinless and point-like charged 'particles' (with mass m) and spinless and massless 'bosons' mimicking electrons and photons:

$$\mathcal{M} = -\mathrm{i}\,(2\pi)^4 g^2 \int \frac{1}{|q|^2}\,\delta^4\left(p_2 - p_2' - q\right)\delta^4\left(p_1 + q - p_1'\right)\mathrm{d}^4 q\,. \tag{161}$$

Integration of the delta-function is done by inspection. Choosing the second delta-function to integrate, we substitute $q \mapsto p_1' - p_1$ into (161) and obtain

$$\begin{aligned}\mathcal{M} &= -\mathrm{i}\,(2\pi)^4 g^2 \int \frac{1}{|q|^2}\,\delta^4\big(p_1 + p_2 - p_1' - p_2'\big)\delta^4\big(q - [p_1' - p_1]\big)\,\mathrm{d}^4 q \\ &= -\frac{\mathrm{i}\,g^2}{(p_1' - p_1)^2}\,(2\pi)^4\delta^4\big(p_1 + p_2 - p_1' - p_2'\big)\end{aligned} \tag{162}$$

since $\int \delta^4(q - [p_1' - p_1])\,\mathrm{d}^4 q = 1$.

Discarding the left-out delta-function $(2\pi)^4\delta^4(p_1+p_2-p_1'-p_2')$, which just re-enforces the overall conservation of energy and momentum at the four external lines (i.e. external 'particles', the mimicked electrons), we get the scattering amplitude in terms of the 4-momenta (cf. Eq. (2.3a) in [2]):

$$\mathcal{M} = -\frac{\mathrm{i}\,g^2}{(p_1' - p_1)^2} = \frac{4\pi\alpha}{(p_1' - p_1)^2}\,. \tag{163}$$

To see the link between $\mathcal{M}$ and the collisional process, the internal 4-momentum squared, $|q|^2 \equiv (p_1' - p_1)^2$, can be expanded further. Consider the 4-momentum (and energy) conservation $|p_{1,2}'|^2 = |p_{1,2}|^2$ for elastic collision in the centre-of-mass frame (Fig. 13). We have $E_{1,2}^2 = E_{1,2}'^2$ and $|\mathbf{p}|_{1,2}^2 = |\mathbf{p}|_{1,2}'^2$ since $p_{1,2} = (E_{1,2}, \mathbf{p}_{1,2})$ and $p_{1,2}^2 = (E_{1,2}^2 - \mathbf{p}_{1,2}^2) \equiv m_{1,2} = m$ for particles of the same mass m. Hence

$$\begin{aligned} p_1' - p_1 = (E_1' - E_1) + (\mathbf{p}_1' - \mathbf{p}_1) = \mathbf{p}_1' - \mathbf{p}_1 \quad &\Longrightarrow \\ (\mathbf{p}_1' - \mathbf{p}_1)^2 = \mathbf{p}_1'^2 + \mathbf{p}_1^2 - 2\mathbf{p}_1'\cdot\mathbf{p}_1 &= \mathbf{p}_1'^2 + \mathbf{p}_1^2 - 2|\mathbf{p}_1'|\,|\mathbf{p}_1|\cos\psi \\ = 2|\mathbf{p}|^2(1-\cos\psi) &= |\mathbf{p}|^2\sin[\psi/2]\,, \end{aligned} \tag{164}$$

in which $\mathbf{p} \overset{\text{def}}{=} \mathbf{p}_1$ is the incident momentum of particle 1 and ψ is the scattering angle between the two momenta $\mathbf{p}_1$ and $\mathbf{p}_1'$ before and after collision. Therefore, in HL units, the amplitude $\mathcal{M}$ takes the form

$$\mathcal{M} = \frac{4\pi\alpha}{|\mathbf{p}|^2\sin^2[\psi/2]} \quad\Longrightarrow\quad \big|\mathcal{M}\big|^2 = \left(\frac{e^2}{|\mathbf{p}|^2\sin^2[\psi/2]}\right)^2 \equiv \sigma(|\mathbf{p}|,\psi)\,. \tag{165}$$

The scattering amplitude $\big|\mathcal{M}\big|^2$ is thus identified with the differential cross-section $\sigma(|\mathbf{p}|,\psi)$ of the two-electron collisional process.

Comment: Compare (165) with the cross-section $\sigma(\psi)$ of a Coulomb classical (non-quantal) Rutherford scattering process, Eq. (36).

At this point the calculations are still far from finished, and also they are not easy to perform. After some difficult manipulations the rate of change of the emittances, $\mathrm{d}\varepsilon_u/\mathrm{d}t$ of Eq. (159), can be recast in the form given by Eq. (166) below. See [2] for details of the lengthy calculations used to derive the Bjorken–Mtingwa Eq. (3.4) and then Eqs. (4.5)–(4.7), which yield growth rate expressions that are convenient to use.

3.3.3 Intrabeam scattering growth rates

In deriving Eq. (166), Bjorken and Mtingwa considered a zero vertical dispersion function D_z, so that $\phi_z = 0$ and $H_z = 0$, reducing L_z (168) to a matrix with all components $L_{z_{i,j}} = 0$ except for $L_{z_{3,3}} = \beta_z/\varepsilon_z$:

$$L_z = \frac{\beta_z}{\varepsilon_z}\begin{pmatrix}0&0&0\\0&0&0\\0&0&1\end{pmatrix} \text{ (Eq. (2.37d) of [2]) compared to } L_z = \frac{\beta_z}{\varepsilon_z}\begin{pmatrix}0&0&0\\0&\frac{\gamma^2 H_z}{\beta_z}&-\gamma\phi_z\\0&-\gamma\phi_z&1\end{pmatrix} \text{ in Eq. (168)}.$$

Moreover, in solving (166) Bjorken and Mtingwa did an approximation by neglecting the ratios $\beta_{x,z}/\varepsilon_{x,z}$ relative to $\gamma^2 D_x^2/(\varepsilon_x\varepsilon_z)$, $(\beta_x/\varepsilon_z)\gamma^2\phi_x^2$ and γ^2/σ_η.

To conclude, for bunched beams, the IBS growth rates τ_u^{-1} in the horizontal, vertical and longitudinal directions ($u = x, z, s$) are written in the form similar to that obtained by Bjorken and Mtingwa [2],

$$\begin{aligned}\frac{1}{\tau_u} &= \frac{1}{\sigma_u}\frac{d\sigma_u}{dt} = \frac{1}{\sqrt{\langle\varepsilon_u\rangle}}\frac{\mathrm{d}\sqrt{\langle\varepsilon_u\rangle}}{\mathrm{d}t} = \frac{1}{2\,\langle\varepsilon_u\rangle}\frac{\mathrm{d}\langle\varepsilon_u\rangle}{\mathrm{d}t} = \\ &= \mathcal{A}_{\mathrm{BM}}\,C_{\log}\left\langle\int_0^\infty \frac{\mathrm{d}\lambda\,\sqrt{\lambda}}{\sqrt{\det[L+\lambda I]}}\left\{\mathrm{Tr}[L_u]\,\mathrm{Tr}\left[\frac{1}{L+\lambda I}\right] - 3\,\mathrm{Tr}\left[L_u\Big(\frac{1}{L_u+\lambda I}\Big)\right]\right\}\right\rangle,\end{aligned} \tag{166}$$

in which we have introduced the growth rates (134), the rough momentum spread squared $\langle H\rangle \approx \langle\eta\rangle^2 = \sigma_\eta^2$, and the Bjorken-Mtingwa scattering constant $\mathcal{A}_{\mathrm{BM}}$ in analogy with (128):

$$\begin{aligned}\mathcal{A}_{\mathrm{BM}}\,C_{\log} = 4\pi\mathcal{A}_{\mathrm{P}}\,C_{\log} &= \frac{c r_{\mathrm{i}}^2 N_b\,C_{\log}}{16\pi\beta^3\gamma^4\varepsilon_x\varepsilon_z\varepsilon_s} \equiv \frac{\pi^2 N_b\,c_0\,r_{\mathrm{i}}^2\,C_{\log}}{2\gamma\Gamma},\\ \Gamma = (2\pi)^3(\beta\gamma)^3\varepsilon_x\varepsilon_z\varepsilon_s, &\qquad \frac{1}{\tau_s} = \frac{1}{\sigma_\eta}\frac{\mathrm{d}\sigma_\eta}{\mathrm{d}t},\end{aligned} \tag{167}$$

where Γ is the six-dimensional phase volume for bunched beams and $\varepsilon_s \overset{\mathrm{def}}{=} \sigma_\eta\,\sigma_s$. Moreover, the longitudinal growth rate τ_s, has been remodelled in the handy form above, better suited for practical usage (cf. [30] chapter 13.2 and [37] footnote[3]). Unlike Eq. (134) and (166) the growth rates in Ref. [37] are expressed as the time-derivative of the emittances, yielding a factor 2 difference between both versions. Also, the longitudinal emittance can be written instead as $\varepsilon_s = \sigma_s\sigma_E/\beta^2$ using the relative energy spread $\Delta E/E$ since the relationship between the momentum and energy spreads is $\Delta p/p = (\Delta E/E)/\beta^2$, the two relative spreads being equal at high energy.

The present formulation (cf. [37]) includes the vertical dispersion D_z and its derivative D_z'. The matrix $L = L_x + L_z + L_s$ is composed of the 3×3 matrices defined below in (168), I is the identity matrix, and the brackets $\langle\,\cdot\,\rangle$ represent averaging over the lattice period.

$$L_x = \frac{\beta_x}{\varepsilon_x}\begin{pmatrix}1&-\gamma\phi_x&0\\-\gamma\phi_x&\frac{\gamma^2 H_x}{\beta_x}&0\\0&0&0\end{pmatrix},\quad L_z = \frac{\beta_z}{\varepsilon_z}\begin{pmatrix}0&0&0\\0&\frac{\gamma^2 H_z}{\beta_z}&-\gamma\phi_z\\0&-\gamma\phi_z&1\end{pmatrix},\quad L_s = \frac{\gamma^2}{\sigma_\eta^2}\begin{pmatrix}0&0&0\\0&1&0\\0&0&0\end{pmatrix} \tag{168}$$

with

$$\phi_{x,z} = \frac{D_{x,z}\alpha_{x,z} + D'_{x,z}\beta_{x,z}}{\beta_{x,z}},\quad H_{x,z} = \frac{D_{x,z}^2 + \beta_{x,z}^2\phi_{x,z}^2}{\beta_{x,z}} = \gamma_{x,z}D_{x,z}^2 + 2\alpha_{x,z}D_{x,z}D'_{x,z} + \beta_{x,z}D_{x,z}'^2\,.$$

In Eqs. (166)-(168), N_b is the number of particles per bunch, c_0 is the speed of light reintroduced here in SI units, r_{i} is the classical ion radius [m] given in (90); it reduces to the classical proton radius r_0 for unit ion mass and charge A, Z (for leptons of charge Z, A is the lepton-to-electron mass ratio), $\gamma = \left(E_0^2 + p^2\right)^{1/2}/E_0$ and $\beta = \left(1-\gamma^{-2}\right)^{1/2}$ are the Lorentz factors, E_0 is the particle rest energy [eV],

and p is the particle momentum [eV/c]. The matrices inside the brackets depend on the optics parameters $\alpha_{x,z}, \beta_{x,z}, D_{x,z}$ and $D'_{x,z}$, on the r.m.s. unnormalized transverse emittances $\varepsilon_{x,z}$ [m], and on the r.m.s. relative momentum spread σ_η and bunch length σ_s [m] (or the r.m.s. longitudinal emittances [m] ε_s defined above). For matched beams, the longitudinal emittance is defined as $\varepsilon_s = \pi p \sigma_\eta \sigma_s (\beta c)^{-1}$ [eVs]. $C_{\log}$ in Eq. (166) is the Coulomb logarithm, with typical values in the range $[10,\ 20]$.

After expansion of the integrand in the brackets in (166) and some lengthy computations, the growth rates are recomputed to include the vertical dispersion function and cast in the form (cf. [36, 37])

$$\frac{1}{\tau_u} = \frac{\pi^2 N_b\, c_0\, r_i^2\, C_{\log}}{2\gamma\Gamma}\, \Delta_u \left\langle \int_0^\infty \frac{\mathrm{d}\lambda \sqrt{\lambda}\,(a_u\lambda + b_u)}{(\lambda^3 + a\lambda^2 + b\lambda + c)^{3/2}} \right\rangle \tag{169}$$

with $u = x, z, s$ and

$$\Delta_x = \frac{\gamma^2 H_x}{\varepsilon_x}, \quad \Delta_z = \frac{\beta_z}{\varepsilon_z}, \quad \Delta_s = \frac{\gamma^2}{\sigma_\eta^2}.$$

The nine coefficients a, b, c, a_x, b_x, a_z, b_z, a_s and b_s depend on the optics parameters and on the approximation used. They are not reproduced here; see [37] for a complete list, including three variants.

Comment: A high energy approximation to Bjorken-Mtingwa theory [2] has been developed by Bane [27] to give formulae for the IBS growth rates that can be rapid and easy to apply. For instance, IBS effects in high energy storage rings, operating above transition, can induce emittance growth during beam coasts. So, numerical simulations of the emittance evolution caused by IBS involves performing the integrals appearing in the growth rates formulae over numerous storage ring turns, averaging the growth rates for each turn around the storage ring and then deriving the emittance variation for this turn. This task may be quite cumbersome and computationally intensive if one has to use plain growth rates formulae without approximation (see also [28, 30, 33]). Although the Piwinski and Bjorken-Mtingwa formulae for the growth rates look dissimilar, the Piwinski model (assuming weak-focussing lattices) and the Bjorken-Mtingwa one (intrinsically ready-made for strong-focussing lattices) are in good agreement has also shown by Bane, with sure assumptions.

For illustration, Fig. 15 plots the evolution of the Coulomb logarithm for the ELENA 100 keV low-energy antiproton decelerator ring, computed with Eqs. (170) and (171) below.

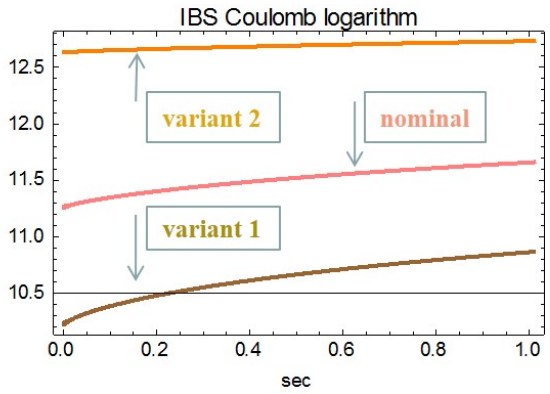

Fig. 15: Evolution of the calculated Coulomb logarithm during 1 s on a 100 keV plateau for the nominal ELENA beam and the first two variants in Table 4.

In [2] the Coulomb logarithm is taken to be the fixed value $C_{\log} = 20$. Here the Coulomb logarithm is defined by the expression (see [23])

$$C_{\log} \equiv \ln\left[r_{\max}/r_{\min}\right] \quad \text{with} \quad r_{\max} = \min[\sigma_x, \lambda_D], \quad r_{\min} = \max\left[r_{\min}^{C}, r_{\min}^{QM}\right], \tag{170}$$

where $r_{\max}$ is the smaller of the mean r.m.s. beam size σ_{x_β} and the Debye length $\lambda_{\rm D}$, and $r_{\min}$ is the larger of the distance of closest approach $r_{\min}^{\rm C}$ and the quantum diffraction limit from the nuclear radius $r_{\min}^{\rm QM}$. These quantities are given by

$$\lambda_{\rm D} = \frac{7.434}{Z}\sqrt{\frac{2E_\perp}{\rho}}, \quad \rho = \frac{N_b \times 10^{-6}}{\sqrt{64\pi^3 \langle\beta_x\rangle \varepsilon_x \langle\beta_z\rangle \varepsilon_z \sigma_s^2}}\,, \quad E_\perp = \frac{(\gamma^2-1)E_0}{2}\frac{\varepsilon_x}{\langle\beta_x\rangle}\,,$$
$$r_{\min}^{\rm C} = \frac{1.4410\times 10^{-9} Z^2}{2E_\perp}, \quad r_{\min}^{\rm QM} = \frac{1.97310\times 10^{-13} Z^2}{\sqrt{8E_\perp E_0}}\,, \tag{171}$$

in which ρ is the particle volume density [m^{-3}] and $E_\perp$ is the transverse beam kinetic energy in the centre-of-mass frame [eV].

4 Examples

4.1 First example: LHC and SLHC at 7 TeV

4.1.1 Nominal LHC, first interaction region upgrade and SLHC

The effects of intrabeam scattering and synchrotron radiation on the expected evolution of the LHC and SLHC beam emittances during coasts at 7 TeV are examined for the nominal beam and beams with reduced emittances. The study was carried out in 2010 for the first 'interaction region' (IR) upgrade and for the SLHC. The nominal beam and LHC parameters and those with reduced emittances have been selected to study the effect of IBS on emittance evolution in a coast [5].

Figure 16 shows the betatron functions along the LHC ring circumference for the LHC 'IR phase 1 triplet' beam and for the lattice parameters of Case 2 in Table 1 with $\beta^* = 0.3$ m, used for all subsequent IBS calculations (small disparities among the other three β^* values were negligible). Except at the interaction points, LHC is a fairly smooth storage ring and so more or less fulfils the *smooth focusing approximation* criteria. The vertical dispersion (see Fig. 17) is generated by the vertical crossing angles at interaction points 1 and 2 and by the detector fields of ALICE and LHCB [37].

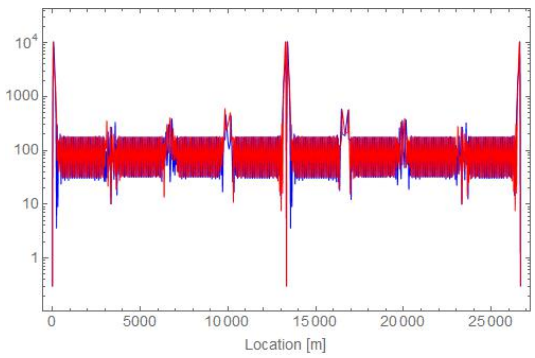

Fig. 16: SLHC betatron functions [m] for $\beta^* = 0.30$ m (at interaction points IP1 and IP5).

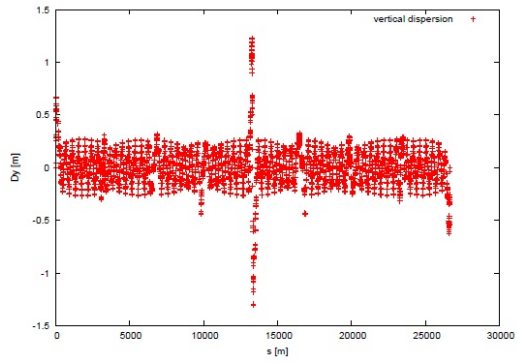

Fig. 17: Vertical dispersion [m] as a function of position [m], for the LHC at 7 TeV.

Table 1 displays a list of beam and lattice parameters related to the luminosity characteristics of the LHC and SLHC. Cases 1 and 2 in the table show the LHC luminosity with a nominal beam intensity of 1.15×10^{11} protons, and Cases 3 and 4 show the SLHC luminosity for the 'highest' ultimate beam intensity of 2.36×10^{11} protons.

Table 1: LHC nominal beam intensity luminosity and SLHC luminosity with improved variants

LHC and SLHC beam parameters	Case 1[a]	Case 2[b]	Case 3[c]	Case 4[d]
N_b $(\times 10^{11})$	1.15	1.15	1.70	2.36
$\varepsilon^n_{H,V} = \gamma\varepsilon$ [μm] (normalized)	3.75	2.54	2.65	2.60
β^* [m]	0.55	0.30	0.25	0.15
$\sigma^*_{H,V}$ [μm]	16.58	10.11	9.40	7.21
σ_L [mm]	75.5	75.5	75.5	75.5
$\sigma_{\Delta p/p}$ $(\times 10^{-4})$	1.13	1.13	1.13	1.13
ε_L r.m.s. [eV s]	0.62	0.62	0.62	0.62
Crossing angle θ [μrad]	285	337	355	452
ΔQ_{bb} head-on[e]	1	1.09	1.43	1.37
Luminosity $\mathcal{L}$ $(\times 10^{-34})$ [cm^{-2} s^{-1}]	2	1.09	4.65	10.29

[a] Initial IR triplet: nominal beam with LHC at top energy gives the nominal luminosity.
[b] IR phase 1 triplet: new optics foreseen for interaction region to give lower β^*, reduced emittance and improved luminosity.
[c] Ultimate N_b: with the ultimate beam intensity and the reduced emittance raise ΔQ_{bb} to still improve the luminosity.
[d] 'Highest' ultimate N_b: top luminosity can be obtained by reducing β^* and raising N_b within an emittance again reduced.
[e] The head-on beam–beam tune shift ΔQ_{bb} is normalized to the value of the nominal beam.

4.1.2 Intrabeam scattering effects in the LHC and SLHC

Figure 18 shows the initial IBS growth times in the LHC and SLHC computed with the beam parameters in Table 1. The simulations were performed with a dedicated *Mathematica* notebook based on the Bjorken–Mtingwa model [2], which handles the vertical dispersion function and its derivative [36].

The *Mathematica* code accounts for the variation of the optical parameters $\beta_{H,V}, \beta'_{H,V}, D_{H,V}$ and $D'_{H,V}$ over the lattice. Table 2 displays the increase in beam emittance due to IBS for a 7 TeV proton

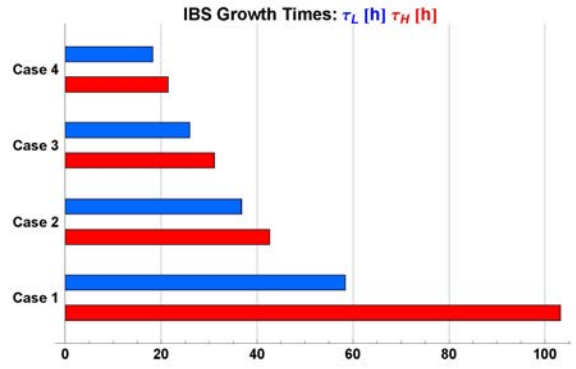

Fig. 18: Initial IBS growth times in hours for the four cases in Table 1. For the nominal LHC parameters (Case 1): $\tau_L = 58$ h, $\tau_H = 103$ h and $\tau_V = -359$ years. The vertical growth times are not shown as they are negative, approximately -100 years, i.e. $\tau_V^{-1} \approx 0$.

beam at the end of 10 hours' storage in the LHC/SLHC.

Figures 19 and 20 plot the emittance evolution over the 10-hour period of coast, assuming a constant beam intensity for the duration of the storage. The *synchrotron radiation* damping effect is not accounted for in the simulations. IBS growth times are calculated iteratively in time steps of 5 minutes.

At each iteration i, the emittances are updated as follows:

$$\varepsilon_{\mathrm{LHV}}(i+1) = \varepsilon_{\mathrm{LHV}}(i) \exp\left[\frac{\Delta t}{\tau_{\mathrm{LHV}}(i)}\right] \;\rightleftarrows\; i = i+1, \quad \frac{1}{\tau_{\mathrm{LHV}}(i+1)} = \frac{1}{\Delta t} \ln\left[\frac{\varepsilon_{\mathrm{LHV}}(i+1)}{\varepsilon_{\mathrm{LHV}}(i)}\right]. \qquad (172)$$

Table 2: IBS emittance growth after a 10-hour beam coast, considering only the IBS effect

		$\Delta\varepsilon_L/\varepsilon_L$	$\Delta\varepsilon_H/\varepsilon_H$	$\Delta\varepsilon_V/\varepsilon_V$
Case 1	Initial IR triplet: $\beta^*=0.55$ m	16%	9%	−0.0001%
Case 2	IR phase 1 triplet: $\beta^*=0.30$ m	24%	21%	−0.001%
Case 3	Ultimate N_b: $\beta^*=0.25$ m	32%	27%	−0.001%
Case 4	'Highest' ultimate N_b: $\beta^*=0.15$ m	44%	37%	−0.001%

$$\varepsilon_{\mathrm{L,H,V}}(i+1)=\varepsilon_{\mathrm{L,H,V}}(i)\exp\left[\frac{\Delta t}{\tau_{\mathrm{L,H,V}}(i)}\right] \;\rightleftharpoons\; i=i+1 \quad \frac{1}{\tau_{\mathrm{L,H,V}}(i+1)}=\frac{\ln\varepsilon_{\mathrm{L,H,V}}(i+1)-\ln\varepsilon_{\mathrm{L,H,V}}(i)}{\Delta t} \tag{173}$$

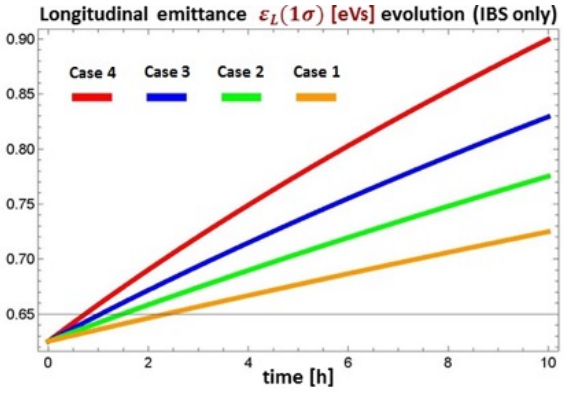

Fig. 19: Evolution of the r.m.s. longitudinal emittance due to IBS effect for the 4 cases of Table 1.

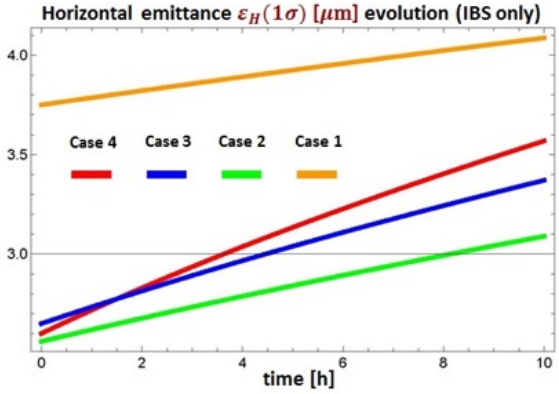

Fig. 20: Evolution of the r.m.s. horizontal emittance due to IBS effect for the 4 cases of Table 1.

4.1.3 Cumulative intrabeam scattering and radiation damping effects in the LHC and SLHC

The *synchrotron radiation* turns into a visible effect for the LHC/SLHC proton beams at 7 TeV collision energy. Emittances shrink with damping times $\tau_{\mathrm{srd_L}}=12.9$ h and $\tau_{\mathrm{srd_{HV}}}=26.0$ h in the transverse planes. Synchrotron radiation damping (SRD) is modelled by replacing $\tau_{\mathrm{LHV}}(i)$ with $(\tau^{-1}_{\mathrm{LHV}}(i)-\tau^{-1}_{\mathrm{srd_{LHV}}})^{-1}$ in Eq. (173).

Figures 21–22 show the evolution of the longitudinal and transverse emittances over a 10-hour beam coast. Synchrotron radiation dominates IBS growth in the longitudinal and vertical planes for all of Cases 1–4; in the horizontal plane the emittance damps continuously during the coast only in Case 1, whereas for Cases 2–4 it expands at some point during the coast. Table 3 displays the increase in beam emittance due to IBS and SRD for a 7 TeV proton beam at the end of 10 hours' storage in the LHC/SLHC.

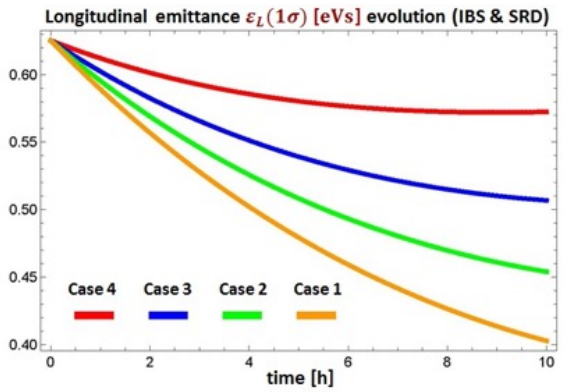

Fig. 21: Evolution of the r.m.s. longitudinal emittance due to IBS and SRD effects for the 4 cases of Table 1.

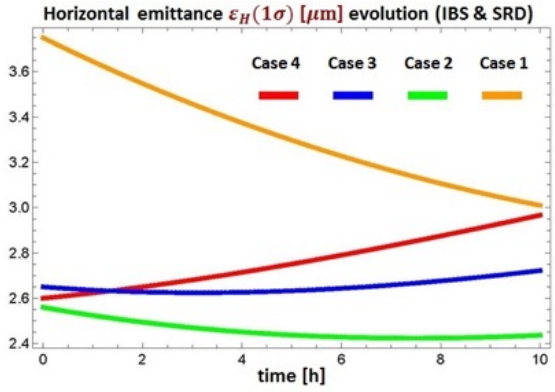

Fig. 22: Evolution of the r.m.s. horizontal emittance due to IBS and SRD effects for the 4 cases of Table 1.

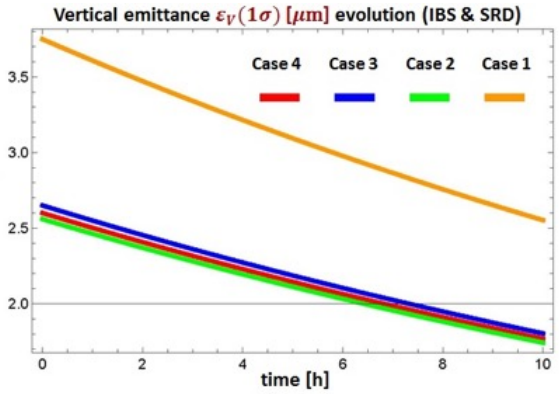

Fig. 23: Evolution of the r.m.s. vertical emittance due to IBS and SRD effects for the 4 cases of Table 1.

Table 3: IBS emittance growth after a 10-hour beam coast, considering both IBS and SRD effects

		$\Delta\varepsilon_L/\varepsilon_L$	$\Delta\varepsilon_H/\varepsilon_H$	$\Delta\varepsilon_V/\varepsilon_V$
Case 1	Initial IR triplet: $\beta^* = 0.55$ m	-36%	-20%	-32%
Case 2	IR phase 1 triplet: $\beta^* = 0.30$ m	-27%	-5%	-32%
Case 3	Ultimate N_b: $\beta^* = 0.25$ m	-19%	3%	-32%
Case 4	'Highest' ultimate N_b: $\beta^* = 0.15$ m	-8%	14%	-32%

In summary, the longitudinal and vertical emittances of all the luminosity scenarios are kept within target specifications for Cases 1–4. Horizontal emittances stay within requirements for Cases 1 and 2; a small blow-up of approximately 3% is anticipated for Case 3, and a larger blow-up of approximately 14% for Case 4. Globally, for most scenarios, the evolution of emittances during the 10-hour coast is kept within the range of design values. Observe that, without the counterbalancing damping effect of the synchrotron radiation, the longitudinal and horizontal emittances would grow continuously during a coast, while the vertical emittance would stay roughly the same. This is because at 7 TeV the LHC is far above the transition energy, as $\gamma = 7461 \gg \gamma_t \approx 53.8$.

4.2 Second example: ELENA at 100 keV

4.2.1 Study of nominal beam parameters and variants

ELENA is a compact hexagonal synchrotron of about 30 m circumference, equipped with an electron cooler. It was designed to allow greater deceleration of the antiprotons ($\bar{p}$) with 5.31 MeV kinetic energy sent by the Antiproton Decelerator (AD), to yield dense beams at 100 keV kinetic energy with a beam population of approximately 2.5×10^7 cooled $\bar{p}$. *Electron cooling* is used to counteract the increase in emittance and momentum due to the deceleration process. The plan is to increase the intensity of the antiprotons delivered to the anti-hydrogen-based experiments at the AD by one to two orders of magnitude [38, 39]. In [38], the joint effects of electron cooling and IBS on the beam equilibrium phase space dimensions are computed using the code BETACOOL [3].

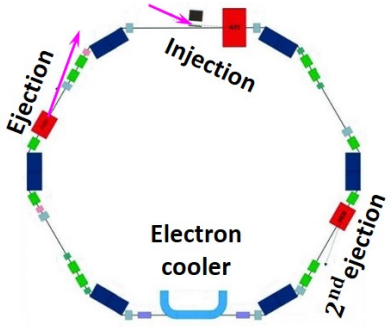

Fig. 24: The ELENA (Extra Low Energy Antiproton) ring (8.6 m×10.0 m, ≈30 m circumference) is a below-transition-energy ring with $\gamma = 1.00001 < \gamma_t \approx 1.9$.

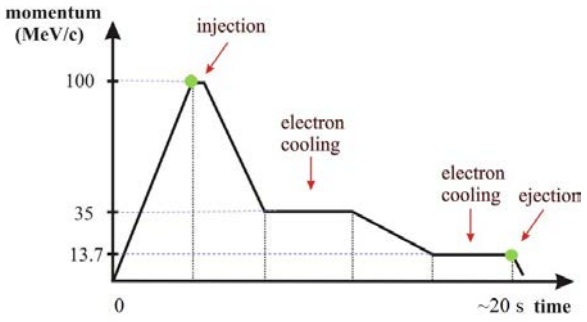

Fig. 25: ELENA cycle, with first injection plateau at 100 MeV/c, second cooling plateau at 35 MeV/c and third cooling plateau at 13.7 MeV/c (100 keV).

The cycle has one injection plateau at 100 MeV/c momentum for the *coasting* $\bar{p}$ beam injection from the AD. Hence, the beam is decelerated down to a first plateau at 35 MeV/c for a cooling period of about 8 s, followed by deceleration down to a second plateau at 13.7 MeV/c for about 3 s extra cooling of the $\bar{p}$ beam. Before the end of the plateau, the beam is *bunched* and further cooled for approximately 0.3 s to the emittances needed for ELENA experiments, up to the extraction of four bunches consisting of approximately 6.25×10^6 antiprotons to the transfer lines between ELENA and the experimental areas.

Figures 24 and 25 show schematically the ELENA ring and its deceleration cycle.

Figure 26 displays the optics of the ELENA ring lattice with working points $Q_H = 2.3$ and $Q_V = 1.3$ (P. Belochitskii, 2012). We see that, unlike the LHC lattice (Fig. 16), ELENA is not a smooth lattice.

Table 4 shows the initial length, momentum spread, and longitudinal and transverse emittance values of the nominal bunch and five variants (prior to IBS), used to evaluate how the bunch parameters behave under IBS effects. This is an important issue, as the bunch length and momentum spread must be kept close to their nominal values. This study was undertaken in 2012.

Table 4: Initial nominal beam emittances on the 100 keV plateau and five variants. The longitudinal emittance is defined as $\varepsilon_L = \pi p \sigma_{BL} \sigma_{\Delta p/p} (\beta c)^{-1}$, where c is the speed of light and σ_{BL} is the r.m.s. bunch length.

	σ_{BL}	$\sigma_{\Delta p/p}$	ε_L^{rms}	ε_{HV}^{rms}
Nominal	0.325 m	7.5×10^{-5}	2.4×10^{-4} eV s	1.0 μm
Variant 1	0.325 m	2.5×10^{-5}	0.8×10^{-4} eV s	0.5 μm
Variant 2	0.325 m	1.25×10^{-4}	4.0×10^{-4} eV s	2.5 μm
Variant 3	0.325 m	2.5×10^{-4}	8.0×10^{-4} eV s	1.0 μm
Variant 4	0.325 m	3.75×10^{-4}	12.0×10^{-4} eV s	1.0 μm
Variant 5	0.325 m	5.0×10^{-4}	16.0×10^{-4} eV s	1.0 μm

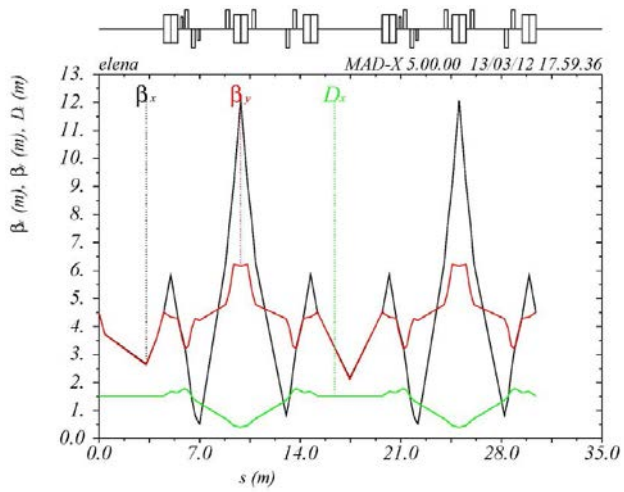

Fig. 26: ELENA ring betatron functions and dispersion function in [m]

4.2.2 Intrabeam scattering simulations for bunched beams on the 100 keV *plateau*

The IBS simulations for ELENA were performed with two different *Mathematica* notebooks for cross-checking. The first consists of the code used for LHC/SLHC simulations. The code in the second notebook is based on an algorithm derived by A. Piwinski [6] and implemented by Ch. Carli [7], which takes the linear coupling into account exactly. The lattice is described in terms of magnets and their strengths, and the program analyses linear properties such as the betatron-oscillation coupling (solenoid and skew quadrupole magnets). The process is applied to the generalized emittances specified via the betatron-oscillation eigenvectors (e.g. as calculated by MADX). Then this information is used to compute IBS growth rates. Simulations using the second code show that the coupling effect has negligible influence on the IBS growth rates and hence on the vertical dispersion function.

Figures 27–29 plot, for bunched beams, the longitudinal τ_{L}^{-1}, horizontal τ_{H}^{-1} and vertical τ_{V}^{-1} growth rates 'without cooling', as functions of the transverse emittance $\varepsilon_{\mathrm{HV}}^{\mathrm{rms}}$ and the relative momentum spread $\sigma_{\Delta\mathrm{p/p}}$. Each bunch contains 6.25×10^6 antiprotons. The plotted growth rates are computed using an initial r.m.s. bunch length of $\sigma_{\mathrm{BL}} = 0.325\,\mathrm{m}$. Alternative plots of τ_{LHV}^{-1} versus $\varepsilon_{\mathrm{H}}^{\mathrm{rms}}$ and $\varepsilon_{\mathrm{V}}^{\mathrm{rms}}$, with nominal $\sigma_{\Delta\mathrm{p/p}} = 7.5 \times 10^{-5}$ and $\sigma_{\mathrm{BL}} = 0.325\,\mathrm{m}$, look similar and so are not shown.

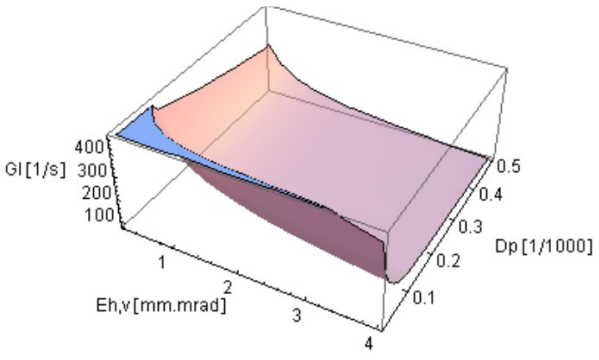

Fig. 27: Longitudinal growth rate τ_{L}^{-1} ($\mathrm{G_L}$) as $\varepsilon_{\mathrm{H,V}}$ and $\sigma_{\Delta\mathrm{p/p}}$ are varied, with $\varepsilon_{\mathrm{H}} \equiv \varepsilon_{\mathrm{V}}$ and $\sigma_{\mathrm{BL}} = 0.325\,\mathrm{m}$.

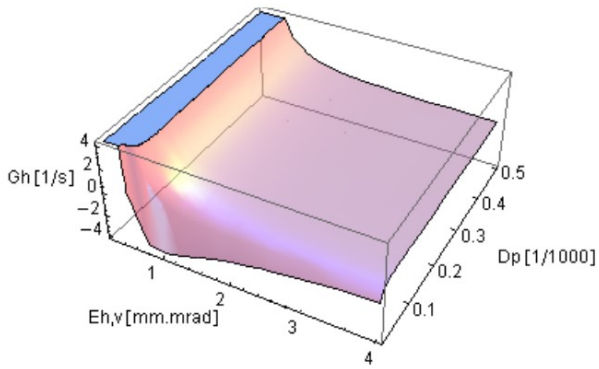

Fig. 28: Horizontal growth rate τ_{H}^{-1} ($\mathrm{G_H}$) as $\varepsilon_{\mathrm{H,V}}$ and $\sigma_{\Delta\mathrm{p/p}}$ are varied, with $\varepsilon_{\mathrm{H}} \equiv \varepsilon_{\mathrm{V}}$ and $\sigma_{\mathrm{BL}} = 0.325\,\mathrm{m}$.

Figures 30 and 31 plot the transverse and longitudinal growth times τ_{LHV} 'without cooling' for bunched beams (where each bunch contains 6.25×10^6 antiprotons). The simulation was performed for the nominal beam and the first two variants given in Table 4.

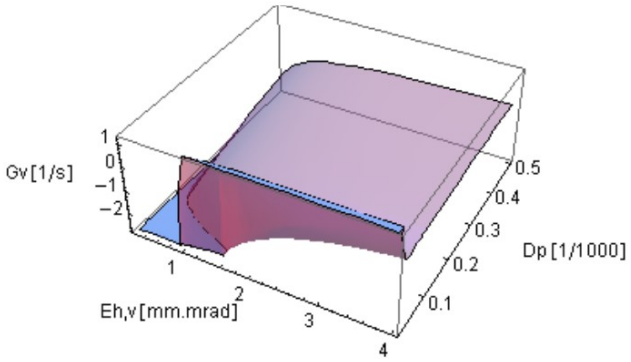

Fig. 29: Vertical growth rate τ_V^{-1} (G_V) as $\varepsilon_{H,V}$ and $\sigma_{\Delta p/p}$ are varied, with $\varepsilon_H \equiv \varepsilon_V$ and $\sigma_{BL} = 0.325$ m

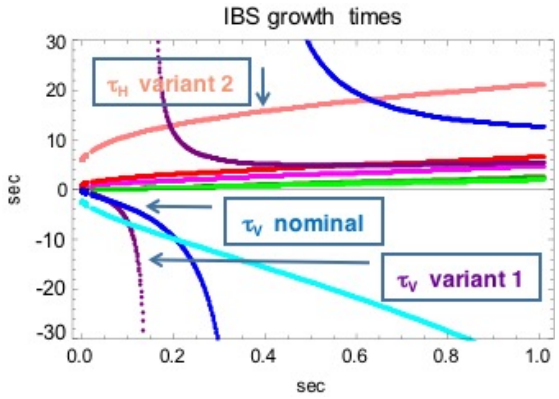

Fig. 30: Evolution of the transverse IBS growth times τ_{HV} (on the linear scale) over 1 s ($\varepsilon_L = \pi p \sigma_{BL} (\beta c)^{-1}$).

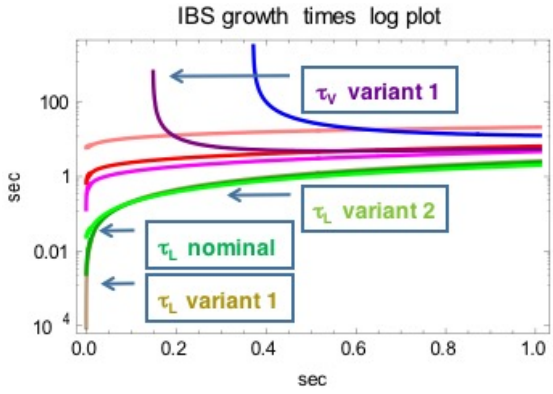

Fig. 31: Evolution of the longitudinal and vertical IBS growth times τ_{LV} (on the logarithmic scale) over 1 s.

4.2.3 Performance of nominal beam and variants for bunched beams on the 100 keV *plateau*

Figures 32 and 33 plot the transverse emittance ε_{HV} 'without cooling' for the nominal beam and the five variants given in Table 4.

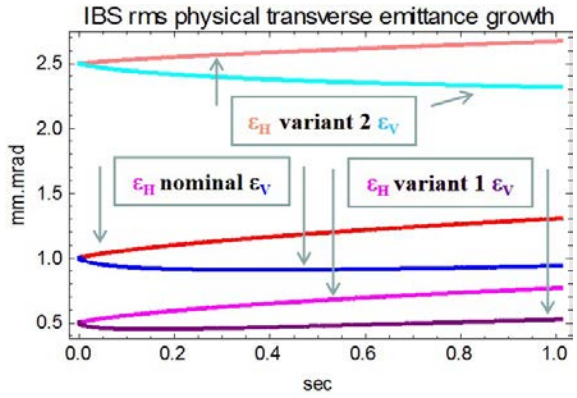

Fig. 32: Evolution of the emittances ε_{HV} over 1 s for the nominal beam and the first two variants in Table 4.

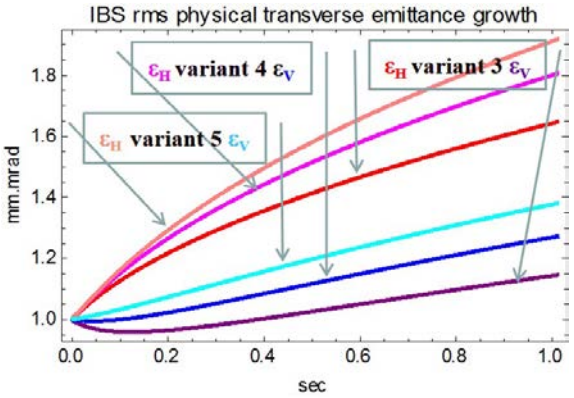

Fig. 33: Evolution of the transverse emittances ε_{HV} over 1 s for variants 3–5 in Table 4.

Figure 34 plots the relative momentum spread $\sigma_{\Delta p/p}$ with IBS effects and without cooling for the nominal beam and the first two variants. Figure 35 plots the bunch length σ_{BL} and the momentum spread

$\sigma_{\Delta p/p}$ for variants 3–5. The bunch length is given in [m] and the momentum spread in [permille], with both units shown on the same vertical scale (e.g. $\sigma_{BL}(1) = 0.42$ m, $\sigma_{\Delta p/p}(1) = 0.65$ permille for variant 5).

Finally, Fig. 36 displays the bunch length σ_{BL} [m] for the nominal beam and the first two variants.

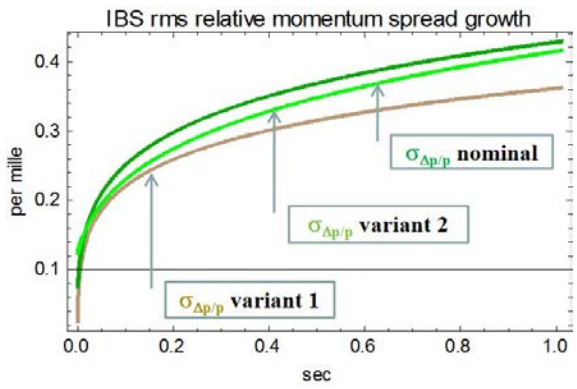

Fig. 34: Evolution of the momentum spread $\sigma_{\Delta p/p}$ over 1 s for the nominal beam and for variants 1–2.

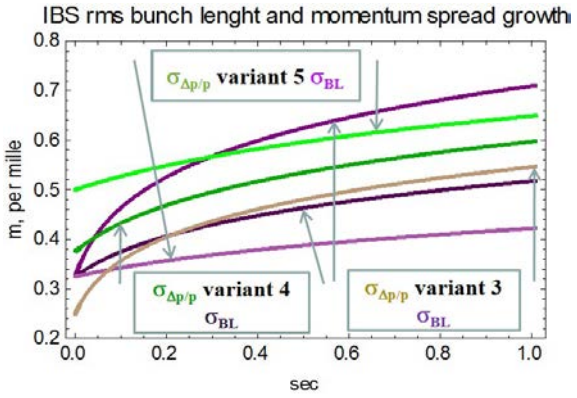

Fig. 35: Evolution of the bunch length σ_{BL} and relative momentum spread $\sigma_{\Delta p/p}$ over 1 s for variants 3–5.

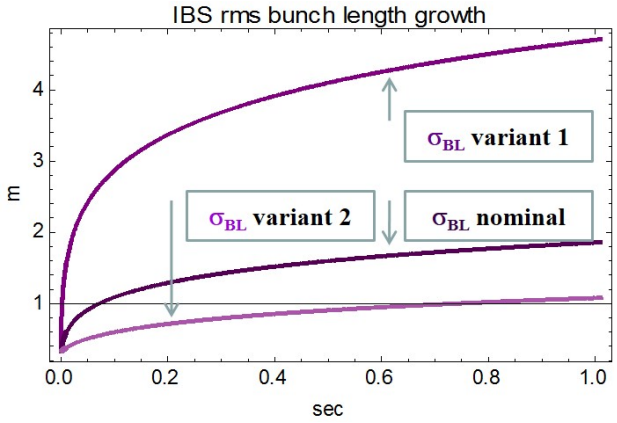

Fig. 36: Evolution of the bunch length σ_{BL} over 1 s for the nominal beam and the first two variants

From Figs. 32–36 we can see that an equilibrium between the transverse and longitudinal emittances does not strictly take place, even though ELENA at 100 keV is below the transition energy, with $\gamma \approx 1 < \gamma_t \approx 1.9$. Unlike the LHC collider, ELENA is a compact decelerator ring made of a non-regular lattice (see Fig. 26) and so does not satisfy the smooth focusing approximation criteria. Table 5 shows the bunch length, relative momentum spread and emittance increase for the nominal bunch and the five variants under IBS effects for 1 s at 100 keV without cooling. This allows us to quantify the bunch parameters with IBS, which is important because bunch length and momentum spread must be kept close to their nominal values.

Table 5: IBS beam growth ratios for the nominal beam and five variants; the ratios are of parameters experiencing the IBS effect for 1 s on the 100 keV plateau without cooling to those same parameters not enduring IBS effects.

	$\sigma_{\mathrm{BL}}(t)/\sigma_{\mathrm{BL}}(0)$	$\varepsilon_{\mathrm{L}}^{\mathrm{rms}}(t)/\varepsilon_{\mathrm{L}}^{\mathrm{rms}}(0)$	$\varepsilon_{\mathrm{H}}^{\mathrm{rms}}(t)/\varepsilon_{\mathrm{H}}^{\mathrm{rms}}(0)$	$\varepsilon_{\mathrm{V}}^{\mathrm{rms}}(t)/\varepsilon_{\mathrm{V}}^{\mathrm{rms}}(0)$
Nominal	5.7	32.5	1.31	0.94
Variant 1	14.5[a]	205.1	1.25	1.05
Variant 2	3.3	11.0	1.07	0.93
Variant 3	2.19	4.78	1.65	1.15
Variant 4	1.59	2.54	1.81	1.27
Variant 5	1.30	1.69	1.92	1.38

[a]Variant 1 is the worst scenario as the bunch length grows by a factor of 14.5 under IBS effects in relation to a bunch without IBS. Likewise, the nominal beam experiences a 5.7 growth factor due to IBS effects. The best scenario is variant 5, as the bunch grows by only a small factor of 1.3, compatible to that of the bunch length before IBS starts.

Figure 37 displays the IBS beam parameter growth factor ratios for the nominal beam and the five variants in Table 5. Compared to the longitudinal emittance, the transverse beam emittances are not as significantly altered by the IBS effects.

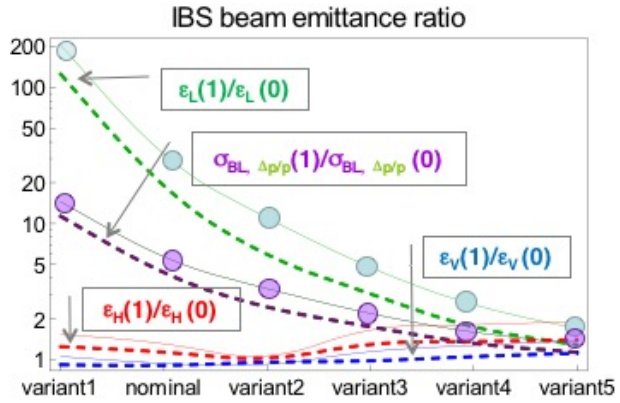

Fig. 37: Longitudinal and transverse emittance growth ratios, $\varepsilon_{\mathrm{LHV}}(t)/\varepsilon_{\mathrm{LHV}}(0)$, and the r.m.s. bunch length growth ratio $\sigma_{\mathrm{BL}}(t)/\sigma_{\mathrm{BL}}(0)$ (equal to that of the relative momentum spread $\sigma_{\Delta_{\mathrm{p/p}}}$) plotted for the nominal beam and the five variants. The growth ratios are shown for IBS simulations over 1 s (large circles represent IBS raw simulation data, while continuous and dashed lines are interpolated).

To finish, let us summarize our observations for the nominal beam and variants 1 and 5 in Table 5.

- **Nominal:** The increase in bunch length and relative momentum spread after the beam circulates for 1 s on the 100 keV plateau is *large*; the r.m.s. bunch length increases to $\sigma_{\mathrm{BL}}(1) = 1.85\,\mathrm{m}$ compared with $\sigma_{\mathrm{BL}}(0) = 0.325\,\mathrm{m}$ before IBS begins (also $\sigma_{\Delta_{\mathrm{p/p}}}(1) = 0.04\%$). This corresponds to a 95% bunch length increase equal to 7.4 m ($\approx 4\sigma_{\mathrm{BL}}(0)$), instead of the nominal 95% bunch length of $1.3\,\mathrm{m}$ at $t = 0$ without IBS effects. The longitudinal emittance varies as the product of the bunch length and the momentum spread since $\varepsilon_{\mathrm{L}} = \pi p \sigma_{\mathrm{BL}} \sigma_{\Delta_{\mathrm{p/p}}} (\beta c)^{-1}$.
- **Variant 1:** The bunch length and momentum spread after 1 s are *huge*. Indeed, the r.m.s. bunch length increases to $\sigma_{\mathrm{BL}}(1\,\mathrm{s}) = 4.7\,\mathrm{m}$, while the 95% bunch length peaks at 18.8 m!
- **Variant 5:** This is the best scenario, because the bunch length and momentum spread will suffer only 30% blow-up due to IBS after circulating for 1 s on the 100 keV plateau; their r.m.s. values are $\sigma_{\mathrm{BL}}(1) = 0.42\,\mathrm{m}$, compared with 0.325 m before IBS starts ($\sigma_{\Delta_{\mathrm{p/p}}}(1) = 0.065\%$). Similarly, the 95% bunch length is 1.7 m.

Appendix A: Complementary proof of growth rate formula

The Piwinski's model [1] derives the formulae for the variations of the mean transverse emittances and momentum spread per time unit due to a scattering event. The derivative of the betatron and dispersion functions and the vertical dispersion function with respect to the longitudinal beam axis are neglected. The growth rates are calculated in accordance with the expression (154) for Gaussian probability law, derived from (147). Here, the aim to show clearly as possible the link between these formulations.

Let us define the functions

$$f_i = 2\,k_i \int_0^{\pi} \mathrm{d}\mu \int_0^{2\pi} \mathrm{d}\nu \int_0^{\infty} \mathrm{d}r\, \sin[\mu]\, g_i[\mu,\nu] \log[r] \exp\Big[-r\, D(\mu,\nu)\Big] \quad \text{for} \quad i = 1,2,3\,. \tag{A1}$$

where $k_1 = \dfrac{1}{c^2}$, $k_2 = \dfrac{a^2}{c^2}$, $k_3 = \dfrac{b^2}{c^2}$, and

$$D(\mu,\nu) = \frac{1}{c^2}\Big(b^2\cos^2[\mu] + \sin^2[\mu]\big(\cos^2[\nu] + a^2\sin^2[\nu]\big)\Big)\,.$$

$D(\mu,\nu)$ is Eq. (145) and $g_1[\mu,\nu]$, $g_2[\mu,\nu]$, $g_3[\mu,\nu]$ are Eqs. (146). Now, we pass from the spherical to Cartesian coordinates $(\sqrt{r},\mu,\nu) \to (u,v,w)$ using (143)

$$\big(u = \sqrt{r}\sin\mu\cos\nu,\ v = \sqrt{r}\sin\mu\sin\nu,\ w = \sqrt{r}\cos\mu\big) \implies u^2+v^2+w^2 = r\,,$$

from which we can write the three functions f_i as follows, since the functions $g_i(\mu,\nu)$ and $D(u,v,w)$ transform into

$$g_1 = \frac{1}{r}(-2u^2+v^2+w^2)\,, \quad g_2 = \frac{1}{r}(u^2-2v^2+w^2)\,, \quad g_3 = \frac{1}{r}(u^2+v^2-2w^2)\,, \tag{A2}$$
$$D(u,v,w) = \frac{1}{r}(u^2-a^2\,v^2+b^2\,w^2)\,, \quad \frac{2}{\sqrt{r}}\,du\,dv\,dw = \sin[\mu]\,\mathrm{d}r\,\mathrm{d}\mu\,\mathrm{d}\nu$$

$$\begin{pmatrix} f_1 \\ f_2 \\ f_3 \end{pmatrix} = 4 \begin{bmatrix} k_1 \\ k_2 \\ k_3 \end{bmatrix} \int_{-\infty}^{\infty}\mathrm{d}u \int_{-\infty}^{\infty}\mathrm{d}v \int_{-\infty}^{\infty}\mathrm{d}w \begin{Bmatrix} -2u^2+v^2+w^2 \\ u^2-2v^2+w^2 \\ u^2+v^2-2w^2 \end{Bmatrix}$$
$$\times \frac{\ln[u^2+v^2+w^2]}{\big(u^2+v^2+w^2\big)^{3/2}} \exp\left[-\frac{1}{c^2}\big(u^2+a^2v^2+b^2w^2\big)\right]\,, \tag{A3}$$

Next, a trick is used: In f_1 let $u = w, v = u, w = v$, in f_2 let $u = u, v = w, w = v$, do not change f_3 (i.e. $u = u, v = v, w = w$ remain the same). We obtain (cf. [24])

$$\begin{pmatrix} f_1 \\ f_2 \\ f_3 \end{pmatrix} = \frac{4}{c^2} \begin{bmatrix} 1 \\ a^2 \\ b^2 \end{bmatrix} \int_{-\infty}^{\infty}\mathrm{d}u \int_{-\infty}^{\infty}\mathrm{d}v \int_{-\infty}^{\infty}\mathrm{d}w\, \big\{u^2+v^2-2w^2\big\}$$
$$\times \frac{\ln[u^2+v^2+w^2]}{\big(u^2+v^2+w^2\big)^{3/2}} \begin{Bmatrix} \exp\left[-\frac{1}{c^2}\big(a^2u^2+b^2v^2+w^2\big)\right] \\ \exp\left[-\frac{1}{c^2}\big(u^2+b^2v^2+a^2w^2\big)\right] \\ \exp\left[-\frac{1}{c^2}\big(u^2+a^2v^2+b^2w^2\big)\right] \end{Bmatrix} \mathrm{d}u\,\mathrm{d}v\,\mathrm{d}w\,, \tag{A4}$$

Switching back to spherical coordinates leads to, with

$$\frac{u^2+v^2-2w^2}{r^{3/2}} = \frac{1-3\cos^2[\mu]}{r^{1/2}}\,, \quad \text{reintroducing} \quad \rho = \frac{r}{c^2} \quad \Longrightarrow \quad \frac{2}{\sqrt{r}}\,du\,dv\,dw = c^2\sin[\mu]\,\mathrm{d}\rho\,\mathrm{d}\mu\,\mathrm{d}\nu\,,$$

$$\begin{pmatrix} f_1 \\ f_2 \\ f_3 \end{pmatrix} = 2\int_0^{\pi} \mathrm{d}\mu \int_0^{2\pi} \mathrm{d}\nu \int_0^{\infty} \mathrm{d}\rho\, \sin[\mu]\, \left(1-3\cos^2[\mu]\right) \ln[\rho c^2]$$
$$\times \begin{Bmatrix} \exp\left[-\rho\left(\sin^2[\mu]\left(a^2\cos^2[\nu]+b^2\sin^2[\nu]\right)+\cos^2[\mu]\right]\right. \\ a^2\exp\left[-\rho\left(\sin^2[\mu]\left(\cos^2[\nu]+b^2\sin^2[\nu]\right)+a^2\cos^2[\mu]\right]\right. \\ b^2\exp\left[-\rho\left(\sin^2[\mu]\left(\cos^2[\nu]+a^2\sin^2[\nu]\right)+b^2\cos^2[\mu]\right]\right. \end{Bmatrix} \equiv \begin{pmatrix} f\left(a,b,c\right) \\ f\left(\frac{1}{a},\frac{b}{a},\frac{c}{a}\right) \\ f\left(\frac{1}{b},\frac{a}{b},\frac{c}{b}\right) \end{pmatrix} . \qquad \text{(A5)}$$

in which $f\left(a,b,c\right)$ is the scattering matrix (148) and $D_0(\mu,\nu)$ is (149). The first equation of (A5) can be written

$$f_1 = 2\int_0^{\pi} \mathrm{d}\mu \int_0^{2\pi} \mathrm{d}\nu \int_0^{\infty} \mathrm{d}\rho\, \sin[\mu]\, \left(1-3\cos^2[\mu]\right) \ln[\rho c^2] \exp\left[-\rho\, D_0(\mu,\nu)\right] \equiv f\left(a,b,c\right) ,$$

Referring to Eqs. (147) the IBS growth rates can then given in terms of f_1, f_2, f_3 as

$$\begin{pmatrix} \tau_\eta^{-1} \\ \tau_x^{-1} \\ \tau_z^{-1} \end{pmatrix} = \frac{\mathcal{A}_\mathrm{P}}{c^2} \int_0^{\infty} \mathrm{d}\rho \int_0^{\pi} \mathrm{d}\mu \int_0^{2\pi} \mathrm{d}\nu\, \sin[\mu] \exp\left[-\rho D(\mu,\nu)\right] \ln[\rho c^2]$$
$$\times \begin{Bmatrix} \left(1-d^2\right) g_1[\mu,\nu] \\ a^2 g_2[\mu,\nu] + d^2 g_1[\mu,\nu] \\ b^2 g_3[\mu,\nu]) \end{Bmatrix} \equiv \mathcal{A}_\mathrm{P} \begin{bmatrix} \left(1-d^2\right) f_1 \\ f_2 + d^2 f_1 \\ f_3 \end{bmatrix} \equiv \mathcal{A}_\mathrm{P} \begin{bmatrix} \left(1-d^2\right) f\left(a,b,c\right) \\ f\left(\frac{1}{a},\frac{b}{a},\frac{c}{a}\right) + d^2 f\left(a,b,c\right) \\ f\left(\frac{1}{b},\frac{a}{b},\frac{c}{b}\right) \end{bmatrix} . \qquad \text{(A6)}$$

where $f\left(a,b,c\right) = f_1,\ f\left(\frac{1}{a},\frac{b}{a},\frac{c}{a}\right) = f_2,\ f\left(\frac{1}{b},\frac{a}{b},\frac{c}{b}\right) = f_3$. Eq. (A6) is thus equal to Eq. (154).

Appendix B: Scattering matrix

Decay rates and *cross-sections* are experimentally measurable quantities, predicted in quantum physics through probabilities given by squared inner products of particle quantum states. These inner products can be written as matrix elements $\langle f;t_f|\, i;t_i\rangle$ where $|i;t_i\rangle$ is the *initial* state before the scattering of a physical system and $|f;t_f\rangle$ is the *final* state after the scattering event (cf. [35, 40–42]). The notation $\langle f;t_f|\, i;t_i\rangle$ refers to the so-called *Schrödinger picture* (SP), where the states $|\psi\rangle_\mathrm{S}$ evolve in time while the operators $\mathcal{O}_\mathrm{S}$ are independent of time. In contrast, in the *Heisenberg picture* (HP), the states $|\psi\rangle_\mathrm{H}$ are fixed and the operators $\mathcal{O}_\mathrm{H}(t)$ vary in time:

$$\begin{aligned} &\text{SP:} \quad \mathrm{i}\frac{\mathrm{d}|\psi\rangle_\mathrm{S}}{\mathrm{d}t} = H|\psi\rangle_\mathrm{S} \text{ and } \mathcal{O}_\mathrm{S} \text{ is time-independent} \\ &\text{HP:} \quad |\psi\rangle_\mathrm{H} = \exp(\mathrm{i}Ht)|\psi\rangle_\mathrm{S} \text{ and } \mathcal{O}_\mathrm{H}(t) = \exp(\mathrm{i}Ht)\mathcal{O}_\mathrm{S}\exp(-\mathrm{i}Ht) \end{aligned}$$

(where HL units, with $\epsilon_0 = \hbar = c = 1$, are used). The *interaction picture* (IP) is a hybrid of SP and HP. The Hamiltonian H is split up into a part H_0 that can be handled exactly and a part H_int to be treated as a perturbation: $H = H_0 + H_\mathrm{int}$. Thus, the time dependence of operators $\mathcal{O}_\mathrm{I}$ is driven by H_0 and the time dependence of states $|\psi\rangle_\mathrm{I}$ by H_int so that the corresponding IP state vector and operator are defined by

$$|\psi(t)\rangle_\mathrm{I} = \exp(\mathrm{i}H_0 t)\,|\psi(t)\rangle_\mathrm{S} \ \text{ and } \ \mathcal{O}_\mathrm{I}(t) = \exp(\mathrm{i}H_0 t)\,\mathcal{O}_\mathrm{S}\exp(-\mathrm{i}H_0 t)$$

$$\overset{\mathcal{O}=H_{\text{int}}}{\Longrightarrow} \quad H_{\text{I}} \equiv (H_{\text{int}})_{\text{I}} = \exp(\mathrm{i}H_0 t)(H_{\text{int}})_{\text{S}} \exp(-\mathrm{i}H_0 t) \ \ \text{(IP)} \ .$$

From this we have the equation of motion for $|\psi(t)\rangle_{\text{I}}$,

$$\mathrm{i}\,\frac{\mathrm{d}|\psi(t)\rangle_{\text{I}}}{\mathrm{d}t} = H_I|\psi(t)\rangle_{\text{I}}, \tag{B1}$$

whose solution is given by *Dyson's expansion*:

$$|\psi(t)\rangle_{\text{I}} = U(t,t_0)|\psi(t_0)\rangle_{\text{I}} \ \ \Longrightarrow \ \ U(t,t_0) = \mathcal{T}\left\{\exp\left[-\mathrm{i}\int_{t_0}^{t} H_{\text{I}}(t')\,\mathrm{d}t'\right]\right\} \tag{B2}$$

with $\mathrm{i} = \sqrt{-1}$, where $U(t,t_0)$ is a time-evolution operator satisfying the properties $U(t,t) = 1$ and $U(t_1,t_2)U(t_2,t_3) = U(t_1,t_3)$. The function $\mathcal{T}\{\,\cdot\,\}$ implies a *time-ordering product* acting on operators such that operators evaluated at later times are placed to the left.

Comment: For two operators $\mathcal{O}_{1,2}$ the function $\mathcal{T}$ is defined by $\mathcal{T}(\mathcal{O}_1(t_1)\mathcal{O}_2(t_2)) = \mathcal{O}_1(t_1)\mathcal{O}_2(t_2)$ if $t_1 > t_2$ and $\mathcal{T}(\mathcal{O}_1(t_1)\mathcal{O}_2(t_2)) = \mathcal{O}_2(t_2)\mathcal{O}_1(t_1)$ if $t_2 > t_1$.

In the case where the particle momentum eigenstates evolve from $t = -\infty$ to $t = +\infty$, the time-evolution operator is denoted by S and called the *S-matrix* (for 'scattering matrix'). It is defined via its components S_{fi} as

$$\langle f|S|i\rangle = \langle f; t=\infty|\, i; t=-\infty\rangle_{\text{Schrödinger}} \equiv S_{\text{fi}} \ . \tag{B3}$$

The S-matrix can equivalently be defined in terms of the time-evolution operator describing scattering experiments, as

$$\langle f|S|i\rangle = \lim_{\substack{t_0\to-\infty \\ t\to+\infty}} \langle f|U(t,t_0)|i\rangle \equiv S_{\text{fi}} \ . \tag{B4}$$

The idea behind this definition is that as time evolves, the particles approach each other and may interact briefly before moving away, with each going along its own path so that the states are free of interactions at $t = \pm\infty$. For that reason it is convenient to separate forward scattering by defining $S = I + \mathrm{i}T$, where I is the identity matrix and T is a *transition matrix* (called the T-matrix) which contributes only when particles undergo scattering. The exponential form of Dyson's expansion, the formula on the right in (B2), is not very useful as the integral in the exponent cannot in general be computed exactly. Therefore, provided H_{I} is small compared with H_0, it should be expanded in a power series of the interaction 'Hamiltonian operator', and thus terms can be obtained to a suitable order since (B2) is related to (B4). Since the S-matrix is the limit $S = U(t\to\infty,\, t_0\to-\infty)$, the Dyson's expansion power series of (B2) can be written as

$$S = I - \mathrm{i}\int_{-\infty}^{\infty} \mathrm{d}t_1 H_{\text{I}}(t_1) + \frac{(-\mathrm{i})^2}{2}\int_{-\infty}^{\infty}\mathrm{d}t_1\int_{-\infty}^{t_1}\mathrm{d}t_2\mathcal{T}\big\{H_{\text{I}}(t_2)H_{\text{I}}(t_1)\big\} + \cdots \ . \tag{B5}$$

However, this approach is rather tedious. Instead, it is better to use the graphical tool of *Feynman diagrams* (together with *Feynman rules*) discussed in the main text. Briefly, Feynman diagrams are qualitative and symbolic figures that represent terms in the perturbation expansion of the S-matrix (see e.g. Fig. 14). Particles in space–time are solid lines with arrows, time runs from left to right, the space direction is perpendicular to time (antiparticles travel backwards in time), arrows show the charge flux relative to time, and wavy lines represent 'virtual particles' that live for only a short time, i.e. bosons mediating the interaction which are emitted and absorbed soon after (e.g. photons in QED). 'Loops' are closed patterns of virtual particles (present in high-order diagrams corresponding to high-order terms of the perturbative Dyson's expansion power series).

In the S-matrix, we are interested in the scattering part of a process and not in the part where no scattering occurs, namely where S reduces to an identity matrix I. Therefore, we just want to calculate $\langle f|S-I|i\rangle$, the 'non-trivial' part of $\langle f|S|i\rangle$. Here we follow [35, 40], where it is emphasized that the matrix elements S_{fi} of the S-matrix should reflect 4-momentum conservation, so that S, or $S-1$, should contain a factor $(2\pi)^4\delta^4(p_i-p_f)$. It is then conventional to extract this factor and define the *invariant amplitude* $\mathcal{M}$ via

$$\langle f|(\mathrm{i}T)|i\rangle \equiv \langle f|S-I|i\rangle = (2\pi)^4\delta^4\Big(\sum p_i - \sum p_f\Big)\,\mathrm{i}\mathcal{M} \tag{B6}$$

where $\sum p_f$ and $\sum p_i$ are the sums of the final and initial 4-momenta, and $\mathrm{i}=\sqrt{-1}$, the complex number i is introduced to motivate the relation $\exp[\mathrm{i}T]\approx I+\mathrm{i}T=S$. The reason the δ-function is included in the S-matrix is to ensure observance of conservation of energy and momentum; so it is useful to factor an overall 'momentum-conserving δ-function' to begin with. Detailed proofs of (B6), which are quite difficult, are given in [43] for non-relativistic scattering and in [44] for the relativistic case. Equation (B6) differs from the expressions in those two proofs by its 2π factor. For a two-particle energy–momentum scattering process, this equation reads

$$\langle f_1f_2|\mathrm{i}T|i_1i_2\rangle \equiv \langle f_1f_2|S-I|i_1i_2\rangle = (2\pi)^4\delta^4(p_{1i}+p_{2i}-p_{1f}-p_{2f})\,\mathrm{i}\mathcal{M}, \tag{B7}$$

also written

$$\langle p_{1f}p_{2f}|\mathrm{i}T|p_{1i}p_{2i}\rangle \equiv \langle p_{1f}p_{2f}|S-I|p_{1i}p_{2i}\rangle = (2\pi)^4\delta^4(p_{1i}+p_{2i}-p_{1f}-p_{2f})\,\mathrm{i}\mathcal{M}\,,$$

where we have used the notation $|i\rangle=|i_1\rangle|i_2\rangle=|p_{1i}\rangle|p_{2i}\rangle$ and $|f\rangle=|f_1\rangle|f_2\rangle=|p_{1f}\rangle|p_{2f}\rangle$ for the two-particle state.

Starting from (B6), the transition probability between the initial state $|i\rangle$ and the final state $|f\rangle$ is given by the square of the S-matrix, $|\langle f|S-I|i\rangle|^2$. As is usual in quantum mechanics and quantum field theory, the probabilities of events are the squared (moduli of the) 'quantum amplitudes', such as the entries of the S-matrix for calculating the probabilities of decay rates and cross-section processes. However, to square the matrix elements we have to square the δ-function in (B6). Using the Dirac δ-function property $\{\delta(x-y)\}^2=\delta(x-y)\delta(0)$, we obtain

$$\Big\{\delta^4\Big(\sum p_i-\sum p_f\Big)\Big\}^2 = \delta^4\Big(\sum p_i-\sum p_f\Big)\delta^4(0)=\infty \quad \text{since} \quad \delta(0)=\lim_{\epsilon\to 0}\frac{1}{\epsilon}=\infty\,,$$

which is meaningless! Nevertheless, such infinities must be eliminated from all physical quantities.

One proper way to solve this problem is to confine the whole system of particles in a closed box of volume V and then let the box volume become infinite, while assuming that the interaction is turned on for only a finite time t. For simplicity the particles are described as 'free-particle plane waves' that spread over infinite volumes and time intervals. Such a finite closed box and finite time interval can be defined using the following representation of a Dirac δ-function on a 4-position $r\stackrel{\mathrm{def}}{=}(t,\mathbf{r})$ and a 4-momentum $p\stackrel{\mathrm{def}}{=}(E,\mathbf{p})$. We find that

$$\begin{aligned}\delta^4(p) &= \frac{1}{(2\pi)^4}\int \exp[-\mathrm{i}rp]\,\mathrm{d}^3r \\ &= \frac{1}{(2\pi)^4}\int_V \exp[-\mathrm{i}\mathbf{r}\cdot\mathbf{p}]\,\mathrm{d}^3\mathbf{r}\int_0^t \exp[-\mathrm{i}t'E]\,\mathrm{d}t' \stackrel{\mathrm{p=E=0}}{\Longrightarrow} \delta^4(0)=\frac{Vt}{(2\pi)^4}\,.\end{aligned}$$

Taking the square of (B6) gives, by virtue of the last two formulae,

$$\mathcal{P}_{i\to f}\stackrel{?}{=}|\langle f|(\mathrm{i}T)|i\rangle|^2 \equiv |\langle f|S-I|i\rangle|^2 = Vt(2\pi)^4\delta^4\Big(\sum p_i-\sum p_f\Big)|\mathcal{M}|^2\,. \tag{B8}$$

Although the probabilities are expressed in terms of the squared amplitudes, we shall proceed differently and replace $|\langle f|(\mathrm{i}T)|i\rangle|^2 \equiv |\langle f|S-I|i\rangle|^2$ in (B8) by the 'normalized' probability

$$\mathcal{P}_{i\to f} = \frac{|\langle f|(\mathrm{i}T)|i\rangle|^2}{\langle f|f\rangle\langle i|i\rangle} \equiv \frac{|\langle f|(S-I)|i\rangle|^2}{\langle f|f\rangle\langle i|i\rangle}, \tag{B9}$$

where the presence of inner products $\langle f|f\rangle$ and $\langle i|i\rangle$ in the denominator of (B9) stems from the fact that they may not be normalized to unity.

As a 'simple' case we envisage (in a toy model framework of structureless, i.e. point-like and spineless, particles) the *decay* of a single initial particle $|i\rangle = |i_1\rangle$, with 4-momentum $|p_{1i}\rangle$, into two distinct final particles $|f\rangle = |f_1\rangle|f_2\rangle$ with 4-momenta $|p_{1i}\rangle|p_{2i}\rangle$ [42]. These inner products can be shown (without proof) to be

$$\langle i|i\rangle \equiv \langle i_1|i_1\rangle = (2E_{1i}V), \qquad \langle f|f\rangle \equiv \langle f_1f_2|f_1f_2\rangle = (2E_{1f}V)(2E_{2f}V), \tag{B10}$$

where $E_{1,2f} = \sqrt{m^2+\mathbf{p}_{1,2f}^2}$ (and E_{1i}) are the particle energies with mass m and V is the volume of the box containing the particles. Observe that $|i_1\rangle$ and $|f_1f_2\rangle$ are not normalized to unity. Therefore, upon substituting (B10) into (B9) the transition probability can be written as

$$\mathcal{P}_{i\to f} = \frac{|\langle f_1f_2|(\mathrm{i}T)|i_1\rangle|^2}{\langle f_1f_2|f_1f_2\rangle\langle i_1|i_1\rangle} = t\frac{(2\pi)^4}{2E_{1i}}\delta^4\big(p_{1i}-p_{1f}-p_{2f}\big)|\mathcal{M}|^2\prod_{n=1}^{2}\frac{1}{2E_{nf}V}\,. \tag{B11}$$

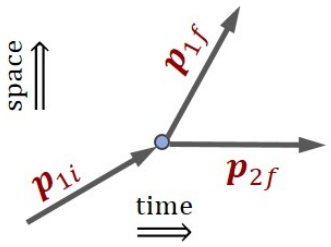

Fig. B.1: Feynman diagram for the decay $\mathbf{p}_{1i} \to \mathbf{p}_{1f} + \mathbf{p}_{2f}$ of one initial structureless particle with 4-momentum $p_{1i} = (E_{1i}, \mathbf{p}_{1i})$ into two final structureless particles with 4-momenta $p_{1f,2f} = (E_{1f,2f}, \mathbf{p}_{1f,2f})$ after decay.

The probability of transition per unit time (called the *transition rate*) between the initial decaying particle state and the final two-particle state created by decay is obtained by dividing (B11) by t, yielding

$$\frac{\mathrm{d}\mathcal{P}_{i\to f}}{\mathrm{d}t} = \frac{1}{2E_{1i}}(2\pi)^4\delta^4\big(p_{1i}-p_{1f}-p_{2f}\big)|\mathcal{M}|^2\prod_{n=1}^{2}\frac{1}{2E_{nf}V} \tag{B12}$$

$$\text{or} \quad \frac{\mathrm{d}\mathcal{P}_{i\to f}}{\mathrm{d}t} = \frac{1}{2E_{1i}}(2\pi)^4\delta^4\big(p_{1i}-p_{1f}-p_{2f}\big)|\mathcal{M}|^2\left(\frac{1}{2E_{1f}V}\right)\left(\frac{1}{2E_{2f}V}\right)$$

which, said differently, is the probability of transition per unit time to one particular final state $|f\rangle = |f_1\rangle|f_2\rangle$ out of all possible final states, made up of two particles with momenta p_{1f} and p_{2f} in that state. In the limit as the box volume $V \to \infty$, the momentum values become continuous, i.e. the $|p_1\rangle + |p_2\rangle$ final states form a continuum, and the *total decay rate*, called Γ, is obtained by integration of $\dot{\mathcal{P}}_{i\to f}$ over the continuum of final states. To determine whether the final momentum of a given particle lies within a domain $\mathrm{d}^3\mathbf{p}$ in the three-dimensional momentum space, Eq. (B12) must be multiplied by the number of states in this domain. To do this, the three-dimensional coordinate space is discretized into cells of size

$(2\pi)^3$ and one state is put into each cell. Hence, in a large box of volume V, the number of single-particle states in a momentum space domain $\mathrm{d}^3\mathbf{p}$ is $V\,\mathrm{d}^3\mathbf{p}/(2\pi)^3$.

Comment: Note that $(2\pi)^3$ is the discretized cell size in HL units, where $\hbar = 1$ and $h \stackrel{\text{def}}{=} 2\pi\hbar = 2\pi$. Expressed in SI units, the cell size is h^3, with $h = 2\pi\hbar = 6.626\times10^{-34}$ J s and $\hbar = 1.054\times10^{-34}$ J s, h being the Planck constant.

Finally, multiplying all the final state particles in Eq. (B12) by the factor $V\,\mathrm{d}^3\mathbf{p}/(2\pi)^3$ and integrating over the two final momenta yields the decay rate Γ (at times the name $\dot{\mathcal{P}}_{i\to f}$ is used for Γ):

$$\Gamma = \frac{1}{2E_{1i}} \int \frac{\mathrm{d}^3\mathbf{p}_{1f}}{(2\pi)^3 2E_{1f}} \int \frac{\mathrm{d}^3\mathbf{p}_{2f}}{(2\pi)^3 2E_{2f}} \, (2\pi)^4 \delta^4\big(p_{1i} - p_{1f} - p_{2f}\big) |\mathcal{M}|^2 \, . \tag{B13}$$

Notice that all the quantities V (and t) have dropped out at the end of the calculations. The amplitude $\mathcal{M}$ will be calculated by means of the Feynman rules (as outlined in the main text). Similar types of calculations are undertaken for the study of scattering *cross-sections*, also referred to as *rate per flux*. An effective application of these powerful computational tools to intrabeam scattering is given by the Bjorken–Mtingwa model. Eq. (B13) agrees with the decay rate formulation [32] (appendix B) and has similarities to the Bjorken's transition rate for the scattering process, Eq. (158).

References

[1] A. Piwinski, Intra-beam scattering, Proc. 9th Int. Conference on High Energy Accelerators, Stanford, CA, 1974 (SLAC, Stanford, CA, 1974), p. 405.

[2] J. Bjorken and S. Mtingwa, *Part. Accel.* **13** (1983) 115.

[3] I. Meshkov *et al.*, BETACOOL Physics Guide, Joint Institute for Nuclear Research, Dubna, Russia (2008).

[4] P. Zenkevich, A. Bolshakov and O. Boine-Frankenheim, *Kinetic effects in multiple intra-beam scattering*, ICFA HB204, Bensheim, 2005 [AIP Conf. Proc. **773** (2005) 425].

[5] M. Martini and A. Vivoli, Effect of intrabeam scattering and synchrotron radiation damping when reducing transverse emittances to augment the LHC luminosity, CERN-sLHC-PROJECT-Report-0032 (2010).

[6] A. Piwinski, in Proceedings of the CAS–CERN Accelerator School and NIKHEF-H, 16–27 June 1991, Amsterdam, the Netherlands, edited by T. Stuart, CERN–1992–001 (CERN, Geneva,1992). http://dx.doi.org/10.5170/CERN-1992-001

[7] Ch. Carli, Private communication, CERN (2012).

[8] M. Kardar, *Statistical Physics of Particles* (Cambridge University Press, Cambridge, 2007). http://dx.doi.org/10.1017/CBO9780511815898

[9] J.A. Bittencourt, *Fundamentals of Plasma Physics* (Springer, New York, 2004). http://dx.doi.org/10.1007/978-1-4757-4030-1

[10] R.L. Liboff, *Kinetic Theory* (Springer, New York, 2003).

[11] L. Landau, E.M. Lifshitz and L.P. Pitaevskii, *Physical Kinetics*, Course of Theoretical Physics, vol. 10 (Butterworth-Heinemann, Oxford, 1981).

[12] D. Tong, *Kinetic Theory*, Graduate Course, University of Cambridge, Cambridge, UK (2012).

[13] K. Huang, *Statistical Mechanics* (Wiley, New York, 1987).

[14] H. Jakobsen, *Chemical Reactor Modeling: Multiphase Reactive Flows* (Springer, New York, 2014). http://dx.doi.org/10.1007/978-3-319-05092-8

[15] N.S. Dikansky and D.V. Pestrikov, *The Physics of Intense Beams and Storage Rings* (AIP Press, Woodbury, New York, 1994).

[16] Ya.S. Derbenev, Collisional relaxation of intense beams of heavy particles in storage rings, Fermilab $\bar{\mathrm{p}}$ Note 176 (1981).

[17] A.H. Sørensen, Intrabeam scattering, US-CERN School on Particle Accelerators, Hilton Head Island, South Carolina, USA (1990).

[18] M. Reiser, *Theory and Design of Charged Particle Beams* (Wiley-VCH, Weinheim, Germany, 2008). http://dx.doi.org/10.1002/9783527622047

[19] H. Wiedemann, *Particle Accelerator Physics* (Springer, Berlin, 2007).

[20] A. Piwinski, Intra-beam scattering, Joint US-CERN School on Particle Accelerators, Texas, USA (1986).

[21] J. Freund, *Special Relativity for Beginners* (World Scientific, Singapore, 2008). http://dx.doi.org/10.1142/6601

[22] A. Piwinski, The Touschek effect in strong focusing storage rings, DESY-98-179, Hamburg, Germany (1998).

[23] M. Zisman, S. Chattopadhyay and J. Bisognano, ZAP user's manual, LBL-21270, E.SG-15 (Lawrence Berkeley Laboratory, Berkeley, CA, 1986).

[24] M. Martini, Intrabeam scattering in the ACOL-AA machines, CERN PS/84 9 (1984).

[25] L.R. Evans and B. Zotter, Intrabeam scattering in the SPS, CERN/SPS/80-15-DI (1980).

[26] K. Kubo and K. Oide, Intrabeam scattering in electron storage rings (2001) 124401. http://dx.doi.org/10.1103/PhysRevSTAB.4.124401

[27] K. Bane, A simplified model of intrabeam scattering, in Proceedings of the eighth European Particle Accelerator Conference, Paris, France, 2002 (EPS-IGA and CERN, Geneva, 2002), p. 1443.

[28] K. Kubo, S. Mtingwa and A. Wolski, Intrabeam scattering formulas for high energy beams (2005) 081001. http://dx.doi.org/10.1103/PhysRevSTAB.8.081001

[29] A. Wolski, Space charge, intrabeam scattering and Touschek effects, Fourth International Accelerator School for Linear Colliders, Beijing, China, 2009.

[30] A. Wolski, *Beam Dynamics in High Energy Particle Accelerators* (Imperial College Press, London, 2014).

[31] D. McMahon, *Quantum Field Theory Demystified* (McGraw-Hill, New York, 2008).

[32] J.D. Bjorken and S.D. Drell, *Relativistic Quantum Mechanics* (McGraw-Hill, New York, 1964).

[33] S. Mtingwa, A New High Energy Approximation of Intrabeam Scattering for Flat Electron and Positron Beams, African Physical Review (2008) 2:0001.

[34] D. Griffiths, *Introduction to Elementary Particles* (Wiley-VCH, Weinheim, Germany, 2010).

[35] I.J.R. Aitchison and A.J.G. Hey, *Gauge Theories in Particle Physics. Vol. 1: From Relativistic Quantum Mechanics to QED* (CRC Press, Boca Raton, FL, 2013).

[36] F. Zimmermann, Refined models of intrabeam scattering, Proc. HB2006, Tsukuba, Japan (2006), p. 265.

[37] F. Antoniou and F. Zimmermann, Revision of intrabeam scattering with non-ultrarelativistic corrections and vertical dispersion for MAD-X, CERN-ATS-2012-066 (2012).

[38] J. Resta-López, J.R. Hunt and C.P. Welsch, Intrabeam scattering effects in ELENA, IPAC2015 Conf., Richmond, Virginia, USA (2015).

[39] V. Chohan (Ed.), Extra low energy antiproton (ELENA) ring and its transfer lines, CERN-2014-002 (2014). http://dx.doi.org/10.5170/CERN-2014-002

[40] M.D. Schwartz, *Quantum Field Theory and the Standard Model* (Cambridge University Press, London, 2014).

[41] A. Lahiri and P.B. Pal, *A First Book of Quantum Field Theory* (Alpha Science, Oxford, 2005).

[42] D. Tong, *Quantum Field Theory*, Lecture notes, University of Cambridge, Cambridge, UK (2007).

[43] S. Weinberg, *Lectures on Quantum Mechanics* (Cambridge University Press, New York, 2013).

[44] S. Weinberg, *Quantum Theory of Fields. Vol. 1* (Cambridge University Press, London, 2005).